Heini Wernli
ETH Zurich, Institute for Atmosphere and Climate Science
Universitaetstrasse 16
8092 Zurich
Switzerland

Dear Dr. Wernli:

Please find enclosed our revised manuscript, "Vertical profile observations of water vapor deuterium excess in the lower troposphere" for publication as a research article in Atmospheric Chemistry and Physics. We have diligently addressed each comment given by the two reviewers. The main changes include a reorganization of separate results and discussions sections into combined sections for each case study flight day. The reviewers also both questioned our application of isotopic model equations from Stewart and Worden to describe the partial evaporation of liquid droplets and subsequent complete evaporation in a different atmospheric layer. We agree with the reviewers that the assumptions of these models do not hold in our observations. We have replaced this discussion with an improved analysis of the relevant timescales for evaporation within cloud layers.

The changes we have made to the manuscript are consistent with the reviewers' comments, and have greatly improved the paper. The submission includes our responses to each of the reviewers' comments, the manuscript and Supporting Information (SI) with changes indicated in "track changes mode", and the final revised manuscript, SI, and figures. We plan to comply with the journal's data policy by providing a DOI once the manuscript is accepted for publication. In the meantime, the data is accessible at https://vapor-isotope.yale.edu/. We hope you agree that we have completely addressed all the reviewers' concerns, and that the paper is now in publishable form. Thank you for your consideration.

Sincerely,

Olivia Salmon and Lisa Welp
Purdue University

Authors' Responses to Reviewer 1

- Author responses are indicated in blue font.
- Locations of our edits in the "strike-through" and final versions of the manuscript are provided with the following convention: ([strike-through version] pg. #, ln # / [final version] pg. #, ln #).

1 Major comments

1. I am not convinced by the way the Rayleigh model is used as an explanation in flights RAY and STC. Even though a Rayleigh model can match much your data, it does not necessarily indicate that the guiding processes are correctly represented. In particular, the presence of a quite homogeneous mixing line of water vapour below the inversion, topped by a pronounced inversion layer, and relative humidity below 10% is in stark contrast to the moist adiabatic profile that would be associated with a Rayleigh model. I recommend to include the possibility of long range advection of air with subsequent mixing into the picture, as well as considering the role of subsidence of air as a contribution to the inversion layer. Can several mixing processes in time and in the vertical combined look like a Rayleigh curve? This analysis should be placed in the context of the critique of Taylor (1984) on Rozanski and Sonntag (1982), and the very valuable study by Gedzelman (1988) to analyze Taylor's (1972) data set. Maybe a conclusion of your study could be a critique rather than a statement of consistency with the Rayleigh model?
The Reviewer makes an excellent point that our flight conditions during the RAY (now CLR) flights are not consistent with moist adiabatic conditions that would be required for Rayleigh rainout processes to be actively occurring. However, the Rayleigh prediction is most consistent with our observations, compared to mixing scenarios as we now show in Figure 7. We have changed this discussion to indicate that observed profile is a fingerprint of previous airmass dehydration conditions that is retained by transport and downward mixing of dehydrated higher altitude FT air, consistent with past studies (Taylor, 1984; Gedzelman, 1988). (pg 19, ln 2-28 / pg 8, ln 10-33)

2. The interpretation of the stratocumulus case study as evaporating cloud drops needs further corroboration. The literature cited on the kinetic fractionation of evaporating droplets, such as Stewart (1975) considers rain drops, which are orders of magnitude larger, and have a vertical downward motion. This provides the potential of partial evaporation, leading to a kinetic fractionation signal in the dexcess. Cloud drops, however, will rapidly evaporate completely as they become unstable at smaller radii, leaving no sign of kinetic fractionation in the d-excess. Furthermore, they are suspended in the atmosphere, thus allowing for equilibrium fractionation. Without the consideration of rain evaporation in addition, or other processes, the explanation of the STC case is thus not viable. What is the potential of the occurrence of rain evaporation from these stratocumulus clouds? Can you estimate how much cloud water specific humidity would have to be added to produce the negative d-excess signal, and is this consistent with the saturation specific humidity in the cloud layer? Could there potentially have been a potential for rain evaporation or ice processes in the airmass upstream earlier instead?
The Reviewer again brought up some excellent details to consider. Our calculations using the equations in Stewart likely apply to cloud droplets evaporating just like rain droplets. Similarly, we realize that the assumptions of the Worden equations are not valid either because that is for a case of a dehydrating airmass (closed system Rayleigh). However, there are 2 important

timescales to consider when exploring the influence of liquid droplet evaporation in the inversion layer. (1) The timescale at which a liquid droplet isotopically equilibrates with its surrounding vapor. (2) The speed at which droplets move through the inversion layer. We calculated the first timescale using Eqn. B5 is Bolot et al., 2013 which is ~2 seconds for a cloud droplet size of 15 microns. For our observations of vertical wind speeds, the time for a droplet to move from the bottom to the top of the inversion is 19 seconds. These calculations do indicate that cloud droplet evaporation starting in the lower inversion and finishing in the top of the inversion during the flight conditions in unlikely. However, if previous inversion conditions were colder, if the droplets were larger than 50 microns (like drizzle), or if the inversion had faster vertical wind speeds, these values could converge. We have edited the discussion of the STC flight day to reflect these new considerations. (pg 24, ln 19 – pg 25, ln 39 / pg 10, ln 17 – pg 11, ln 2)

3. Section 3.3 (DBL case) describes and interesting case of BL development, but is particularly difficult to follow. Consider reorganising the material in a more logical order, and formulate a clearer take-away in the end.
We have consolidated the DBL case study's results (originally Sect. 3.3) and discussion sections (originally Sect 4.3) so that the case study's key isotope features are identified, and their cause(s) immediately discussed. Furthermore, we have extensively revised Section 3.3 (now Section 4.3), which presents the DBL case study results.

4. The material included in the Supplement only seemed marginally useful. It is also confusing to have both an appendix and a supplement in a manuscript. Consider merging the supplement into the Appendix, keeping only Fig. S1.
This is a good suggestion. We have merged the Appendix and the important components of the Supplemental Information (SI) into the SI in order to further limit the length of the paper.

5. It is difficult to follow the description of the cases without additional context of the flight situations. Maybe Fig. 3 could be split up for each case, and supplemented by a weather chart similar to Fig. S6.
We have split up Fig 3a-c to make three plots for the three case studies (Fig 5, 8, 10) so that they can be placed closer to the text where they are being discussed. Weather charts have been added to the SI for each case studies (Fig. S5.1 – S5.3).

6. The discussion sections 4.3 and 4.4 appear repetitive to what has already been presented earlier and can be deleted.
We have consolidated the Results and Discussion sections so that discussion paragraphs directly follow their respective results sections. This reorganization has reduced repetitive parts of discussion sections 4.3 and 4.4. We have also reorganized the manuscript so that discussion of the campaign-wide observations (previously Sect 4.4, now Sect 3) now precedes discussion of the case study observations.

7. The second half of the first paragraph of the Conclusions section should be moved to the introduction/motivation.
We have made the suggested change.

8. Important studies that should be referred to are Taylor (1972, 1984), and He and Smith (1999) and Ehhalt (1975, 2005) and Tsujimura et al., 2007.
We did not focus on these studies because our primary interest was high-frequency deuterium-excess observations, but the reviewer is right that they provide great context for our work. This is why we now point to the the detailed overview of airborne water vapor isotope studies reviewed in the introduction of Sodemann et al., 2017 (pg. 3, ln. 37/ pg. 3, ln. 9).

9. I found the structure of the manuscript somewhat confusing, in that first the flights around both Washington DC and Indianapolis are presented, and then almost all analysis focuses on flights from only one site, before returning to a wider overview in section 3.4. It would be more logical for the reader to move Sec. 3.4 ahead of the case studies, and then zoom into individual aspects. Consider adding a more intuitive way to present an overview of all data than a comparison to Rayleigh in 7.
This is a great suggestion. We have followed the Reviewer's suggestion by reorganizing the manuscript so that the campaign-wide results/discussion precede the case studies' results/discussion sections. We have added a new figure (Fig. 3) which shows dD and $d^{18}O$ vs H_2O_v along every VP descent conducted during the campaign. We no longer present our results relative to Rayleigh by removing the right panel of Fig 7 (now Fig 4 post reorganization).

10. Several times in the writing, wording such as "Fig. x shows ..." is used. For conciseness, consider rephrasing this to sentences talking about what is shown in the figure, added by a figure reference "(Fig. x)".
This is a good suggestion, we have made changes where appropriate.

2 Detailed comments
P3, L8: "However, relatively few...": As far as I am aware there is only one published dataset of airborne d-excess measurements. Why the citation of Schmidt et al., 2005 here?
We have reworded the sentence and deleted the reference to Schmidt et al., 2005, which provides modeled d-excess.

P3, L34: Please state if the inlet or parts of it were heated.
We have added a sentence stating the TWVIA inlet was not heated during the calibrations. (pg 5, ln 27-28 / pg 4, ln 35-36)

P4, L9: How sensitive are the measurements to variations of cavity pressure and temperature during flight?
Once the isotope analyzer has warmed up (i.e. reached the manufacturer recommended pressure and temperature values for operation), cavity pressure and temperature only vary (1σ) by ±0.02 Torr and ±0.08°C, respectively, over a vertical profile descent on average. This is within the operating specification given by the manufacturer. (pg. 5 ln 13-15 / pg 4, ln 21-22)

P9, L21: Worden et al. 2007 formulate their models for rain evaporation (falling condensate), not cloud evaporation, see their supplementary information.
We have removed all discussion of the Worden et al., 2007 model (see our response to major comment #2 for more explanation).

P10, L10: "Rayleigh-consistent observations": Consider rephrasing in light of major comment 1
This is a great suggestion. We have renamed the RAY case study to CLR, which is now representative of the case study's clear sky conditions rather than a possible interpretation of the day's dominant isotopic process.

Fig.4: Consider adding a panel that shows more mixing lines, e.g. between the bottom and top of the inversion, or the bottom and top of the BL, how do these compare with the complete mixing line?
We have split up Fig. 4 into three figures for the three case studies (Fig. 7 CLR, Fig. 9 STC, and Fig 12 DBL). Each new case study figure has an additional panel showing mixing lines for scenarios relevant to the flight day. The new mixing panels are discussed in each case study's respective sections (Sect 4.1-4.3).

P12, L1: Consider using a standard symbol such as q or m for specific humidity or mixing ratio of water vapour, rather than H2O.
We respectfully choose to retain H_2O_v to represent water vapor mole fraction, as it is a common convention in the atmospheric chemistry field.

P14, L8: "relative to Rayleigh" rephrase as e.g. "Rayleigh model predictions"
The sentence now reflects this suggestion.

P14, L16: "d-excess switches to tracking" rephrase
This sentence has been rephrased.

P14, L13-22: hard to follow, rewrite this section for clarity
We thank the Reviewer for identifying this paragraph that could be improved. We have revised this paragraph to include a summarizing, take-away sentence, which highlights the unique d-excess characteristics of the first vertical profile flown on STC (pg 23, ln 17-20 / pg 9, ln 36-40).

P16, L6: "Differences" - difference to what is shown? Are these not absolute values?
This sentence has been rephrased.

Fig.6: How are RL and INV defined? You could provide a quantitative comparison of averaged quantities for both layers that supports their distinction.
To address this comment, we have added a sentence that reads, "We define the base of the RL using the same approach described in Section 2.4 ($d\theta/dz$ and $|d(H_2O_v)|/dz$ threshold values) for determining the base of the INV (z_{INV})."

P17, L14: Not clear what the take-away from this section is. Revise paragraph.
We thank the Reviewer for identifying this paragraph as an opportunity for improvement. We have revised this paragraph about our campaign-wide vertical profile observations. (Sect. 3, paragraph 1-2)

P17, L17: "Figure xxx shows": revise according to major comment 11
We have reworded sentences that begin with "Figure # shows…" throughout the manuscript.

P18, L12: Not clear what the take-away from this section is. Revise paragraph.
We have deleted this paragraph because we decided its inclusion does not benefit the overall story about the campaign-wide observations section.

P18, L16: Why the citation of Lee et al. (2006)? Compare Gedzelman (1988) and the discussion of the Taylor (1972) data (major comment 1).
During our consolidation of the results and discussion sections for each case study, we have removed the indicated sentence. We now discuss the possibility of Rayleigh-consistent condensation occurring upwind of the CLR measurements (see response to major comment #1). We also reference the suggested paper (pg 19, ln 17-28 / pg 8, ln 22-33)

P19, L3: The thermodynamic characteristics of the profiles are not consistent with a Rayleigh processes, even though the isotope composition may be – what is the conclusion from that finding?
We now discuss the possibility of Rayleigh-consistent condensation occurring upwind of the CLR measurements (see response to major comment #1). (pg 19, ln 17-28 / pg 8, ln 22-33)

P19, L15: How would cloud droplets be lofted but not the surrounding vapour? If vapour and droplets move together, how can non-equilibrium fractionation result?
The vapor and droplets do not necessarily have to remain in isotopic equilibrium under changing conditions, including mixing of airmasses. We have revised the indicated sentence so that cloud droplet evaporation is discussed from the framework of timescales, e.g. the time required for condensate and vapor to isotopically equilibrate vs. time required to transport a cloud droplet from the bottom to the top of the inversion. Please see our response to major comment #2 for more detail. (pg 24, ln 19 – pg 25, ln 39 / pg 10, ln 17 – pg 11, ln 2)

P20, L16-20: Consider the possibility of rain evaporation upstream (major comment 2).
We now discuss how rain droplet evaporation in dry, cold conditions upwind of the STC flight measurements could possibly explain the minimum in d-excess at the top of the inversion layer. (pg 25, ln 33-36 / pg 10, ln 36-38)

P21, L10: What relative roles could vertical motion and entrainment of dry air from aloft play in the evaporation of the cloud layer?
This is an interesting question that we believe that stable isotope observations can inform about the occurrence of cloud evaporation, but are not sure that it's possible to distinguish the driver of that evaporation (cloud drops moving into the FT versus entrainment of dry air into the cloud) using our observations downwind of clouds. This would require a sophisticated cloud microphysics model, similar to Bolot et al. (2013). Respectfully, it is outside of the scope of this paper, but an exciting future application. We do, however, cite papers that give evidence for stratocumulus cloud droplet evaporation occurring within and above the cloud layer due to differences in entrainment efficiency (pg 24, ln 36- pg 25 ln 2 / pg 10, ln 12-15).

P21, L20-29: Rephrase for clarity. Could ice-phase processes have been relevant further upstream, earlier in time?
We have rephrased the paragraph about the effect condensation in the presence of ice has on vapor d-excess for clarity. We also now include the following sentence, "It is possible, however,

that condensation under ice-supersaturated conditions occurred prior to the STC flight, and that the resulting isotopic imprint was maintained during transport to Indianapolis." (pg 26, ln 28-30 / pg 11, ln 15-17)

P22, L12: What is the Rapid Refresh Model? Could be deleted here.
Reference to the model name has been deleted.

P22, L7-34: reorganize and rewrite this section for clarity
We have revised the entire results/discussion sections related to the DBL case study to improve their clarity. (now Sect 4.3)

P22, L36: "so we look" rephrase
This phrase has been deleted as part of the manuscript reorganization.

Fig. A1: What is the reason for the large scatter between both instruments in the mid-range of humidities? Does longer averaging of the data provide a better agreement? Was the scatter similar for each of the flight? How is the scatter for the downward profiles only?
The scatter corresponds to few points relative to most of the points that show good agreement. The mid-range humidities in Fig. A1 (now Fig. S1 due to the Appendix-SI merger) correspond to vertical profiles. These few points that do not show as good agreement result from the TWVIA data being low pass filtered relative to the Picarro due to a longer residence time, as we mention in Sect 2.2.2 (SI pg 5, ln 23 / SI pg 4, ln 31).

Authors' Responses to Reviewer 2

- Author responses are indicated in blue font.
- Locations of our edits in the "strike-through" and final versions of the manuscript are provided with the following convention: ([strike-through version] pg. #, ln # / [final version] pg. #, ln #).

Major Comments

1. The results could be better distilled. The paper is quite lengthy and detailed. As a result, it is easy for key points to become buried. Usually, I would not list this as a major concern, but in this case, I found much of the critical interpretation for the analysis was lost among the long-winded descriptions of the data. It might help readers if the critical arguments and conclusions were emphasized near the beginning and/or end of each sub-section. One place where this is very much needed is in Section 3.3, which discusses the developing boundary layer case (DBL). Here, more time could be spent on the interpretation of the causes of the fascinating differences in atmospheric structure among the profiles rather than on re-describing Figure 6.
To address the Reviewer's comment, we have consolidated the case studies' results (originally Sect. 3.1-3.3) and discussion sections (originally Sect 4.1-4.3) so that each case study's key isotope features are identified, and their possible cause(s) immediately discussed. The consolidated sections are now located in Section 4.1-4.3. We have also extensively revised Section 3.3 (now Section 4.3), which presents the DBL case study results.

2. Section 4.2 is another section that is somewhat difficult to follow, largely because of confusing terminology. How do the "scenarios" relate back to the equations presented in the methods? Also, "partial evaporation" and "near complete evaporation of a semidehydrated drop" could easily be confused as one and the same. As a result, it is not at all clear which "scenario" best represents the data.
We thank the Reviewer for identifying Section 4.2 as an area that could see improvement. We have chosen to remove the cloud evaporation equations (see our response to comment #4), and by association, the paragraphs which discussed the degree of droplet evaporation under two scenarios. In their place, we have added text which evaluate the likelihood of cloud evaporation and its impact on d-excess under meteorologically-relevant time scales. We believe our changes have greatly improved the clarity of Section 4.2. (pg 24, ln 19 – pg 25, ln 39 / pg 10, ln 17 – pg 11, ln 2)

3. I am not convinced by the analysis that Rayleigh distillation is the dominant process determining the vertical isotopic structure of the boundary layer. First and foremost, there are many papers that show the contrary; a few case studies are not sufficient to prove otherwise. Previous papers that have measured water vapor isotope ratio vertical profiles in situ (and have shown profiles consistent with processes other than distillation) include He and Smith 1999, Galewsky et al 2007, Noone et al 2013, Bailey et al 2013, Sodemann et al 2017, and Kelsey et al 2018. These studies contrast, to some degree, with the early work of Ehhalt, which was re-published as Ehhalt et al 2005.

We thank the Reviewer for these suggested literature citations. We have revised our interpretation of the RAY (now CLR) case study to express that the Rayleigh-consistent

observations likely reflect the isotopic imprint of prior condensation under saturated conditions, followed by advection of this imprinted signal to the Indianapolis study site. Additionally we note that the lower free troposphere measurements appear more consistent with mixing lines, which is indicative of mixing between subsiding free troposphere air and boundary layer air. We include the some of the suggested references to support this discussion (pg 19, ln 2-28 / pg 8, ln 10-33).

Second, I am not entirely convinced that Rayleigh distillation gives the best physical interpretation for the Indianapolis "Ray" profiles. The paper argues that Rayleigh distillation is a good model when the boundary layer is dry adiabatic (and therefore that no clouds or precipitation exist). This is contrary to expectation: distillation depends on condensation and precipitation. Furthermore, other studies (see above) have shown nearly the opposite: that Rayleigh is appropriate when the boundary layer follows a moist adiabat but not when it follows a dry one. A clear exception, of course, is if the distillation occurs upwind and imprints an isotopic signature that is then advected downwind. One of the earliest papers discussing this phenomenon is Gedzelman 1988. Is it possible that advection is affecting the Indianapolis isotope ratio profiles? If so, this could make for an interesting discussion on whether moist convective processes regionally set the humidity structure of the lower atmosphere locally, which others have argued for tropical/subtropical regions (e.g. Brown et al 2008, Lee et al 2011, Bailey et al 2013).

The reviewer make an excellent point that our fight conditions during the RAY (now CLR) flights are not consistent with moist adiabatic conditions. However, the Rayleigh prediction is most consistent with our observations, compared to mixing scenarios. We have changed this discussion to indicate that observed profile is an imprint of previous airmass dehydration conditions, and cite the suggested studies (pg 19, ln 17-28 / pg 8, ln 22-33).

Third, extra care must be taken in matching data to hypothetical Rayleigh curves since these can be designed to fit many data. A good example of this is found in Noone et al 2013. Consequently, it may be difficult to truly distinguish Rayleigh from mixing processes unless the theoretical end-members are well constrained. It is not clear in the manuscript from whence the theoretical end-members for Figure 4 are derived. Some description of the assumptions made would be a valuable addition to the analysis and perhaps make the case that the Ray flights are, in fact, illustrative of (upwind?) Rayleigh distillation in a much more compelling manner.
The Reviewer makes a good point. We do note, however, that our Rayleigh curves are calculated using an objective method (Sect. 2.5; Eq (1)). The initial isotopic composition of the Rayleigh air parcel (R_o) is determined from the average observed boundary layer delta values. The equilibrium fractionation factors are calculated for the lifting condensation level temperature. We also demonstrate in Fig. S4 that varying the equilibrium fractionation factor by observed temperature does not lead to significantly different shaped Rayleigh curves. We now note that mixing endmembers are informed by actual observed delta values in different atmospheric layers (pg 10, ln 26 / pg 6, ln 26). Figure 7 now makes a direct comparison of our observations to Rayleigh theory and mixing scenarios.

4. Some care should be taken in describing the Worden et al 2007 and Stewart 1975 models and applying them to the case of stratiform clouds. Both models were designed to describe freely falling raindrops. In the original presentation of the model, Worden suggests raindrops undergo both an equilibrium fractionation and an effective fractionation, and that "this assumption is

unlikely to be valid when raindrops are small…". I note that Equation 3 substitutes a kinetic fractionation coefficient in place of the effective factor. What impact does this have? How does the model work if the assumptions of large falling drops are violated? The Worden model describes isotopic depletion with a loss of water from an air parcel. How can it be applied to describe a gain of moisture by the atmosphere? I have similar concerns with use of the Stewart model and would like to see more justification for these model choices for the case of stratiform clouds. Also, the equations presented from Stewart are from Equations 2 and 3 of the original paper, and there is an alpha missing in the denominator of the beta equation.
We have opted to remove the Worden et al, 2007 and Stewart, 1975 equations from the paper for the reasons that both reviewers mention. Instead of calculating the impact different degrees of evaporation could have on surrounding vapor, we have reframed this discussion by evaluating the likelihood of cloud droplet evaporation impacts based on transport and equilibration time scales. We now show that a droplet would isotopically equilibrate with surrounding vapor faster than the time required for transport of a droplet from the bottom to the top of the inversion (Equation B5 in Bolot et al., 2013). These calculations suggest cloud droplet evaporation may not be responsible for the observed d-excess minimum during the STC flight. However, we maintain that a negative d-excess signal resulting from cloud or rain droplet evaporation could have been transported from an area upwind of the STC measurements. (pg 24, ln 19 – pg 25, ln 39 / pg 10, ln 17 – pg 11, ln 2)

5. I found it difficult to identify the case studies in the flight figures due to distinct nomenclature. The figures use numbers, the text uses pseudonyms, and only the table provides both these plus dates. I would recommend one naming convention, preferably related to flight number or date. The reason being that a priori, it seems difficult to know whether the "Ray" days will really be Rayleigh-like.
The Reviewer brings up an excellent point. We have deleted any reference to research flight codes (RF#), and now refer to the flights by date. We maintain pseudonyms for the case study flights, but we have made sure that figures include both the flight date and case study pseudonym where appropriate. We have renamed the RAY case study to CLR (for clear skies) so that the pseudonym characterizes the day's meteorology, rather than a possible interpretation of the isotopologue data.

6. The Isotope Theory section suggests there are "three common ways the isotopic composition of the atmospheric H2Ov can change." I would have thought these would be condensation, evaporation, and mixing. Rayleigh distillation is just an example model for condensation processes. Similarly, cloud evaporation is just one type of evaporation that can affect the atmosphere's isotopic composition.
We have reworded this section to indicate that we employ different models to represent condensation and mixing processes. Please refer to our response to comment #4 for our explanation for removing the cloud evaporation equations. (pg 9, ln 24-26 / pg 6, ln 1-4)

7. I have some trouble understanding how partial cloud evaporation can cause a minimum of deuterium excess near the inversion layer. Evaporation tends to favor the diffusion of the D relative to 18O. Why wouldn't partial evaporation result in an enrichment of the surrounding vapor? Perhaps I am missing something, but my hunch is most readers will also have this

impression. It might be worth explaining the physical underpinning behind these conclusions in greater depth, perhaps in Sections 4.2 or 4.4.
The Reviewer is correct that evaporation (from an infinitely large source) typically imparts a positive d-excess signal on the surrounding vapor. This is why we believe cloud evaporation to be responsible for the slight increase in d-excess in the middle of the inversion (Fig. 6b). As a droplet evaporates, its own d-excess signal becomes more negative, so subsequent complete evaporation of the droplet in another region would act to decrease the surrounding vapor d-excess (Aemisegger et al., 2015; Sodemann et al., 2017). We also now include a calculation (Bolot et al., 2013) showing that a droplet would isotopically equilibrate with surrounding vapor faster than the time a droplet would be transported from the bottom of the inversion to the top of the inversion. This calculation indicates cloud evaporation during the STC flight may not be responsible for the observed d-excess minimum. We do, however, maintain that evaporation of cloud/rain droplets upwind might have caused the d-excess minimum. We support this possible explanation with references that show that stratocumulus cloud droplet evaporation occurs at different altitude in and above the cloud layer, and that the inversion layer above stratocumulus clouds are not homogeneous in terms of depth or thermodynamic properties. (pg 24, ln 19 – pg 25, ln 39 / pg 10, ln 17 – pg 11, ln 2)

8. The calibration documentation is quite thorough and comprehensive. I was prompted, however, to ask a few follow up questions regarding the variations in concentration dependence shown for dD. Is it possible one would get a different answer if concentration biases were adjusted first and VSMOW-scaling applied separately? It also appears that there are higher errors in dD at low isotopic values at all water vapor concentrations, not just at the low concentrations. Is it possible that lower precision at low isotope ratios causes the appearance of "irreproducibility" in the concentration dependence?
Our calibration procedure does begin with concentration-dependence corrections (Sect. S2; note that the Appendix has been merged with the SI). We determined that VSMOW scaling of the concentration dependence-corrected delta values was not necessary (Figure S2.3). The Reviewer makes an interesting point about the apparent dD irreproducibility. However, we note that the "irreproducibility" at mid-range humidities (3000-8000 ppmv) only lie on one side of the correction curve (Fig. S2.2b), so it is an offset. On the other hand, variability on either side of the correction curve is observed for drier conditions (550-3000 ppmv; Fig. S2.2b), which indicates the low precision idea could be a possible explanation. We note that the uncertainty is only consequential for very low H_2O_v mole fractions, where these depleted delta values are observed. We have added a sentence discussing the possible low precision and offset ideas (strike-through SI: pg 5, ln 5 / final SI: pg 5, ln 7).

Minor comments
Page 1 Line 35 – no need for ":" after "include"
The ":" has been removed.

Page 2 Line 10 –I had trouble distinguishing the conditions at a moisture source region from "surface H2Ov sources." Perhaps it might be more clear to say "an air parcel's moisture source region, including the geography of the source and its meteorological conditions?"
This sentence has been changed to reflect the Reviewer's suggestion.

Page 2 Line 19 – I think "further exchange" is meant instead of "equilibrium?"
"Equilibrium" has been replaced by "further exchange".

Page 3 Line 3 – I might remove "point in" before time, since I initially confused "point" with space.
"Point in" has been removed.

Page 3 Line 6 – Perhaps best to say "higher…resolution" since aircraft is not as high resolution as slower-moving platforms.
This is a good point, "high" has been changed to "higher".

Page 3 Line 11 – Perhaps best to say that "measurements of vertical profiles" were conducted.
We have incorporated this suggestion.

Page 4 Line 28 – Perhaps "produce" for "emit?"
Thank you for this suggestion, we have replaced "emit" with "produce".

Page 6 Figure 2 – Could the three analyzed flights be emphasized, perhaps by making the other flight lines dashed?
This is a good suggestion, the case study flight paths are now indicated with solid lines, and all other flight paths are indicated with dashed lines.

Page 7 Table 1 – Table caption/title should provide some explanation of the "codes" and what is meant by "support study"
Per the Reviewer's comment #5, we have modified the flights codes so that the flights are identified by their date.

Page 9 Line 13 – One of many examples of the great care that was taken in the analysis

Page 9 Line 31 – This appears to be the only place where "q" is used instead of "H2Ov." Consistency would help.
Thank you for catching this. As noted in our response to major comment #4, we no longer include the Worden et al., 2007 equation that the Reviewer is referencing.

Page 10 Equations – This appears to be the only place "Rvap" is used instead of "Rv." Again, consistency would help.
Thank you for catching this oversight. As noted in our response to major comment #4, we have removed the Stewart, 1975 equation that the Reviewer is referencing.

Page 11 Figure 4 – All the lines are "solid," thus it might be best to say the "black" line to distinguish it from the "pink" one. Also, I don't fully understand how the average mixing ratio is given by a gray envelope. Shouldn't the average be a point?
Thank you for these suggestions. We have replaced "solid" with "black", and we have clarified that the grey envelope indicates the inversion layer, which is defined by the average H_2O_v mole fraction observed at z_{INV} and z_{FT} during the vertical profiles. (Fig 4 has been split into three figures for each of the case studies, Fig 7- CLR; Fig 9 – STC; Fig 12 – DBL)

Page 12 Line 7+ - Here is an example where it's easy for the reader to become lost in all the number-reporting. This paragraph would greatly benefit from a sentence that provides a bit more of a picture of what is going on physically.
Thank you for this suggestion. We have added text to identify the important meteorological characteristics of each atmospheric layer on this day, and also decreased the amount of number-reporting. (pg 17, ln 6-19 / pg 7, ln 35 – pg 8, ln 9)

Page 12 Line 18 – I might say "predictions" instead of "theory."
We have made this substitution.

Page 13 Figure 5 – Caption should explain what the shaded area for the inversion is and what the envelopes around the profiles are.
The caption now indicates that the inversion layer (previously grey bands, now blue bands) lies between z_{FT} and z_{INV}, and that the shading around the isotope VP measurements correspond to total measurement uncertainty. (Now Fig 6)

Page 14 Line 6 – How was the average range of the inversion calculated? From how many days or which days of data?
Similar to our changes to the caption of Fig. 4 (now Fig 7, 9 and 12) and Fig. 5 (now Fig. 6), we now specify that the bounds of the inversion layer range, which are unique to each flight, are defined by the average H_2O_v mole fractions observed at z_{FT} and z_{INV} for each flight.

Page 14 Line 16 – I'm not sure I agree that the data start "tracking" the mixing line. There just aren't enough points for me to be convinced of that. Perhaps "approaches" the mixing line?
We have made this substitution.

Page 14 Line 26 – This seems like an important argument explaining how is STC different from Ray, and yet it is buried halfway down the page. Perhaps it could be moved up in the sub-section.
We have moved this sentence to the second paragraph of Sect 4.2. (pg 21, ln 7 / pg 9, ln 18)

Page 15 Figure 6 – Most axes appear consistent across panels except for theta. Was this purposeful?
Good catch! We have modified the theta range of Fig 6a (now Fig. 11a) for consistency.

Page 17 subtitle – I'm not really sure what "general observations" means. Would "observations from other flights" be more descriptive?
We have renamed this subsection: "Airborne campaign observations of H_2O_v isotopologues in the lower troposphere". (Now Sect. 3 title)

Page 17 Line 21 – which observations are used here for this argument?
We now specify that the "DBL" case study observations are being discussed in this sentence.

Page 19 Line 19 – A sentence or couple words reminding the reader what "Scenario 1" is would be appreciated.

We have revised the STC discussion paragraphs (see our response to major comment #2), and no longer reference cloud evaporation scenarios 1 and 2.

Page 19 Line 22 – I think "drier" is meant.
Great catch, we did mean "drier". During our revision of this section, we have deleted "drier".

Page 21 Figure 9 – I would recommend dots (or some symbol) instead of vertical lines to indicate the values of dxs expected. Otherwise, it is not clear that the reader should look for the intersection of the various lines.
We have revised Section 4.2 per major comment #2, and in doing so, we have removed Figure 9 from the manuscript.

Page 22 Line 24 – Excellent synthesis sentence: highlights the key point nicely.

Page 22 Line 36 – I disagree that these are some of the few data of this kind. There are quite a few studies that are not cited in this work. Please see my major comments for ideas.
We have reworded this sentence to express that there are few studies that report vertical profiles of d-excess.

Page 23 Line 24 – Kelsey et al 2018 also report dxs profiles.
Thank you for this suggestion, we now reference the Kelsey et al, 2018 study here, and in the introduction.

Page 24 Line 4 – Perhaps "investigate" for "interrogate."
We have made the suggested replacement.

Page 27 Line 5 – "To check calibration…" against? of?
We have rephrased this sentence.

Page 30 Line 14 – The notation seems to change here. Should all isotopologues have subscript "v?"
Thank you for catching this, we have added missing subscripted *v*'s to the isotopologue ratios. (Now in the SI, Section S6)

Page 31 Figure D1 – At first I thought the black square was a symbol in the legend. It might be more clear simply to use the caption to say that the striped region shows the expected range for the observations, or something to that effect.
Thank you for this observation. We have modified the legend to better represent the slanted line region, and we have added a sentence to the caption describing the saturation values that the slanted lines represent. (Now in the SI, Figure S6)

Vertical profile observations of water vapor deuterium excess in the lower troposphere

Olivia E. Salmon[1†], Lisa R. Welp[2,3], Michael Baldwin[2,3], Kristian Hajny[1], Brian H. Stirm[4], Paul B. Shepson[*1,2,3]

[1]Department of Chemistry, Purdue University, 560 Oval Dr, West Lafayette, IN, 47907, USA
[2]Department of Earth, Atmospheric, and Planetary Sciences, Purdue University, 550 Lafayette St, West Lafayette, IN, 47907, USA
[3]Purdue Climate Change Research Center, 203 S Martin Jischke Dr, West Lafayette, IN, 47907, USA
[4]School of Aviation and Transportation Technology, Purdue University, 1401 Aviation Dr, West Lafayette, IN, 47907, USA
†Now at Lake Michigan Air Directors Consortium, 101 S Webster St, Madison, WI, 53703, USA
*Now at School of Marine and Atmospheric Sciences, Stony Brook University, 145 Endeavour Hall, Stony Brook, NY, 11794, USA

Correspondence to: Lisa R. Welp (lwelp@purdue.edu)

Abstract. We use airborne measurements of water vapor (H_2O_v) stable isotopologues ~~pic~~ ~~vertical profile measurements~~ and complementary meteorological observations to examine how boundary layer dynamics, cloud processing, and atmospheric mixing ~~processes~~ influence the vertical structure of δD, $\delta^{18}O$, and deuterium-excess (d-excess = $\delta D - 8\times\delta^{18}O$) in the boundary layer, inversion layer, and lower free troposphere. ~~Airborne measurements of water vapor (H_2O_v) stable isotopologues~~Flights were conducted around two continental U.S. cities in February – March 2016~~. Nine research flights were designed to characterize the δD, $\delta^{18}O$, and d-excess~~ and included vertical profiles extending from near the surface to ≤2 km. We examine observations from three unique case study flights in detail. One case study shows observations ~~H_2O_v isotopologue vertical profiles~~ that are consistent with Rayleigh isotopic distillation theory coinciding with clear skies, dry adiabatic lapse rates within the boundary layer, and relatively constant vertical profiles of wind speed and wind direction. This suggests that the air mass retained the isotopic fingerprint of dehydration during moist adiabatic processes upwind of the study area. Also, observed d-excess values in the free troposphere were sometimes ~~observed~~ larger than Rayleigh theory predicts, which may indicate mixing of extremely dehydrated air from higher altitudes. The two remaining case studies show ~~that H_2O_v~~ isotopic ~~signatures above the boundary layer are sensitive to cloud processes and complex air mass mixing patterns. These two case studies indicate~~ anomalies in the d-excess signature relative to Rayleigh theory, ~~such as low d-excess values at the interface of the inversion layer and the free troposphere, which is possibly indicative of~~and indicate cloud ~~evaporation~~processes and complex boundary layer development. The most notable case study with stratocumulus clouds present had extremely low (negative) d-excess values at the interface of the inversion layer and the free troposphere, which is possibly indicative of cloud or rain droplet evaporation. We discuss how ~~We discuss possible explanations for the observed d-excess anomalies, such as cloud evaporation, wind shear, and vertical mixing. I~~*in situ* H_2O_v stable isotope measurements, and d-excess in particular, could be useful for improving our understanding of moisture processing and transport mixing occurring between the boundary layer, inversion layer, and free troposphere.

1 Introduction

Water vapor (H_2O_v) in the lower troposphere modulates processes including cloud formation, precipitation, severe weather development, atmospheric circulation, radiative forcing, and climate feedbacks (Held and Soden, 2000; Kunkel et al., 2012; Tompkins, 2001; Trapp et al., 2007; Trenberth, 2011). Accurately representing these dynamic, mesoscale processes in models can be difficult, and efforts to improve parameterizations are on-going (Gerber et al., 2013; de Lozar and Melledo, 2015; Park et al., 2017; Wood, 2012; Yamaguchi and Feingold, 2013). Some active areas of research include~~:~~ quantifying the inversion layer entrainment flux (Wood, 2012), refining entrainment-cloud evaporation relationships (Gerber et al., 2013; Yamaguchi and Feingold, 2013), and updating cloud evaporation schemes with new cloud classes (Park et al., 2017).

Free troposphere entrainment and cloud evaporation influence the maintenance of the cloud layer, which in turn influences radiative forcing (Gerber et al., 2013; Yamaguchi and Feingold, 2013). The nature of H_2O_v as a climate feedback agent adds further complexity to our understanding of H_2O_v's role in weather. Anthropogenic greenhouse gas emissions have resulted in increasing global temperatures, enhanced evaporation from soil and the oceans, and higher atmospheric concentrations of H_2O_v, the dominant absorber of infrared radiation (Held and Soden, 2006; Hurley and Galewsky, 2010; Willett et al., 2007). Warmer temperatures and more humid conditions have caused a shift towards less frequent, but more intense precipitation events, increasing the risk of both floods and droughts (Roque-Malo and Kumar, 2017; Trenberth, 2011). H_2O_v also modulates production of the dominant atmospheric oxidant, the hydroxyl radical (Thompson, 1992). Thus, accurately representing H_2O_v in mesoscale processes is of great importance in a warming world.

H_2O_v stable isotopologue measurements are a potential tool to inform our understanding of the distribution and dynamics of H_2O_v in the lower troposphere (see review by Galewsky et al., 2016). H_2O_v stable isotopologue ratios, i.e. the ratio of heavy (HDO or $H_2{}^{18}O$) to light ($H_2{}^{16}O$) molecules, capture~~s~~ the origin and mixing of moisture sources as well as the condensation and cloud processes that modified that moisture. The δ-notation indicates the sample's heavy-to-light isotope ratio reported relative to an international standard ($\delta = R_{sample}/R_{standard} - 1$), where δ is multiplied by 1000 to report in units of per mil (‰). Both equilibrium fractionation, which separates heavy and light ~~isotopolougues~~isotopologues based on their unique vapour-pressure differences, and kinetic fractionation, which is controlled by differences in diffusion rates of the isotopologues, ~~lead to differentchanges to~~modulate the isotopic signature~~s~~ ~~in the~~ of atmospheric H_2O_v~~e~~ (Dansgaard, 1964). Isotopic fractionation processes act to enrich/deplete both HDO and $H_2{}^{18}O$ relative to $H_2{}^{16}O$ in atmospheric waters, resulting in co-varying δD and $\delta^{18}O$ signatures. The Rayleigh distillation model describes the equilibrium fractionation between vapour and condensation that dominates the variability of H_2O_v isotopes in the troposphere. This model can be used to calculate the degree to which condensate is removed from an air parcel as it cools, such as when it ~~is undergoes ascent~~ascends from the surface to higher altitudes. Variability in δD and $\delta^{18}O$ often co-vary by a factor of approximately 8 because the ratio of the δD and $\delta^{18}O$ equilibrium fractionation factors is approximately 8:1 at typical surface temperatures (Dansgaard, 1964). The second-order isotope parameter deuterium excess (d-excess = $\delta D - 8\times\delta^{18}O$) can be used to help identify the non-equilibrium kinetic fractionation processes. For example, remoistening of the atmosphere by raindrop evaporation imparts a kinetic isotopic fingerprint on H_2O_v d-excess (Field et al. 2010; Lawrence et al. 2004; Risi et al. 2008; Worden et al. 2007; Wright et al. 2009).

Tropospheric vapor d-excess measurements may provide important information about cloud microphysics, convection processes, precipitation recycling, and free troposphere (FT) entrainment. ~~H_2O_v stable isotopologue ratios, i.e. the ratio of heavy (HDO or $H_2{}^{18}O$) to light ($H_2{}^{16}O$) molecules, can contain information about the~~ Local-scale studies have examined the role of moisture source, condensation history, ~~meteorological conditions at an air parcel's moisture source~~and land surface

evapotranspiration~~ region~~ on d-excess signatures~~, including the geography of the source and its meteorological conditions surface H_2O_v sources, like evapotranspiration, as well as its temperature-dependent phase change history since that point~~ (Benetti et al., 2014; Delattre et al., 2015; Kelsey et al., 2018; Lai and Ehleringer, 2011; Uemura et al., 2008; Welp et al., 2012). ~~The δ-notation indicates the sample's heavy-to-light isotope ratio reported relative to an international standard ($\delta = R_{sample}/R_{standard} - 1$), where δ is commonly multiplied by 1000 to report in units of per mil (‰).~~

~~Isotopic fractionation processes act to enrich/deplete both HDO and $H_2{}^{18}O$ relative to $H_2{}^{16}O$ in atmospheric waters, resulting in co-varying δD and $\delta^{18}O$ signatures. Rayleigh distillation theory can be used to calculate the degree of equilibrium fractionation that occurs when condensate is removed from an air parcel as it cools, such as when it is undergoes ascent from the surface to higher altitudes. Rayleigh theory assumes that when saturation is reached, the condensate is removed immediately from the system via precipitation, thus no equilibrium further exchange occurs between the two phases. The second-order isotope parameter deuterium excess (d-excess = $\delta D - 8 \bullet \delta^{18}O$) can be used to identify the type of fractionation occurring, equilibrium or kinetic, given that the ratio of the δD and $\delta^{18}O$ equilibrium fractionation factors is approximately 8:1 at typical surface-level temperatures (Dansgaard, 1964). The ratio of the δD to $\delta^{18}O$ kinetic fractionation factors is typically less than 8 and decreases with decreasing relative humidity.~~

~~Observations of d-excess have been used to deduce meteorological conditions at the evaporation source, assuming it is a conservative tracer not changed by transport and rainout processes (Benetti et al., 2014; Delattre et al., 2015; Steen-Larsen et al., 2014; Uemura et al., 2008), but there is also evidence that d-excess is not a conserved tracer of evaporative origin if other significant sources of vapor exist, especially outside of the marine environment (Aemisegger et al., 2014; Gorski et al., 2015; Griffis et al., 2016; Fiorella et al., 2018, Parkes et al., 2017; Welp et al., 2012). For example, the unique d-excess signature of combustion-derived H_2O_v has been used to quantify the contribution of combustion emissions to boundary layer vapor (Fiorella, et al., 2018; Gorski et al., 2015), and several studies have demonstrated the influence of sublimation, vapor deposition, and land surface evapotranspiration on the atmospheric H_2O_v d-excess signature (Aemisegger et al., 2014; Casado et al., 2016; Galewsky, 2015; Griffis et al., 2016; Lai and Ehleringer, 2011; Lowenthal et al., 2016; Moore et al., 2016; Parkes et al., 2017; Schmidt et al., 2005; Samuels-Crow et al., 2014; Welp et al., 2012).~~

~~Airborne d-excess measurements may provide information about cloud processes, precipitation recycling, FT entrainment, and more generally, the vertical structure characteristics of d-excess over different land cover and in different seasons.~~ Measurements of d-excess have been used to estimate below-cloud precipitation evaporation (Aemisegger et al., 2015; Froehlich et al., 2008; Wang et al., 2016), and mixing between the boundary layer (BL) and~~ free troposphere (~~FT~~)~~ from stationary platforms near the surface or at high-altitude mountain sites (Bailey et al., 2015; Benetti et al., 2015; 2018; Froehlich et al., 2008; Galewsky, 2015; Lowenthal et al., 2016; Samuels-Crow et al., 2014). Kelsey et al. (2018) conducted mobile traverses along leeward and windward slope roads of a mountain in an instrumented vehicle to report vertical profiles of d-excess. While ~~some~~ high-elevation surface monitoring ~~sites~~ has~~ve~~ the advantage of sampling BL and FT air over a diurnal cycle, ~~they~~ it does not provide a complete picture of the H_2O_v isotope vertical profile (VP) at a discrete ~~point in~~ time. Satellite measurements, which can provide discrete VP measurements, currently only ~~currently~~ provide middle troposphere δD profiles (Herman et al., 2014; Worden et al., 2012). Airborne platforms are capable of δD, $\delta^{18}O$, and d-excess VP measurements at higher spatiotemporal resolution, and have been conducted since the 1960s extending from the lower troposphere to the stratosphere to investigate a variety of ~~science~~ scientific questions (overview in Sodemann et al. (2017))~~)~~. ~~However, relatively few~~~~d~~Due to either ~~the~~ study~~'s~~ objectives or limitations of the instrumentation (Dyroff et al., 2015; Herman et al., 2014), however, only one airborne H_2O_v isotope study~~ies~~, to our knowledge,

has~~ve~~ reported d-excess measurements in the lower troposphere to provide high vertical resolution snapshots at discrete time points in the boundary later (~~Schmidt et al., 2005;~~ Sodemann et al., 2017)~~, due to either the study's objective or limitations of the instrumentation (Dyroff et al., 2015; Herman et al., 2014)~~. Additional airborne d-excess observations may improve our understanding of the role that cloud processes and convection have on determining the moisture distribution of the troposphere (Noone, 2012; Bolot et al., 2013).~~Our stable H_2O_v isotope measurements over two continental sites is a starting point in filling the field's gap in understanding variability in the lower troposphere d-excess profile, and what it reveals about lower troposphere moisture processing on relatively small regional scales.~~

In this study~~,~~ we present stable H_2O_v isotope measurements over two continental sites. These measurements provide a unique data set for understanding variability in the lower troposphere d-excess profile, and what it reveals about lower troposphere moisture processing on relatively small regional scales. H_2O_v stable isotope VP measurements were conducted in the lower troposphere during four flights around the Washington, D.C.-Baltimore, MD area in February 2016 and during five flights around the Indianapolis, IN metropolitan area in March 2016. We compare and contrast observations of the unique vertical structure of δD, $\delta^{18}O$, and d-excess from three representative case study days. The case studies provide information about meteorological conditions that produce H_2O_v isotopic VP profiles ~~consistent with~~~~consistent with a memory of~~ indicative of past Rayleigh ~~distillation~~dehydration of the airmass ~~theory~~ and those where other processes must explain the observations. The case study observations reveal d-excess features unique to ~~stratocumulus cloud~~cloud droplet or rain droplet evaporation and show the influence of synoptic weather patterns and urban versus rural differences on BL development. Interpretations of case study VPs are supported with observations from the remaining flight days in Washington, D.C.-Baltimore and Indianapolis areas.

2 Methods

2.1 Study sites

Flights were conducted around the Washington, D.C.-Baltimore, MD area in February 2016 and around Indianapolis in March 2016. Washington, D.C.-Baltimore~~-~~ is a metropolitan area of 9.8 million residents that includes the District of Columbia and ~~encompassing~~ encompasses parts of Maryland, Virginia, West Virginia, and Pennsylvania (U.S. Census Bureau, 2018). The Appalachian Mountains lie to the west of Washington, D.C.-Baltimore, and the Chesapeake Bay and the Atlantic Ocean lie to the east side of Washington, D.C.-Baltimore. By contrast, Indianapolis has a population of 2.0 million and is relatively isolated from other metropolitan areas by agricultural fields (U.S. Census Bureau, 2018). The closest large body of water to Indianapolis is Lake Michigan, over 200 km to the north.

2.2 Instrumentation

2.2.1 Airborne Laboratory for Atmospheric Research (ALAR)

The Purdue Airborne Laboratory for Atmospheric Research (ALAR) is a modified twin-engine ~~Beachcraft~~ Beechcraft Duchess aircraft. The ALAR's two rear passenger seats have been removed to make room for scientific instrumentation. Ambient air at the nose of the aircraft is pulled through a forward-facing unheated 5-cm diameter PFA Teflon inlet called the "main manifold" at a flow rate of 1840 L min^{-1} using a blower installed at the rear of the aircraft. Residence time in the main manifold is ≤0.1 second. Instruments sample from the main manifold with individual Swagelok "T" connections and Teflon sampling lines. The Purdue ALAR is equipped with a global positioning and internal navigation system (GPS/INS) for 50 Hz geopositional measurements and a Best Air Turbulence (BAT) probe for 50 Hz three-dimensional winds and pressure measurements (Crawford

and Dobosy, 1992; Garman et al., 2006; 2008). Temperature measurements are made with a microbead thermistor installed in the center pressure port of the BAT probe (Garman, 2009). Although not the focus of this study, measurements of carbon dioxide, methane, and H_2O_v mole fraction were made with a Picarro G2301-m cavity ringdown spectrometer. The Picarro data frequency was 0.5 Hz and the flow rate was 850 sccm. This system provides an independent evaluation of H_2O_v mole fraction measurements by the isotope analyser described in the next section. A full description of the ALAR instrumentation suite has been provided by Salmon et al. (2017).

2.2.2 Water vapor mixing ratio and stable isotope measurements

H_2O_v, δD and $\delta^{18}O$ measurements (1 Hz) were made with a Los Gatos Research, Inc. (LGR) Triple Water Vapor Isotope Analyzer (TWVIA; model: 911-0034). The TWVIA was configured as a rack-mount, extended-range model, operating with an internal cell pressure of 80 Torr, and is suggested by the manufacturer for isotopic measurements over the H_2O_v mole fraction range from 4,000 – 60,000 ppmv. The ~~analyser~~ analyzer can make measurements at H_2O_v mole fractions below 4,000 ppmv, but the instrument precision worsens (discussed below). The TWVIA sampled ambient air from the main manifold at a flow rate of 500 sccm using the analyzer's internal pump. Cavity pressure and temperature were observed to vary (1σ) by ±0.02 Torr and ±0.08°C, respectively, over a vertical profile descent on average, which is within the operating specification given by the manufacturer. Measurements of H_2O_v, δD, and $\delta^{18}O$ were identically lag adjusted for the sample residence time (average: 8 s) to match geopositional and meteorological measurements. Depending on the ambient air temperature, the cabin of the aircraft was heated to prevent condensation inside tubing and for the comfort of the pilot and mission scientist.

H_2O_v mole fractions reported by the LGR TWVIA and the Picarro instrument were calibrated on the ground (not in flight) throughout the campaign (on 7 and 17 March 2016) using a LI-COR dewpoint generator (model: LI-610) over the H_2O_v mole fraction range from 7,000 – 12,000 ppmv. This H_2O_v mole fraction range corresponds to saturation vapor pressures for temperatures ranging from approximately 3°C – 10°C. The LGR TWVIA (and Picarro) H_2O_v mole fraction calibration curve slope, y-intercept, and R^2 value are 0.9845 (0.94), -280 ppmv (-200 ppmv), and 0.99978 (0.99895), respectively. ~~Figure A1 shows that t~~The calibrated H_2O_v mole fractions from the Picarro and LGR analysers were consistent in flight (Fig. S1). LGR H_2O_v measurements are low-pass filtered relative to the Picarro measurements due to the longer LGR residence time.

The LGR TWVIA isotopic measurements were calibrated in the lab for H_2O_v concentration dependence before and after the field campaign using an LGR Water Vapor Isotope Standard Source (WVISS; model: 908-0004-9003) with five standards ranging in isotope enrichment from -39.9‰ to -573.7‰ in δD and -8.7‰ to -76.2‰ in $\delta^{18}O$ (Table ~~B1~~S2). Neither the Teflon sampling line between the TWVISS and TWVIA, nor the TWVIA inlet were heated. The range in the standards' δ values brackets the range of δ values measured during the campaign. The concentration dependence was characterized over the H_2O_v mole fraction range from 550 ppmv – 14,000 ppmv, which corresponds to the lowest H_2O_v mole fraction the WVISS could consistently ~~emit~~ produce (~~Appendix B~~Section S2) and the highest H_2O_v mole fraction observed during the research flights. The TWVIA's H_2O_v concentration dependence was monitored between January 2016 and June 2017, with no appreciable instrument drift observed. H_2O_v concentration-dependence calibration and residual curves are provided in Fig. S2.~~B~~1 ($\delta^{18}O$) and ~~B2~~Fig. S2.2 (δD), along with a discussion of the non-linear calibration curve line fitting (~~Appendix B~~Section S2). There was no need for an additional correction to normalize to the VSMOW-SLAP (Vienna Standard Mean Ocean Water – Standard Light Antarctic Precipitation) scale (discussed in ~~Appendix B~~Section S2; Fig. S2.3). Discussion of the instrument precision and calibration uncertainties are provided in ~~Appendix C~~Section S3. ~~Instrument precision and concentration-dependence calibration uncertainties are summed in quadrature to yield the total uncertainty in δD, $\delta^{18}O$, and d-excess. Figure 1 shows the total uncertainty in δD, $\delta^{18}O$, and d-excess versus H_2O_v.~~ Total u~~U~~ncertainties, the quadrature sums of instrument precision and calibration uncertainties, increase as H_2O_v

mole fraction decreases below 4,000 ppmv (Fig. 1). Flight measurements of δD, $\delta^{18}O$, and d-excess reported here are smoothed using a 20-second moving average which corresponds to the time required for the TWVIA-reported δ values to stabilize after a change in the sample's H_2O_v mole fraction or isotopic signature (~~Appendix~~ Section S3~~C~~).

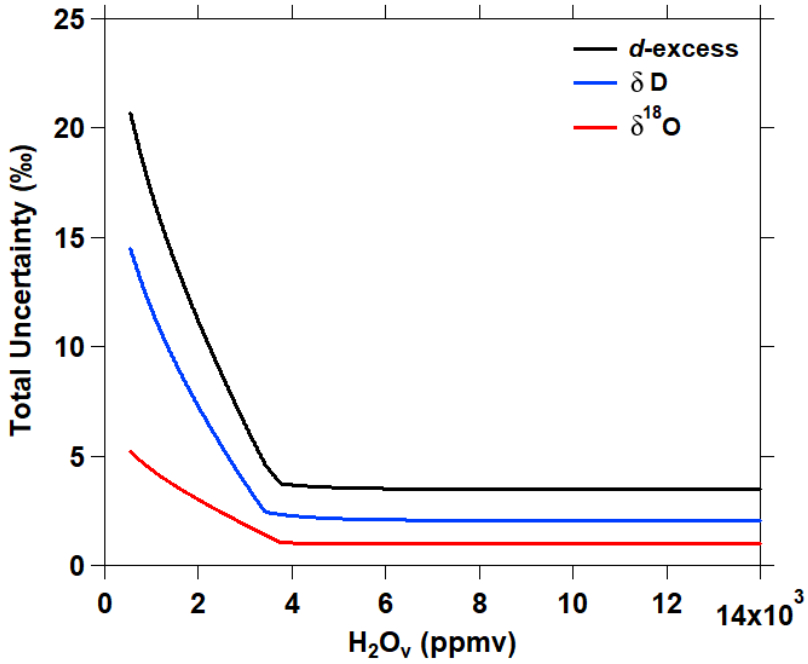

Figure 1: Total uncertainty of δD, $\delta^{18}O$, and d-excess over the range of H_2O_v mole fractions observed in flight.

2.3 Flight design

Nine daytime research flights were conducted around Washington, D.C.-Baltimore and Indianapolis in February and March of 2016 (Table 1; Fig. 2). Flight paths were designed to maximize the number of vertical profiles (VPs) conducted while also characterizing upwind/downwind gradients in H_2O_v isotopic signature. VPs were sometimes conducted in a spiral pattern to limit the horizontal spatial coverage of the measurements, while other VPs were conducted in a sawtooth pattern ("porpoising"; Gerber et al., 2013) between the BL and FT. The aircraft flew up to ~1600 m above sea level (msl) on average during the VPs. Only data collected on the descents of the VPs, when sampled air transitions from relatively dry to relatively humid, are presented here to minimize the potential influence of memory effects. However, similar features were observed on the ascents and descents. The number of VPs (Table 1) conducted on each flight was limited by air traffic and restricted air space (which was worse for the Washington, D.C.-Baltimore study site), cloud cover, and available flight time. The research aircraft typically does not fly through clouds during experimental flights as the BAT probe has electronics exposed to air. Flights included other maneuvers, such as transects conducted upwind, intersecting, and downwind of the urban centers, the interpretation of which is beyond the scope of this paper (Fig. 2).

~~Figure 2 shows the flight paths conducted around Washington, D.C. Baltimore and Indianapolis. Specific flight dates and times are provided in Table 1. We focus on three particular daytime experiments conducted around Indianapolis as representative case studies based on their unique features and the consistency and height of the vertical profiles (Table 1). H_2O_v isotope measurements on March 6 (RAY) appear consistent with Rayleigh distillation theory, the observations on March 4 (STC) may reflect moisture processing in a stratocumulus topped BL, and the March 18 (DBL) observations may reveal differences in urban versus rural BL development and the influence of changing synoptic conditions. Conclusions about the processes influencing the~~

~~isotopic features observed during the case studies are supported by measurements from the remaining Washington, D.C. and Indianapolis flights (Table 1).~~

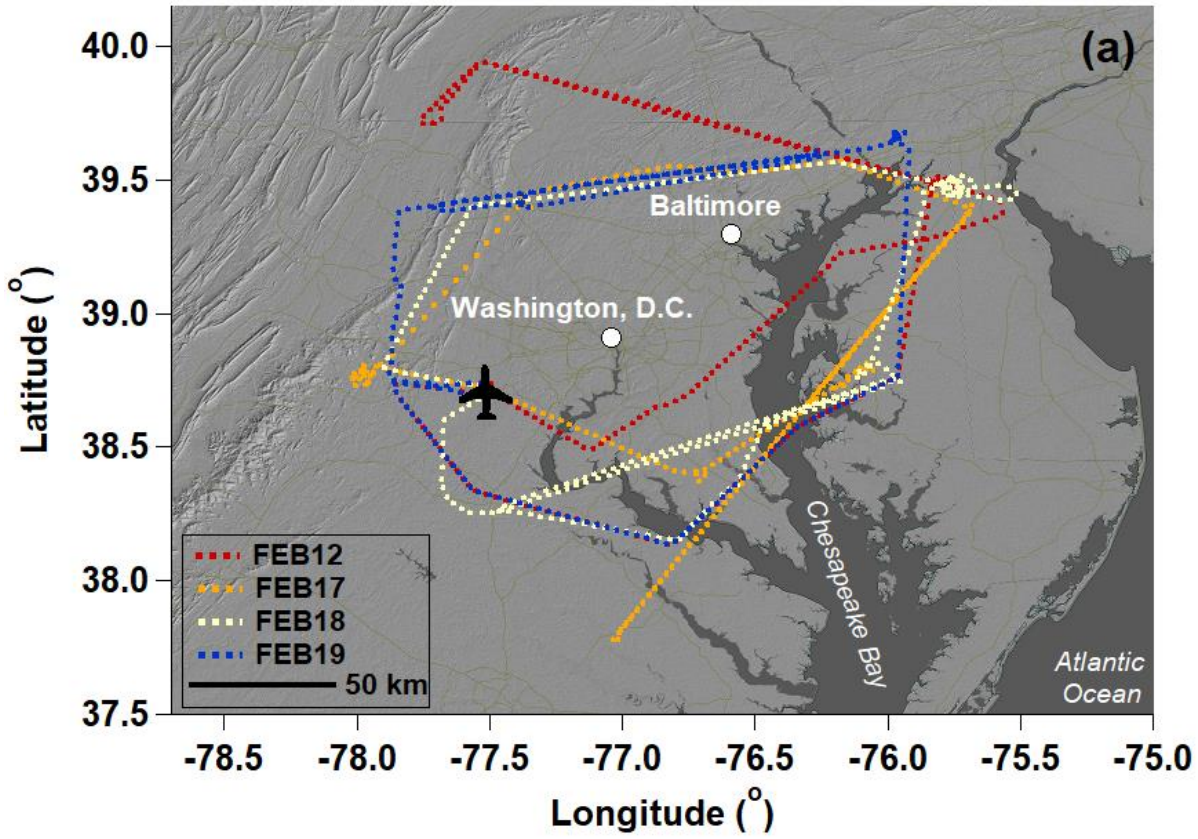

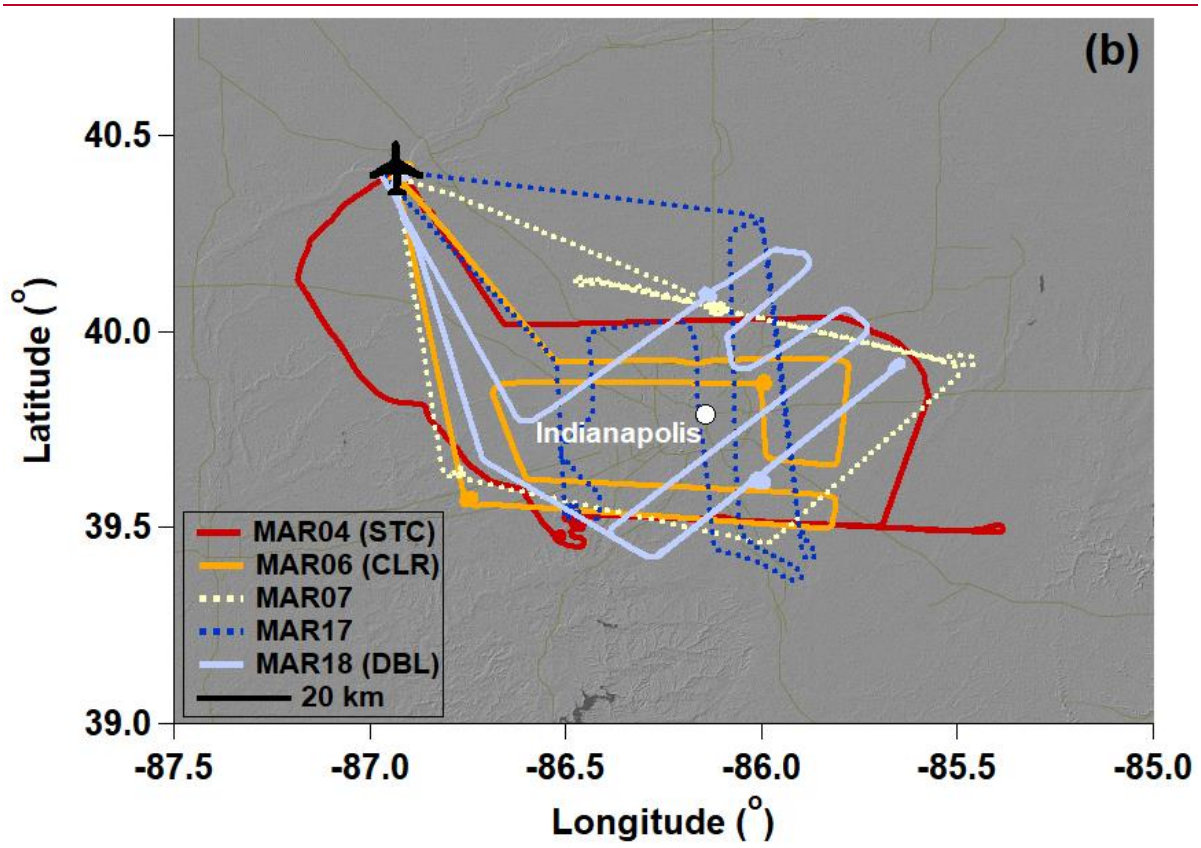

Figure 2: Flight paths conducted around the (a) Washington, D.C.-Baltimore and (b) Indianapolis study sites for the research flights ~~(RF) dates~~ listed in Table 1. Case study flight paths are indicated with solid lines, while all other flight paths are indicated with dotted lines.

Table 1: Flight ~~log listing flight~~ date, research flight ~~(RF) and case study~~ codes ~~used in this manuscript~~, flight time (local time, LT), number of vertical profiles conducted, and the observed range of potential temperature (θ) and ambient temperature (T) during the flights.

Flight Date (2016)	Research Flight Code - Case Study	Flight Time (LT)	Vertical Profiles	θ (ºC)	T (ºC)
12 February	~~RF01~~FEB12	11:45 – 17:30	1	-3.0 – 6.9	-8.9 – 9.3
17 February	FEB17~~RF02~~	11:40 – 18:15	1†	6.4 – 12.5	1.6 – 10.4
18 February	FEB18~~RF03~~	12:10 – 17:25	1	-0.4 – 17.7	-6.1 – 10.7
19 February	FEB19~~RF04~~	11:55 – 17:10	1	0.9 – 14.6	-0.6 – 10.1
4 March	~~RF05~~MAR04 - STC	13:55 – 16:30	5	3.5 – 15.4	-2.8 – 4.2
6 March	~~RF06~~MAR06 - CLR	12:55 – 15:25	4	9.6 – 21.1	4.4 – 11.6
7 March	~~RF07~~MAR07	14:10 – 16:45	6	15.8 – 26.5	10.2 – 18.7
17 March	~~RF08~~MAR17	12:15 – 15:00	2	13.6 – 17.5	1.6 – 17.3
18 March	~~RF09~~MAR18 - DBL	11:40 – 14:20	4†	7.8 – 17.8	0.2 – 10.7

~~*The supporting research flight days share similarities with the indicated case study, but some caveats exist (Discussion 4.4).~~

†Measurements of meteorological variables are completely or partially unavailable during one of the vertical profiles due to temporary failure of winds measurement system.

~~Nine daytime research flights were conducted around Washington, D.C. Baltimore and Indianapolis in February and March of 2016 (Table 1; Fig. 2). Flight paths were designed to maximize the number of VPs conducted while also characterizing upwind/downwind gradients in H_2O_v isotopic signature. VPs were sometimes conducted in a spiral pattern to limit the horizontal spatial coverage of the measurements, while other VPs were conducted in a sawtooth pattern ("porpoising"; Gerber et al., 2013) between the BL and FT (b and c panels of Figures #, #, and #) when the research aircraft travelled between the West Lafayette, IN, Purdue airport and the Indianapolis study site. Figure 3 shows examples of these two types of VPs conducted during the case study flights. The aircraft flew up to ~1600 m above sea level (msl) on average during the VPs. Only data collected on the descents of the VPs, when sampled air transitions from relatively dry to relatively humid, are presented here to minimize the potential influence of memory effects. However, similar features were observed on the ascents and descents. The number of VPs (Table 1) conducted on each flight was limited by air traffic and restricted air space (which was worse for the Washington, D.C. Baltimore study site), cloud cover, and available flight time. The research aircraft typically does not fly through clouds during experimental flights. Flights included other maneuvers, such as transects conducted upwind, intersecting, and downwind of the urban centers, the interpretation of which is beyond the scope of this paper (Fig. 32).~~

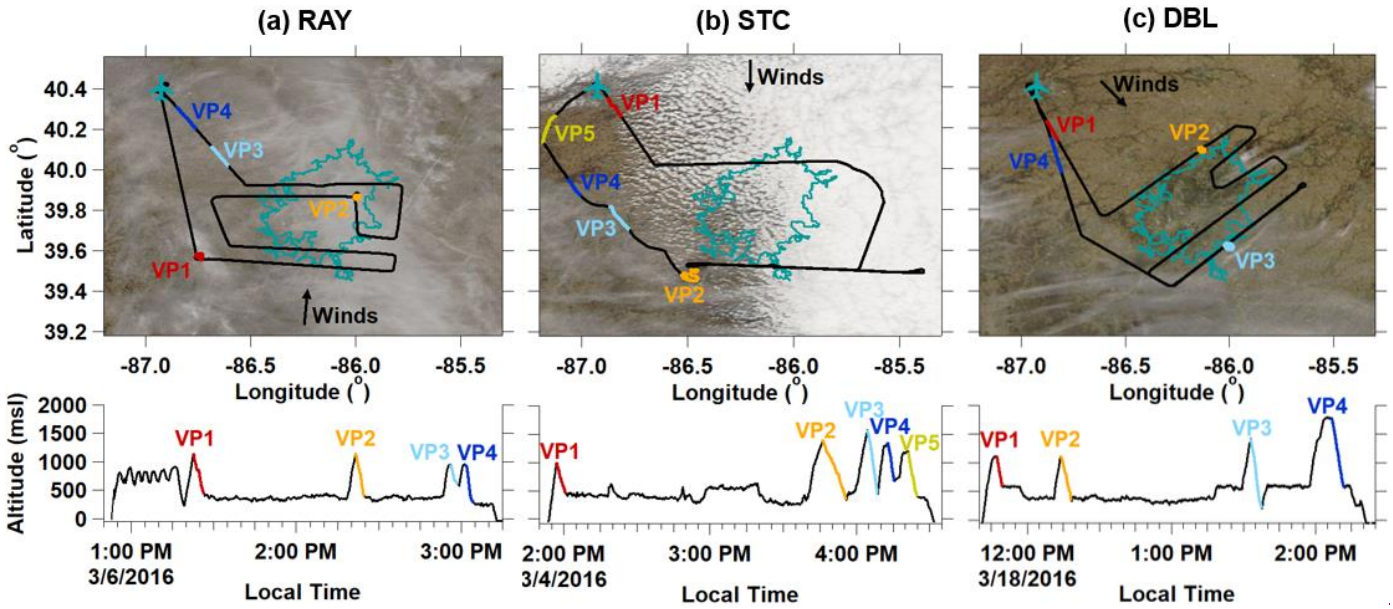

~~**Figure 3: The (a) RAY, (b) STC, and (c) DBL flight path and altitude time series with vertical profiles (VP) highlighted. Flight paths overlay the study site's cloud cover captured at approximately 12:30 local time by the Terra MODIS satellite (https://worldview.earthdata.nasa.gov/). The teal outline indicates the Indianapolis city boundaries. The West Lafayette, IN, Purdue airport is indicated by the airplane marker.**~~

2.4 Atmospheric layer identification

We classify regions of the atmosphere into the boundary layer (BL), inversion layer (INV), and free troposphere (FT), to compare and contrast ~~features~~ observed ~~in δD, δ^{18}O, and d-excess~~ isotopic ~~signatures~~ features during the research flights. The altitude at the base of the INV (z_{INV}) is defined as the lowest altitude at which the change in potential temperature (θ) ~~with altitude~~ exceeds 0.5 K for a 10 m change in altitude ($d\theta/dz > 0.05$ K m^{-1}). Rates of $d\theta/dz > 0.05$ K m^{-1} were commonly observed within the INV during the research flights. The altitude at the base of the FT (z_{FT}) is defined as the altitude above z_{INV} at which dθ/dz transitions to <0.05 K m^{-1}. A recent evaluation of methods for determining boundary layer height from aircraft measurements indicate the potential temperature gradient approach is most reliable (Dai et al., 2014). However, if layers are not definable using the $d\theta/dz >$ or < 0.05 K m^{-1} criterion, the secondary criterion of $|d(H_2O_v)|/dz > 20$ ppmv m^{-1} and $|d(H_2O_v)|/dz < 20$ ppmv m^{-1} is used to define z_{INV} and z_{FT}, respectively. These threshold values are appropriate for our wintertime, mid-latitude observations, but may not be universally appropriate in different locations or seasons. If neither criterion is met, the profiles of θ, dθ/dz, H_2O_v, and $d(H_2O_v)/dz$ are collectively considered, and z_{INV} is visually defined as the point at which H_2O_v and θ begin decreasing and increasing, respectively. Similarly, z_{FT} is visually determined as the altitude at which the rate of change of H_2O_v and θ with altitude begins to decrease.

2.5 Isotope theory

There are ~~three common ways~~ many processes that can influence the isotopic composition of atmospheric H_2O_v; here we examine two common ways ~~can change~~: condensation and mixing. We use the Rayleigh distillation model to represent condensation ~~as~~ of an ascending air parcel and ~~we use~~ a simple two-member mixing model to represent atmospheric mixing. ~~is dehydrated as it cools with altitude, mixing of different air masses, and~~ We calculate the influence of these processes using R

notation, but present the results by converting to delta notation ($\delta = R_{sample}/R_{standard} - 1$) using VSMOW as the standard. cloud formation and evaporation. We show here how each of these processes is are expected to change the isotopic signatures of atmospheric H_2O_v as H_2O_v mixing ratios change.

As air is dehydrated, for example during ascent, the heavier isotopologues are preferentially condensed first. The Rayleigh distillation model describes the effects of equilibrium fractionation on the isotopic composition of a dehydrating air parcel, for example during ascent (Dansgaard, 1964). Condensate that is formed as an ascending air parcel expands and cools is isotopically enriched in the heavier isotope relative to the vapor and in the open form of the Rayleigh model is assumed to be immediately removed from the system. The isotopic composition of the parcel as predicted by Rayleigh theory is given by the (eq. (1)).

$$R_{Ray} = R_o \left(\frac{H_2O_v}{H_2O_{v_o}}\right)^{\alpha_e - 1} \quad (1)$$

Here R_o and R_{Ray} are the heavy to light isotopologue ratios ($\frac{HDO}{H_2O}$ or $\frac{H_2{}^{18}O_vO}{H_2O}$) of the parcel prior to the ascent and at any point throughout the ascent, respectively. The remaining fraction of H_2O_v left in the ascending parcel relative to initial conditions is given by $\frac{H_2O_v}{H_2O_{v_o}}$. We determined the initial R_o and $H_2O_{v_o}$ input values for each day from the average BL values measured along the VP descents. The temperature-dependent equilibrium fractionation factor, α_e, for each isotopologue is calculated for the temperature corresponding toof the air parcel's lifting condensation level (LCL) altitude using Horita and Wesolowski (1994) for LCL temperatures greater than 0°C and Ellehøj et al. (2013) for LCL temperatures less than 0°C. The LCL is the height at which an air parcel would become saturated if lifted adiabaticallyalong a dry adiabatic ascent and is often used as an estimate of cloud base height (Romps, 2017). The VP observations show that ambient temperatures vary with altitude along the vertical profiles. However, Rayleigh distillation curves calculated with α_e values defined by the varying ambient temperatures measured along the vertical profiles are nearly identical to Rayleigh curves calculated with a single LCL-defined α_e value (Fig.ure S41).

The mixing of two air parcels (*A* and *B*) results in a heavy-to-light isotopologue ratio of an air parcel, R_{mix}, given by eq. (2) using HDO_v and H_2O_v ($H_2{}^{16}O_v$) as an example, $\frac{HDO}{H_2O}_{mix}$. In eq. (2), R_{mix} is the ratio of the weighted average of the heavy isotopologue to the weighted-average of the light isotopologue. The fraction of air parcel *A*, f_A, and air parcel *B*, f_B, sum to unity. The mixture's H_2O_v mole fraction is simply the weighted average of each parcels' individual H_2O_v mole fraction. $H_2{}^{18}O_v$ can replace HDO_v in eq. (2).

$$R_{mix} = \left(\frac{HDO_v}{H_2O_v}\right)_{mix} = \frac{f_A[HDO_v]_A + f_B[HDO_v]_B}{f_A[H_2O_v]_A + f_B[H_2O_v]_B} \quad (2)$$

We consider mixing processes in our observations by choosing two regions of the VPs as potential end-members, for example, the BL and the FT, and use the observed H_2O_v and isotopic ratios to define end-member values. The isotopic influence of cloud evaporation on the surrounding water vapour is complicated and depends on the mass of water in the vapour and liquid phases (Noone, 2012). Here, we compare two simplified approaches, described in detail below, but outlined here. In the first approach, we use the model from Worden et al. (2007) to describe cloud evaporation into a completely dry atmosphere. In the second approach using the model from Stewart (1975), we assume that cloud evaporation happens in two distinct regions of the inversion layer. First, cloud liquid is formed in equilibrium with atmospheric vapour at the LCL temperature. Next, that liquid is partially evaporated in the lower portion of the INV, changing its isotopic composition. Finally, that partially evaporated cloud droplet is moved to the upper portion of the INV where it evaporates completely.

The Worden et al. (2007) model describes the isotopic signature of an air parcel that is influenced by the evaporation of cloud droplets using a modified Rayleigh model shown in eq. (3).

$$\frac{\partial\delta}{\partial H_2O_v} = \frac{1}{H_2O_v}\left[\alpha_e\left(\frac{1-f_{evap}/\alpha_k}{1-f_{evap}}\right) - 1\right] \quad (3)$$

Here $\frac{\partial\delta}{\partial q}$ represents the change in the air parcel's δ signature with change in H_2O_v concentration. The fraction of the cloud droplet that has evaporated is given by f_{evap}. The kinetic fractionation coefficient is given by α_k, and is calculated according to Merlivat and Jouzel (1979). This is a simplified model that assumes the relative humidity at the surface of the evaporating cloud droplet is 0% (Worden et al., 2007; Noone, 2012).

The isotopic signature of a cloud droplet that undergoes partial evaporation and kinetic isotope fractionation within the INV is calculated according to eqs. (4) through (6), from Stewart (1975).

$$R_{cloud} = \gamma R_{vap} + (R_{cloud,o} - \gamma R_{vap}) f_{cloud}^{\beta} \quad (4)$$

$$\gamma = \frac{\alpha_e h}{1-\alpha_e\left(\frac{D}{D_i}\right)^n(1-h)} \quad (5)$$

$$\beta = \frac{1-\alpha_e\left(\frac{D}{D_i}\right)^n(1-h)}{\left(\frac{D}{D_i}\right)^n(1-h)} \quad (6)$$

Here R_{cloud} is the isotopic ratio of the remaining cloud droplet, $R_{cloud,o}$ is the initial isotopic ratio of the cloud droplet, R_{vap} is the isotopic ratio of the atmospheric vapor, f_{cloud} is the fraction of the cloud droplet remaining, and h is relative humidity. The ratio of the diffusivity of light water to heavy water, $\frac{D}{D_i}$, is 1.02512 for $H_2{}^{16}O$:HDO and 1.02849 for $H_2{}^{16}O$:$H_2{}^{18}O$ (Merlivat, 1978). The scaling constant, n, is 0.58 and determines the magnitude of kinetic isotope fractionation (Stewart, 1975).

3 Airborne campaign observations of H_2O_v ~~isotopologues~~d-excess in different layers of the lower troposphere

The campaign-wide observations show that values of δD and $\delta^{18}O$ decrease as H_2O_v mole fractions approach zero (Fig. 3). This relationship results from preferential removal of the heavier isotopologues during condensation processes, which becomes more pronounced at colder temperatures, and is consistent with previous airborne and high-altitude measurements of H_2O_v stable isotopologues (Bailey et al 2013; Galewsky et al 2007; He and Smith, 1999; Noone et al 2013; Samuels-Crow et al., 2014; Sodemann et al 2017). Later we will return to examine individual profiles of δD and $\delta^{18}O$ on case study days, but here we focus on identifying common patterns in d-excess signatures observed in the BL, INV, and FT that can be used to understand processes controlling moisture in the lower troposphere.

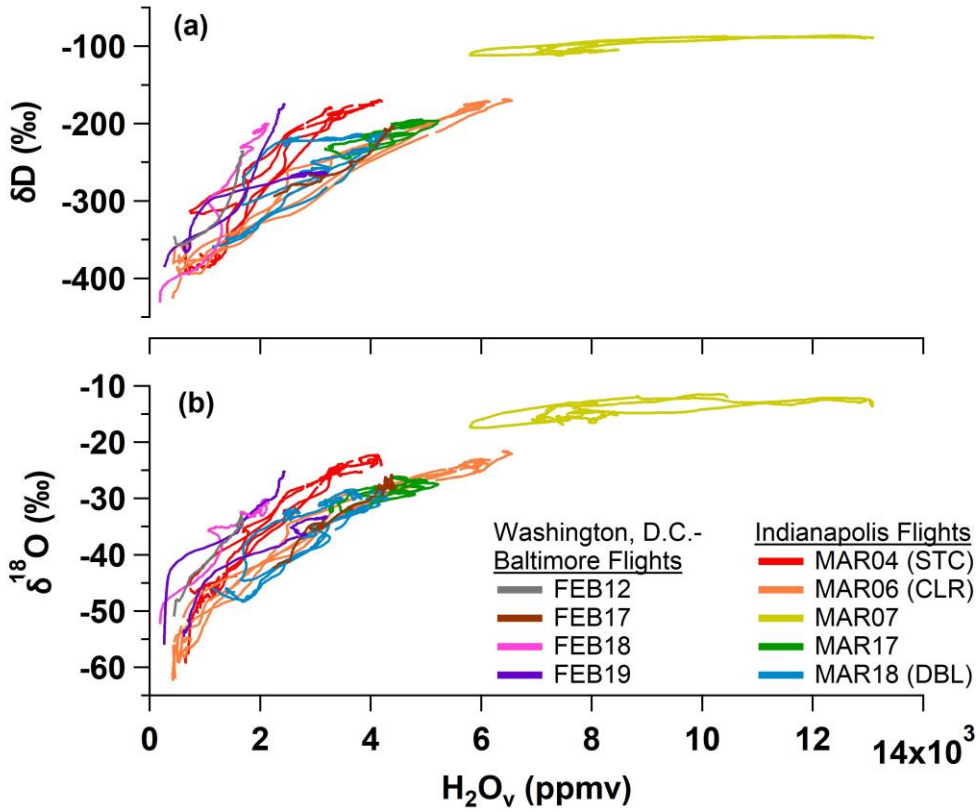

Figure 3: Measurements of (a) δD and (b) $\delta^{18}O$ made during vertical profile (VP) descents on the nine research flights (Table 1).

~~The case study days presented above were chosen for their distinct isotopic features and because several VPs were conducted each day. However, they only represent 30% of the research flight days (Table 1). Figure 7a-c shows t~~The Washington, D.C.-Baltimore and Indianapolis VP ~~absolute~~ d-excess observations within the FT, INV, and BL, are presented as a function of H_2O_v mole fraction in Fig. 4a-c, respectively. ~~Figures 7d-f show the measured d-excess relative to Rayleigh distillation theory, i.e. Rayleigh-predicted d-excess has been subtracted from the observations. Overall, BL d-excess observations at the Indianapolis and Washington, D.C. Baltimore study sites are relatively consistent with Rayleigh theory when using observations on each day as the initial conditions (Fig. 7c).~~ Generally, the air became drier and the d-excess signature exhibited greater variability with increasing altitude (Fig. 4). The greatest ~~departures from Rayleigh theory~~variability ~~-was~~ere ~~most commonly~~ observed in the INV (Fig. 4~~7~~b), where the d-excess signature deviated both positively and negatively from the global average precipitation d-excess value of 10‰ (which is provided in Fig. 4 for reference only). ~~Observations of d-excess in the INV at the Washington, D.C. Baltimore study site in particular were significantly more negative than Rayleigh predictions, by up to -80 ‰ (Fig. 7b).~~ The FT showed low H_2O_v mole fractions as well as large positive d-excess values (Fig. 4a), ~~as~~which are predicted by Rayleigh distillation theory for ~~such~~very low $H2O_v$ mole fractions (Bony et al., 2008).

~~The~~~~Very lowest H_2O_v mole fractions of the campaign were commonly observed in the FT, as were large, positive d-excess values (Fig. 4a). Large positive d-excess values are predicted by Rayleigh distillation theory at low H_2O_v mole fractions. . However, observed FT d-excess values are even more positive than the Rayleigh predictions in Fig. 7a at the lowest H_2O_v mole fractions.~~ High FT d-excess signatures have been reported by other studies, which hypothesize that ~~very~~extremely dry, depleted ~~FT~~ air masses in the mid-to-upper troposphere ~~carrying~~with large positive d-excess signatures, mix downward towards flight-level altitudes in the lower FT (Bony et al., 2008; Samuels-Crow et al., 2014; Sodemann et al., 2017). These FT air masses likely

originated from another source region and possibly underwent multiple condensation cycles to achieve such isotopic depletion prior to mixing with more humid air across the INV. Thus, FT d-excess values likely act as a record of the condensation and isotopic depletion history of a transported air parcel.

The 7 March 2016 flight~~ day~~ in Indianapolis (MAR~~RF~~07) reveals~~stands out as~~ an unusual set of meteorological conditions because, unlike all other flight days of the campaign, the H_2O_v mole fraction increased with altitude in the lower troposphere~~ increased in H_2O_v mole fraction with altitude~~ (Fig. 4~~7~~a-c; gold trace), and it was the most humid day of the entire campaign (Fig. 3; gold trace). A warm, southerly front moved into the Indianapolis study area on this day, and rain preceded the flight measurements~~observations~~. -The relatively high H_2O_v mole fractions in the INV and FT likely reflect residual humidity from the storm. -Overall, the MAR~~RF~~07 VP observations do not exhibit distinctive ~~isotopic features, and~~ d-excess features, ~~generally aligns with the global average d-excess value of precipitation varies around Rayleigh predictions for the BL,~~ i.e. -not deviating much from 10 ~~permil~~ ‰ in the INV~~,~~ and FT (Fig. ~~7~~4). These unique data likely reflect the imprint of the precipitation's isotopic signature on the surrounding vapor via isotopic equilibrium.

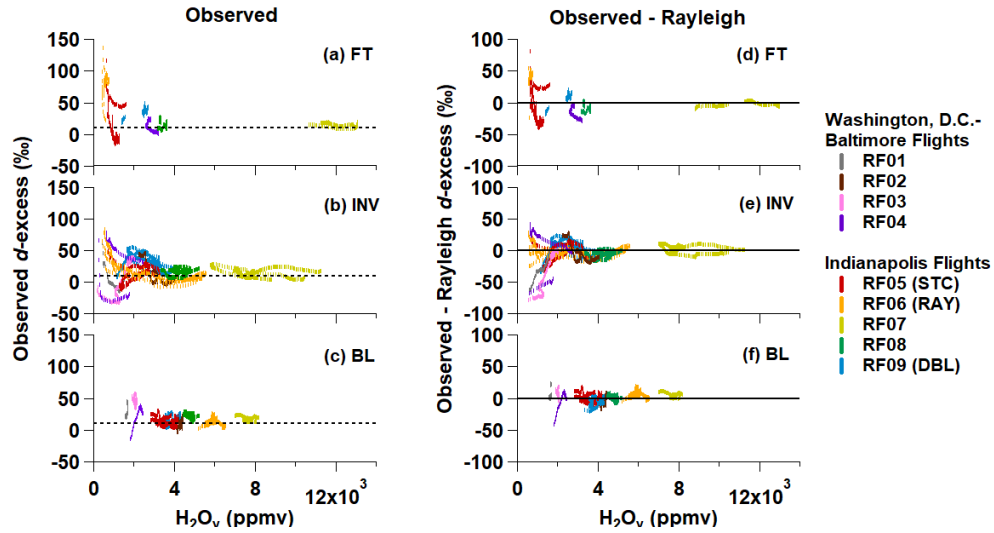

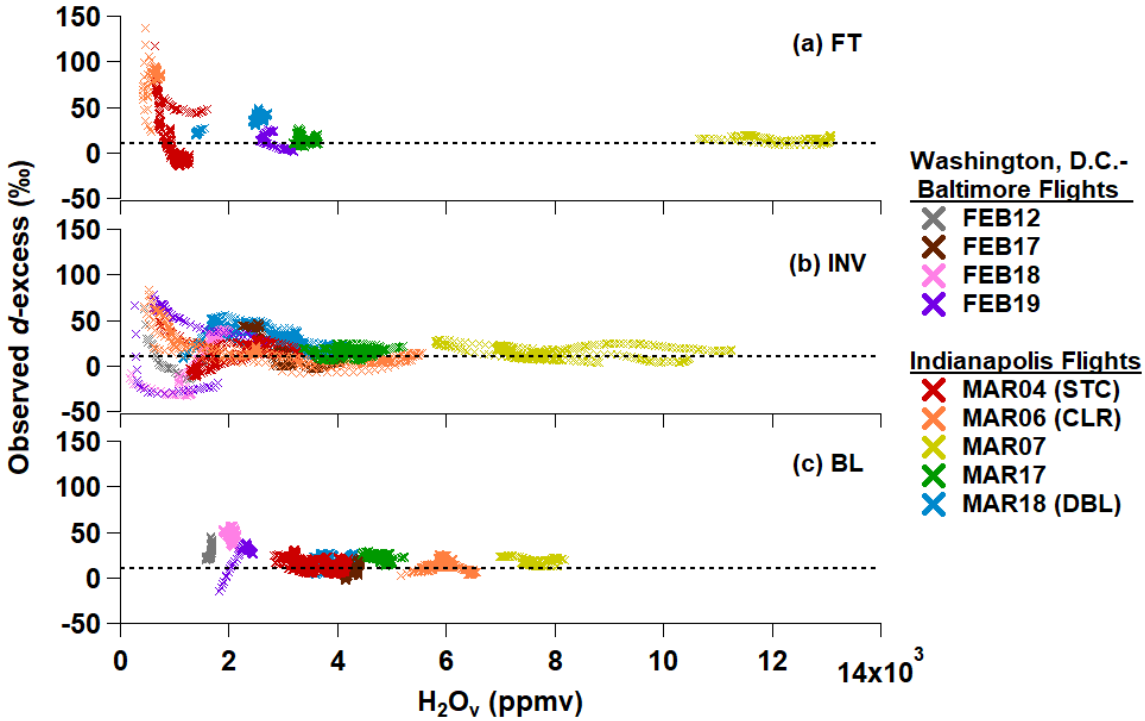

Figure 4~~7~~: Observations of ~~Rayleigh subtracted ddD~~ excess~~s observations~~ in the (a) free troposphere (FT), (b) inversion (INV), and (c) boundary layer (BL) during all the VP descents. Colors indicate each research flight. BL, INV, and FT observations are defined by the rate of change of atmospheric variables~~, and not defined by H_2O_v mole fraction~~. The dashed lines correspond to the global average precipitation d-excess value of 10‰ for reference only.

~~Most measurements of H_2O_v mole fraction in the FT were below 4000 ppmv; the corresponding FT measurements of $\delta^{18}O$, δD, and d-excess are plotted as a function of H_2O_v in Fig. S5. While each Washington, D.C. Baltimore VP (Table 1) extended into the FT, H_2O_v mole fractions were often lower than the humidity range over which the TWVIA was calibrated (lower limit: 550 ppmv; Appendix B). Contributing to the scarcity of Washington, D.C. Baltimore VP measurements is the fact that only one VP was conducted per flight, mainly as a result of congested and restricted air spaces near the capitol. Values of δD range from -30 to -60‰, $\delta^{18}O$ ranges from -200 to -400‰, and d-excess can be close to 10‰, but also increase up to 100‰ below 1000 ppmv.~~

4 ~~Discussion~~Case Studies

We focus on three particular Indianapolis flights as representative case studies based on their distinct features and vertical profiles over large altitude ranges (Table 1). H_2O_v isotope measurements conducted within and above the cloudless, well-mixed boundary layer on March 6 (CLR) represent the meteorologically-simplest observations of the entire campaign, as no clouds, precipitation, or shifting synoptic conditions were observed. Isotopic observations on March 4 (STC) may reflect moisture processing in a stratocumulus topped-BL, and the March 18 (DBL) observations may reveal differences in urban versus rural BL development and the influence of changing synoptic conditions.

~~3~~4.1 ~~Rayleigh-consistent observations~~ Clear sky observations of a well-mixed boundary layer (~~RAY~~CLR)

Four VPs ~~consistent with Rayleigh-distillation theory~~ were conducted on 6 March 2016 ("CLR" case study) around~~in~~ Indianapolis during clear sky conditions~~.~~ (Fig. 5a; weather map is presented in Fig. S5.1). Cloud–top height estimated from the Terra MODIS satellite retrievals (https://worldview.earthdata.nasa.gov/) indicate that the sparse cloud cover shown in Fig. 5a corresponds to higher altitude (>4800 m) clouds. The CLR measurements were made below 1400 m above sea level (Fig. 5b), and as a result, were likely not impacted by higher cloud processes. In terms of meteorology, the CLR case study is the simplest flight day of the airborne campaign. It is a useful case study to examine isotopic signatures across the BL, INV, and FT without the influence of complex atmospheric circulations or vapor-condensate interactions from clouds or precipitation.

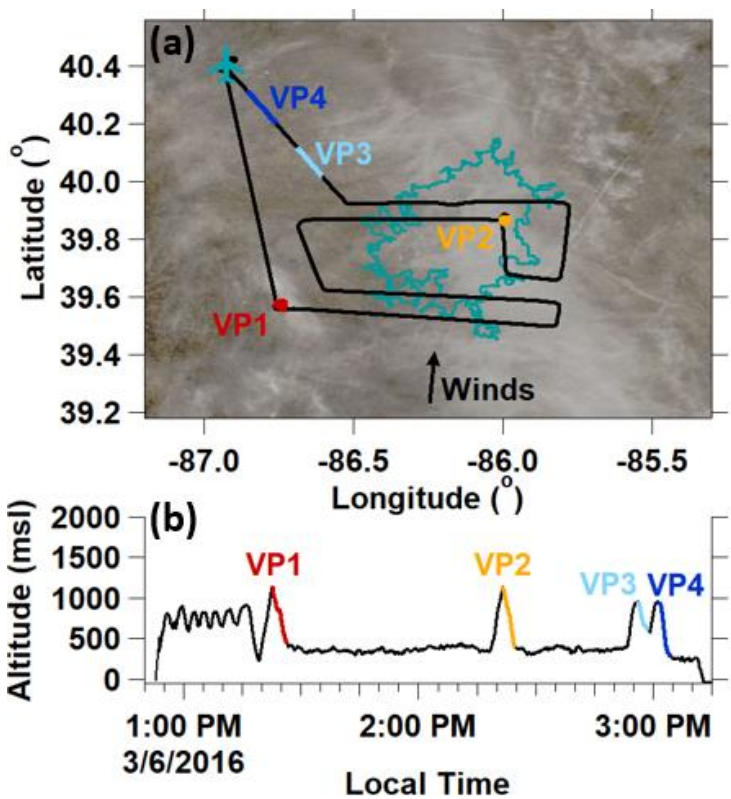

Figure 5. (a) CLR flight path overlaying the study site's cloud cover (https://worldview.earthdata.nasa.gov/) captured at 12:30 local time. The teal outline indicates the Indianapolis city boundaries. The West Lafayette, IN, Purdue airport is indicated by the airplane marker. (b) CLR case study altitude time series.

~~Observations of δD, δ^{18}O, and d-excess measured along the CLR VP descents are plotted as a function of H_2O_v mole fraction in Fig. 4a-c, respectively, along with predictions from Rayleigh distillation theory. The mixing lines in Fig. 4 show an air parcel's isotopic signature if varying proportions of BL and FT air are mixed (Methods 2.5). For the most part, the shape of the Rayleigh predicated δ^{18}O, δD, and d-excess values curvesalong the are similar to the observations four VPs are consistent with the observations from the BL up to the top of the INV (Fig. 4a-c). However, observed δD, δ^{18}O, and d-excess observations values nearat the interface of the INV and FT exhibit a hyperbolic shape (Fig. 4a-c), which is associated with mixing between distinct air parcels (Noone, 2012).~~

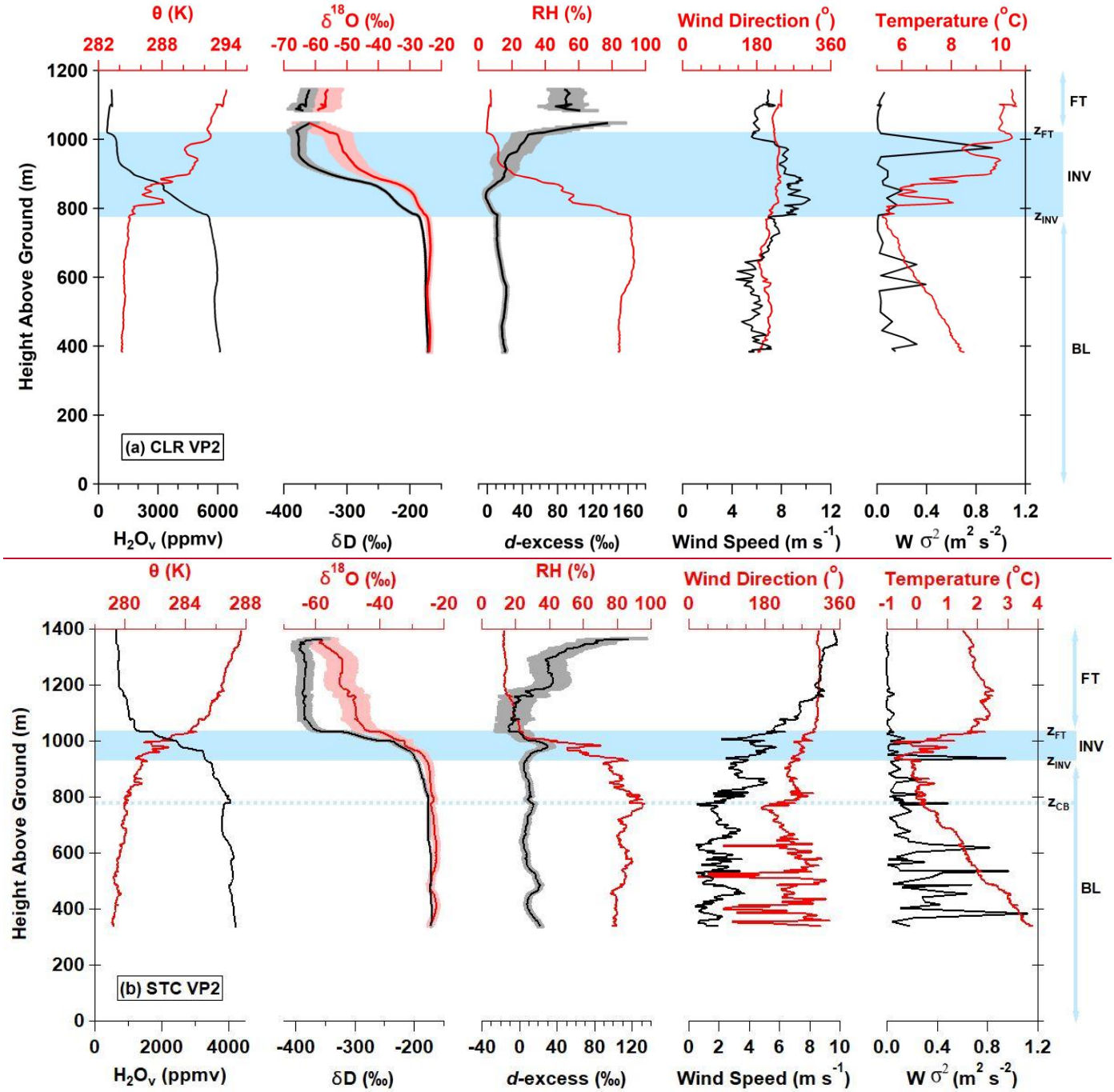

Figure 6: Observations of meteorological and isotope variables along the second VP (VP2) conducted on (a) CLR and (b) STC. Shading around the δ^{18}O, δD, and d-excess VP measurements define measurement uncertainty. Measurements in the boundary layer (BL), inversion layer (INV), and free troposphere (FT) are indicated for reference. The inversion layers,

which are bound at the bottom and top by z_{INV} and z_{FT}, respectively, are identified by blue horizontal bands. The dashed blue line in the Fig. 5b corresponds to stratocumulus cloud base (z_{CB}).

~~VP2 observations are presented as a representative example of RAY because VP2 was conducted approximately midway through the flight, it covers the largest vertical range relative to the remaining VPs, and it was conducted in a spiral formation to minimize the horizontal spatial extent over which the measurements were made (Fig. 3a).~~ The VP measurements made during CLR indicate a well-mixed BL and FT, and wind speed and wind direction were relatively constant from the BL to FT, indicating that BL, INV, and FT air parcels shared recent advection histories.~~.~~ ~~VP2 measurements in the BL, from 380 m – 780 m above ground level, of~~ $\delta^{18}O$, δD, and d-excess are relatively constant with altitude within the BL (surface to z_{INV}), varying by 1.2‰, 15.3‰, and 10.9‰, respectively (Fig. 6a). VP2 observations are presented as a representative example of ~~RAY~~CLR because VP2 was conducted approximately midway through the flight (Fig. 5b), it covers the largest vertical range~~ relative to the remaining VPs~~, and it was conducted in a spiral formation to minimize the horizontal spatial extent over which the measurements were made (Fig. ~~3~~5a~~a~~). The ambient temperature profile approximately follows the dry adiabatic lapse rate to the top of the BL (Fig. ~~5a~~6a), above which, temperature increases within the INV layer. ~~VP2~~ H_2O_v mole fraction decreases ~~by 5095 ppmv~~rapidly in the INV between z_{INV} and z_{FT} before becoming relatively ~~stable~~ constant in the FT. The ~~VP2 INV~~ $\delta^{18}O$ and δD values track the H_2O_v profile within the INV, decreasing by 30.8‰ and 193.2‰, respectively~~, as the heavier isotopologues preferentially condense~~. Observed d-excess values in the INV initially decrease slightly with altitude, and then increase, varying overall by 66.6‰. ~~Just above the INV H_2O_v mole fractions near a minimum, and δD increases while $\delta^{18}O$ decreases, causing FT d-excess values to increase rapidly.~~ Above ~1100 m in the FT, the ~~VP2~~ H_2O_v, $\delta^{18}O$, δD, and d-excess signatures are relatively constant with altitude. ~~Wind speed along the RAY VP2 ranged from 4.3 m s^{-1} to 10.3 m s^{-1}, and wind direction only varied by 60°~~~~were relatively constant~~ ~~from the BL to FT, indicating that BL, INV, and FT air parcels shared recent advection histories~~. ~~In terms of meteorology, the CLR case study is the simplest flight day of the airborne campaign. It is a useful case study to examine isotopic signature across the BL, INV, and FT without the influence of complex atmospheric circulations or vapor-condensate interactions from clouds or precipitation.~~

~~Cloud top height estimated from the Terra MODIS satellite retrievals (https://worldview.earthdata.nasa.gov/) indicate that the sparse cloud cover shown in Fig. 3a corresponds to higher altitude (>4800 m) clouds. The RAY measurements were made below 1400 m above ground level (Fig. 3a), and as a result, were likely not impacted by cloud processes from the sparse, higher altitude clouds.~~

~~Observations on 17 March 2016 (RF08) were also consistent with Rayleigh theory (Table 1). Like RF06 (RAY), skies were clear of clouds and wind speed and wind direction was relatively constant from the BL to the FT and a nearly dry adiabatic lapse rate was present from the surface up to ~3 km on RF08 (Fig. S2). RF06 was chosen for the Rayleigh case study over RF08 because RF08 H_2O_v mole fractions covered a smaller range and only two VPs were conducted that day.~~

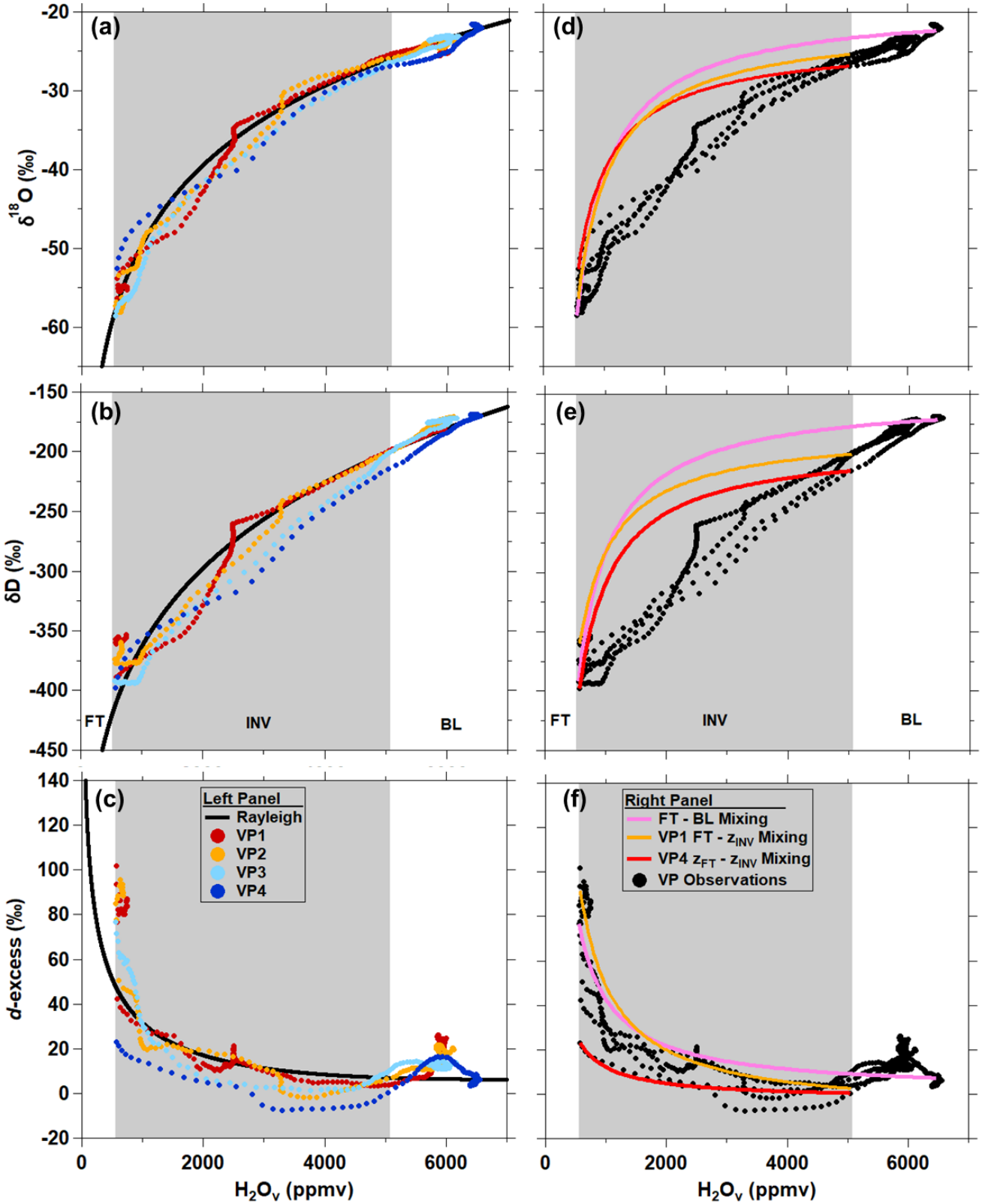

Figure 7: Comparison of vertical profile $\delta^{18}O$ (top panel), δD (middle panel), and d-excess (bottom panel) measurements to Rayleigh theory (left panel) and mixing (right panel) curves for CLR (MAR06). Individual VP descents are indicated by the different-colored points. The bounds of the inversion layer (INV), indicated by grey shading, are defined by the average H_2O_v mole fractions observed at z_{INV} and z_{FT}.

~~CLR~~RAY is the simplest case study day where δ values and d-excess observations generally track the Rayleigh predictions ~~in Fig. 4a-c.~~ Observations of δD, $\delta^{18}O$, and d-excess measured along the CLR VP descents are plotted as a function of H_2O_v mole fraction in Fig. 7, along with predictions from Rayleigh distillation theory (Fig. 7a-c) and different BL-FT mixing scenarios (Fig. 7d-f, Methods 2.5). The measured δ values more closely match Rayleigh curves than the mixing lines from the BL through the INV (Fig. 7). However, -positive deviations relative to ~~from~~ Rayleigh d-excess exist in the upper INV ~~to~~and lower FT (Fig. #7c)~~,~~. ~~and~~ W~~w~~e hypothesize that dry, isotopically-depleted FT air parcels carrying large, positive d-excess values can mix downward into more humid air parcels of smaller d-excess values near the top of the INV (Sodemann et al., 2017). As the H_2O_v mole fraction approaches zero, Rayleigh-predicted d-excess approaches 7000‰ (Bony et al., 2008). Thus, dehydrated lower-altitude FT air masses can carry a more positive d-excess signature for a given H_2O_v mole fraction ~~due to vertical mixing,~~ than is predicted by Rayleigh theory due to vertical mixing in the FT ~~(Fig. S5c)~~. The d-excess signature in the upper INV and lower FT more closely follows the FT-INV~~BL~~ mixing lines ~~-~~(see VP1- and VP4-defined endmember mixing scenarios in Fig. ~~4~~7f~~c~~), which supports this hypothesis.- Our results are consistent with Dyroff et al. (2015), who report lower troposphere δD observations over the Atlantic Ocean~~,~~ and explain the vertical structure of δD at lower altitudes using Rayleigh theory, while mixing scenarios dictate the δD profile based on -higher altitude observations ~~indicate mixing scenarios dictate the δD profile~~.

Despite apparent similarities between observed and Rayleigh d-excess in the BL and INV, the meteorological conditions within the BL are contrary to assumptions of the Rayleigh distillation model. Rayleigh distillation theory describes a two-phase system at saturation, however, no clouds (i.e. condensate) were observed at the flight altitudes where the CLR measurements were made. Furthermore, the BL was dry adiabatic (Fig. 6a). The agreement between the CLR observations and the Rayleigh-predicted d-excess, however, could be described by upwind condensation consistent with Rayleigh distillation theory, followed by subsequent advection to the Indianapolis study site. Given that wind direction and wind speed were observed to be relatively constant throughout the lower troposphere (Fig. 6a), air parcels in the BL, INV, and FT likely share similar trajectories. Thus, the Rayleigh-consistent CLR VP observations at lower flight altitudes likely result from upwind condensation that imprinted an isotopic signature on the air parcels that was maintained during transport, while lower FT observations point to mixing between subsiding FT and INV air. Past studies have also reported on the usefulness of H_2O_v stable isotopes as "imprints" of condensation, mixing, and atmospheric transport (Bailey et al 2013; Brown et al., 2008; Galewsky et al 2007; Gedzelman, 1988; He and Smith 1999; Samuel-Crow et al., 2014; Taylor, 1984).

~~From our measurements, we can comment on what types of atmospheric conditions are likely to produce profiles consistent with Rayleigh theory, i.e. equilibrium fractionation and no vapor-condensate (cloud droplet) equilibration. The RAY meteorological and isotopic observations are very similar to those made on 17 March 2018 (RF08; Table 1). These two flight days' observations provide possible criteria for when it is appropriate to use Rayleigh theory to predict isotopic signature throughout the BL and INV. These criteria include that the study area is free of clouds/precipitation (supported by the presence of a dry adiabatic lapse rate throughout the BL) and wind speed and direction is relatively constant throughout the BL, INV, and FT. The STC and DBL case studies, which do not follow Rayleigh theory, violate one or more these criteria.~~

~~3~~4.2 Stratocumulus-topped boundary layer observations (STC)

~~Figure 3b shows that the~~ The center and eastern portions of the Indianapolis study area were covered by stratocumulus clouds during part of the 4 March 2016 flight (~~RF05,~~ "STC" case study), on which five VPs were conducted (Fig. 8). The cloud cover map in Fig. 8a is provided to show the cloud type and extent during the afternoon of STC, however, it does not necessarily represent the cloud cover conditions throughout the 2.5 h flight. Satellite images (not shown) captured during the early afternoon of STC show that a thick cloud cover was sustained from the beginning into the middle of the flight, particularly over the city of Indianapolis, but eventually transitioned to scattered cover throughout the afternoon. This is consistent with visual observations made by the pilot and mission scientist that thick clouds persisted from the beginning of the flight until approximately 15:30 local time. Vertical profile temperature measurements collected on this day ~~tThe~~support the presence of ~~an earlier~~ cloud layer ~~on STC is supported by the vertical profile temperature measurements collected on this day~~ (Fig. 6b). BL air ~~becomes~~ was nearly saturated at 788 m (z_{CB} for "cloud base") along VP2 on STC (Fig. 6b). The ambient temperature lapse rate is 8.8 K km^{-1} (close to the dry adiabatic lapse rate of 9.8 K km^{-1}) near the surface until an altitude of z_{CB}, where the lapse rate transitions to 2.8 K km^{-1}. These observations are indicative of a stratocumulus cloud layer, which sits directly below the INV, and sustains the temperature inversion via radiative cooling (Wood, 2012). Indeed, a sharp decrease in θ is localized at z_{INV} (Fig. 6b). Evidence of a stratocumulus cloud layer was~~ere~~ apparent on VP1 and VP2, but a clear change in lapse rate below the INV was not observed on the ~~remaining~~ later STC VPs, indicating the air was not saturated below the INV during the later portion of the flight, consistent with visual observations of the thinning cloud layer. The STC flight is a useful case study to investigate how a stratocumulus cloud layer can influence the vertical structure of H_2O_v isotopologues in the lower troposphere.

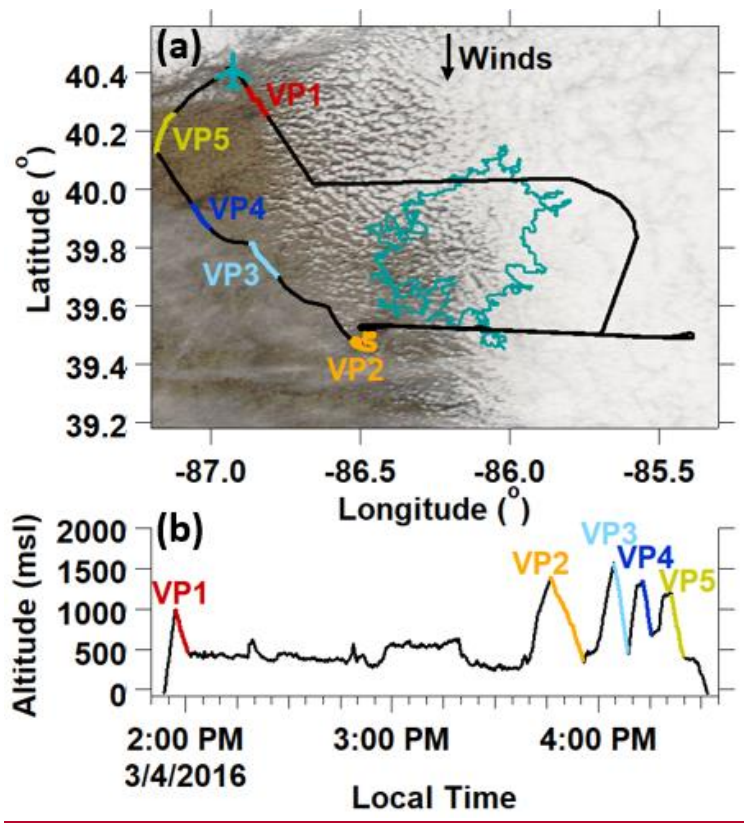

Figure 8. (a) STC flight path overlaying the study site's cloud cover (https://worldview.earthdata.nasa.gov/) captured at 12:30 local time. The teal outline indicates the Indianapolis city boundaries. The West Lafayette, IN, Purdue airport is indicated by the airplane marker. (b) STC case study altitude time series.

Measurements of isotopic and meteorological variables made along VP2 are shown in Fig. 6b. VP2 data is presented because it was conducted approximately mid-flight and it was flown in a spiral formation. ~~minimizing the horizontal spatial extent over which the measurements were made.~~ Measurements of $\delta^{18}O$, δD, and d-excess within the BL varied by 3.3‰, 27.4‰, and 19.1‰, respectively. This is approximately double the variability in δD, $\delta^{18}O$, and d-excess observed within the BL along the CLR VP2 (Fig. 6a). Within the INV, H_2O_v, $\delta^{18}O$, and δD values decrease by 1930 ppmv, 17.6‰, and 159.7‰, respectively from BL values. Similar to CLR, d-excess steadily increases in the FT on STC as H_2O_v mole fractions decrease. Despite general similarities in the vertical structure of the δ values on the CLR and STC flight days, there are notable differences in the d-excess structure near the INV on the two days (Fig. 6). Contrary to the CLR INV d-excess profile (Fig. 6a), d-excess first increases with altitude within the lower INV before decreasing to a minimum at z_{FT} on STC (Fig. 6b). Obvious anomalies in the STC d-excess signature relative to CLR are also apparent when plotted as a function of H_2O_v mole fraction (Fig. 9c and Fig. 7c, respectively).

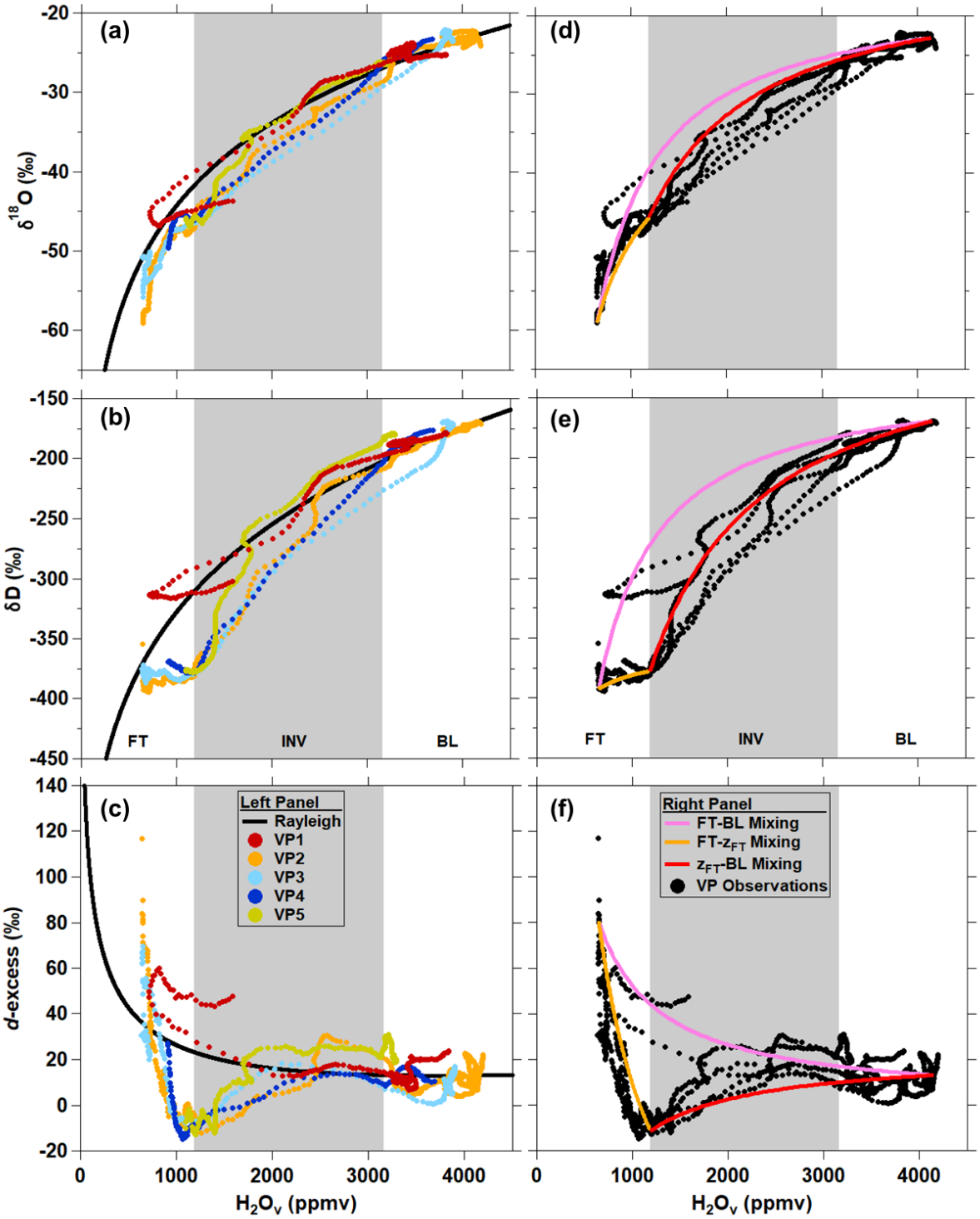

Figure 9: Comparison of vertical profile $\delta^{18}O$ (top panel), δD (middle panel), and d-excess (bottom panel) measurements to Rayleigh theory (left panel) and mixing (right panel) curves for STC (MAR04). Individual VP descents are indicated by the different-colored points. The bounds of the inversion layer (INV), indicated by grey shading, are defined by the average H_2O_v mole fractions observed at z_{INV} and z_{FT}.

~~Measurements on STC reveal unique d-excess features within the INV that may reflect stratocumulus cloud evaporation. Five VPs were conducted on this day.Here we compare the STC observations to Rayleigh curves using the assumptions described in Section 2.5. As mentioned above, the Rayleigh distillation model assumes condensation in a two-phase system at saturation~~

~~(Section 4.1).~~ While the atmosphere on STC was unsaturated at most flight altitudes (except near the cloud base; Fig. 6b), ~~we deem~~ the comparison to open-system Rayleigh curves is a useful exercise ~~,~~ as we showed above in the discussion of the CLR case study. ~~Mixing processes produce $\delta^{18}O$ and δD value that plot above the open-system Rayleigh curve and processes involving non-equilibrium liquid-vapor interactions or closed-system Rayleigh processes can plot below the curve.~~ STC VP $\delta^{18}O$ and δD observations ~~are relatively consistent with Rayleigh predictions (Fig. 4d), with the exception of~~ deviated~~ing~~ ~~but are more~~ negatively from the Rayleigh curve in drier portions of the INV and FT and ~~(Fig. 4b). The grey shading in Fig. 4 is the average range of observed INV H_2O_v mole fractions and does not represent the INV location for every VP on a single day.~~ ~~STC deviations from Rayleigh theory~~ were~~are~~ more pronounced for δD ~~and d-excess~~ than $\delta^{18}O$ (Fig. ~~4~~9a~~d-be f~~). ~~The INV ranges (grey shading in Fig. 4) are defined by each day's average H_2O_v mole fractions observed at z_{INV} and z_{FT}. STC deviations from Rayleigh theory are more pronounced for δD and d-excess than $\delta^{18}O$ (Fig. 4e-f). With the exception of VP1, the rest~~ Most of the VPs' δD values are more negative relative to Rayleigh in the INV and plateau in the FT which is unusual in water vapour isotope observations (Fig. ~~4e~~9b). Mixing processes can produce $\delta^{18}O$ and δD values that plot very nearly on or above the open-system Rayleigh curve depending on the mixing endmembers (e.g. Fig. 9), whereas processes involving non-equilibrium liquid-vapor interactions or closed-system Rayleigh processes can plot below the Rayleigh curve. While the mixing scenarios presented in Fig 9 (right panel) show remarkable agreement with the VP d-excess observations on STC, the mixing scenarios do not provide an explanation for the minimum at z_{FT}.

The d-excess measurements along VP2 through VP5 (Fig. 9c) reveal two anomalies that yield some insight: ~~(Fig. 4f),~~ (1) the slight increase in d-excess in the middle of the inversion layer (particularly for VP2 and VP5) and ~~the~~ (2) the d-excess minimum at the INV-FT interface (z_{FT}). From this minimum at z_{FT}, the FT d-excess signature becomes more positive with increasing altitude (as the air becomes drier), and eventually transitions to being more positive than the Rayleigh curve (Fig. ~~4f~~9c). ~~Unlike RAY, d-excess first increases with altitude within the lower INV before decreasing to a minimum at z_{FT};~~

The ~~FT~~ d-excess values observed during VP1 represent the only ~~FT~~VP measurements on STC that ~~closely track open-system Rayleigh curve and the BL-FT mixing line, and~~ do not exhibit a minimum at the INV-FT interface (Fig. ~~4~~9c~~f~~). ~~VP1 was conducted immediately after take-off from the Purdue airport. Sky conditions in the vicinity of the airport were clear, but a layer of stratocumulus clouds was observed over Indianapolis.~~ Only ~~one VP (~~VP1~~)~~ was conducted before the research aircraft encountered the thick stratocumulus cloud layer over Indianapolis (Fig. 8a~~3b~~). Unlike VP2 − 5, VP1 d-excess tracks the Rayleigh curve~~line~~ at the INV-FT interface. Slightly above z_{FT}, the VP1 H_2O_v mole fraction ~~began increasing~~increases and ~~the~~ d-excess ~~switches to tracking~~approaches the mixing line (Fig. 9c,f). We believe this VP represents conditions prior to cloud process influences. ~~The FT d-excess values observed during VP1 represent the only FT measurements on STC that closely track the BL-FT mixing line, and do not exhibit a minimum at the INV-FT interface (Fig. 4f). The differences between VP1 and the other VPs are described in more detail later.~~

~~Figure 5b shows vertical profiles of θ, H_2O_v, $\delta^{18}O$, δD, RH, d-excess, wind direction, wind speed, vertical wind variance ($W\text{-}\sigma^2$), and ambient temperature measured along VP2 conducted on STC. VP2 data is presented because it was conducted approximately mid-flight and it was conducted in a spiral formation minimizing the horizontal spatial extent over which the measurements were made. Measurements of $\delta^{18}O$, δD, and d-excess within the BL varied by 3.3‰, 27.4‰, and 19.1‰, respectively. This is approximately double the variability in δD, $\delta^{18}O$, and d-excess observed within the BL along the RAY (RF06; 6 March 2016) VP2 (Fig. 5a). Within the INV, H_2O_v, $\delta^{18}O$, and δD values decrease by 1930 ppmv, 17.6‰, and 159.7‰, respectively from BL values. Unlike RAY, d-excess first increases with altitude within the lower INV before decreasing to a minimum at z_{FT}. Similar to RAY, d-excess steadily increases in the FT on STC as H_2O_v mole fractions decrease.~~

~~One difference between STC and RAY is the presence of a stratocumulus cloud layer for STC (Fig. 3). Figure 5b shows that STC VP2 air becomes nearly saturated at 788 m (z_{CB} for "cloud base"). The ambient temperature lapse rate is 8.8 K km^{-1} (close to the dry adiabatic lapse rate of 9.8 K km^{-1}) near the surface until an altitude of z_{CB}, where the lapse rate transitions to 2.8 K km^{-1}. These observations could indicate a stratocumulus cloud layer, which sits directly below the INV, and sustains the temperature inversion via radiative cooling (Wood, 2012). Indeed, θ decreases sharply at z_{INV} (Fig. 5b). Indications of a stratocumulus cloud layer were apparent on VP1 and VP2, but a clear change in lapse rate below the INV was not observed on the remaining STC VPs, indicating the air was not saturated below the INV during the later portion of the flight.~~

~~Figure 3b shows that stratocumulus clouds covered most of the study area at approximately 12:30 local time on STC. The cloud cover map in Fig. 3b is provided to show the cloud type and extent during the afternoon of STC, however, it does not necessarily represent the cloud cover conditions throughout the 2.5 h flight. Figure S3 is a GIF of satellite cloud cover images captured during the afternoon of STC that shows the cloud cover evolution over the course of the flight. Thick cloud cover was sustained into the middle of the flight, particularly over the city of Indianapolis. As a result, VPs were not conducted within the city limits of Indianapolis. Toward the latter half of the flight the cloud cover transitioned to scattered. Four additional VPs were conducted at the end of the flight west of Indianapolis (Fig. 3b).~~

~~In contrast to RAY (Fig. 5a), STC wind speed is highly variable from the BL to the FT (Fig. 5b). Wind speed values ranged from a minimum of 0.4 m s^{-1} in the BL to a maximum in the FT of 9.8 m s^{-1}. A distinctive wind shear is obvious at z_{FT}. Highly variable wind direction in the BL is a result of low BL wind speeds.~~

~~4.2 Stratocumulus Cloud Evaporation~~

~~Given that~~ T~~t~~he presence of the stratocumulus cloud layer is a defining meteorological characteristic of the STC case study day, ~~we first~~therefore, we evaluate the potential for ~~C~~cloud and rain processes ~~may~~to cause the observed d-excess anomalies ~~from Rayleigh theory in theobserved during the STC case study day~~. ~~As mentioned above, two d-excess anomalies were observed within the INV, (1) a slight increase in d-excess near the middle of the INV, and (2) the minimum in d-excess at the INV-FT interface on VPs 2 – 5 (Fig. 4f).~~ Sodemann et al. (2017) also describe VP observations of a minimum in d-excess (negative values) at the BL top, and hypothesize the negative d-excess signal results from rain droplet evaporation directly below cumulus clouds at the top of the boundary layer. Rehydration processes, like cloud and rain droplet evaporation, have been proposed as mechanisms that could produce negative d-excess anomalies (Bolot et al., 2013~~ and~~; -Sodemann et al., 2017). HDO molecules preferentially evaporate relative to $H_2{}^{18}O$ molecules (Dansgaard, 1964)~~.~~. The result is a relatively positive vapor d-excess, while the d-excess signature of the residual droplet becomes progressively more negative as it evaporates (Aemisegger et al., 2015). Therefore, if liquid droplet evaporation ~~occuring~~occurr~~ing~~ed in separate atmospheric layers from start to finish, such as from the bottom of the INV to the top of the INV, ~~could produce~~ a positive d-excess anomaly could be transferred to the surrounding vapor as the droplet begins evaporating starting in the lower INV. As the liquid droplet is subsequently ~~followed by~~ transported to the upper INV ~~where~~, ~~a~~a negative d-excess anomaly ~~is~~could be transferred to the surrounding vapor~~ in the upper INV~~ as the evaporation of the liquid droplet nears completion.~~.~~ ~~When evaluating the effect that cloud evaporation could have on vertical profiles~~~~VPs of water vapour~~~~H_2O_v~~ ~~isotop~~~~ologues~~~~ic variability, we must consider the altitudes at which clouds form and evaporate. The main difference between the cloud and rain droplet evaporation processes is the size of the liquid droplets: <50 micron for clouds versus >50 micron for rain droplets.~~ Evidence exists that stratocumulus cloud droplets can evaporate at different altitudes, specifically within the cloud layer and within the inversion layer (Kollias and Albrecht, 2000; de Lozar and Melledo, 2015). Furthermore, inversion layer depths are not homogeneous above a stratocumulus cloud layer. Observations show inversion layers to be thicker above downdrafts and thinner near updrafts (Kollias and Albrecht, 2000). Differing INV depths, and associated thermodynamic properties, above the

stratocumulus cloud layer on STC may in part explain why unique d-excess anomalies were observed near the middle of the INV and at z_{FT} (Fig. 6b).

When evaluating the effect that cloud evaporation could have on VPs of H_2O_v isotopologues, we must consider the altitudes at which clouds form and evaporate and the speed of the relevant processes. ~~In the case of evaporation, this may not occur in a single layer, but throughout a range of altitudes or atmospheric layers.~~ Stratocumulus cloud tops are typically ~~present~~ directly below z_{INV} (Wood, 2012). The top of the INV (z_{FT}) is approximately the upper limit of BL mixing (Wood, 2012). Lofting of cloud droplets into the INV would cause droplet evaporation, as the INV was ~~under~~ not saturated (Fig ~~5~~6b). ~~In the cloud evaporation scenarios discussed below, it is assumed that the cloud droplets form at the top of the BL, and the droplets undergo evaporation within the INV.~~ ~~As mentioned above, two d-excess anomalies were observed within the INV, (1) a slight increase in d-excess near the middle of the INV, and (2) the minimum in d-excess at the INV-FT interface on VP2-VP5 (Fig. 4f). Disregarding for the moment the potential isotopic enrichment or depletion cloud droplet evaporation would have on the surrounding vapor, we first~~This hypothesis requires that ~~a~~a negative d-excess anomaly is retained by an ~~partitially~~ evaporat~~ed~~ing droplet while it is transported to the upper INV. This requires us to consider two important timescales. First, t~~(1) T~~he timescale at which a liquid droplet isotopically equilibrates with its surrounding ~~vapor~~vapour, and second, ~~. (2) t~~~~T~~he speed at which droplets move through the INV by ~~way of~~ vertical winds. Using the method described by Bolot et al., 2013, which is -based ~~off of~~on prior work by Jouzel, 1986~~ (Chapter 2)~~, we estimate that the e-folding time required for a cloud droplet with a 15 µm radius to isotopically equilibrate with the surrounding vapor is approximately two seconds, under the conditions observed in the middle of the INV, or about five seconds at the top of the INV. ~~For our observations of vertical wind speeds, T~~~~t~~he time for a droplet to move from the bottom to the top of the INV is 19 seconds, based on vertical wind speed observations. These calculations indicate that a cloud droplet located near the bottom of the INV would ~~isotopically equilibrate~~approach isotopic equilibrium with surrounding vapor before reaching the top of the INV under the observed flight conditions. Thus ~~it is unlikely that~~these calculations do not strongly support the hypothesis that evaporation of stratocumulus cloud droplets ~~observed during the flight had any relationship~~produced ~~to~~ the observed minimum in d-excess at z_{FT}. ~~However, cloud droplet evaporation may explain the local maximum in d-excess at the middle of the INV (Fig. 4f; Fig. 6b).~~

~~HDO molecules preferentially evaporate relative to $H_2^{18}O$ molecules (Dansgaard, 1964). For the case of a rain droplet, evaporation would result in a relative increase in d-excess of the surrounding vapor and a decrease in the droplet's d-excess signature (Aemisegger et al., 2015). Given the time scale of isotopic equilibrium and vertical wind speeds, it is possible that stratocumulus cloud droplet evaporation could be responsible for the slight increase in d-excess within the middle of the INV (Fig. 4f, Fig. 6b).~~

The question of what process or processes are responsible for the minimum in d-excess at the INV-FT interface (z_{FT}) remains. If previous INV conditions on STC were colder, had faster vertical wind speeds, or~~and~~ the liquid droplet radii were larger than 50 microns (e.g. rain drizzle), the timescales associated with isotopic equilibrium and transport across the INV could converge. The main difference between the cloud and rain droplet evaporation processes is the size of the liquid droplets: <50 micron for cloud versus >50 micron for rain droplets (Kollias and Albrecht, 2000). It is possible that such conditions were present prior to when the STC measurements were made, and that the minimum in d-excess is the isotopic imprint of rain droplet evaporation under cold, unsaturated, turbulent conditions. We find discussion of these potential d-excess anomalies in the literature in reference to rain droplets evaporating below the cloud layer (Aemisegger et al., 2015; Gat, 1996), but we believe the same isotopic fingerprint ~~would occur~~ on vapor could occur as liquid cloud or rain drizzle droplets ~~- that are~~ lofted in drier environments- finish evaporating ~~would occur for the vapor~~at the top of the INV, or at the top of the BL, as hypothesized by Sodemann et al. (2017).

~~The slight easterly movement of the cloud layer as shown in Fig. S3 could be interpreted as the stratocumulus cloud layer being advected out of the Indianapolis study area by westerly winds rather than evaporating away. However, Fig. 5b shows that wind speeds at the cloud layer were relatively low (<6 m s^{-1}), and the clouds in Figure S3 transition from opaque to semi-transparent over the flight period. This information taken together suggests there was evaporation of the stratocumulus cloud layer during the flight.~~

~~We believe our observations provide evidence that the process of cloud evaporation may be spread throughout the INV layer with the beginning and end of evaporation separated in space. Within the INV, turbulent updrafts and downdrafts are warmer and cooler than the surrounding air, respectively (Betts, 1985). Updrafts potentially carrying partially-evaporated cloud droplets to the top of the INV may facilitate complete evaporation of the droplets due to the low RH and possibly wind shear-promoted mechanical turbulence at z_{FT} (Fig. 5b). Due to higher RH values within the middle of the INV relative to z_{FT}, it is possible cloud droplet evaporation did not proceed to completion at these INV altitudes. Partial evaporation would impart a positive d-excess signal on atmospheric vapor and act to increase RH (Aemsigger et al., 2015; Sodemann et al., 2017), both of which exhibit a local maximum at ~985 m agl (Fig. 5b).~~

~~Other studies have reported~~ The negative ~~water vapor~~ H_2O_v d-excess observations at z_{FT}~~and hypothesize that the~~ could also have resulted ~~se are~~ from kinetic fractionation of vapor during deposition on ice crystals or snow (i.e. in ice supersaturated conditions) (Bolot et al., 2013; Casado et al., 2016; Galewsky, 2015; Lowenthal et al., 2016; Moore et al., 2016; Samuels-Crow et al., 2014; Schmidt et al., 2005).

Low d-excess values (relative to Rayleigh ~~at~~curves assuming RH = 100%) were sometimes observed within the INV layers during the Washington, D.C.-Baltimore flights (Fig. 4b). Ambient temperatures observed in flight in Washington, D.C.-Baltimore were sometimes less than 0ºC (Table 1), thus vapor deposition on ice crystals could be possible for those scenarios. It is unlikely that ~~ice supersaturation~~vapor deposition on ice occurred during the ~~is responsible for the minimum in vapor d-excess observed at z_{FT} on~~ STC case study flight because temperatures were greater than 0ºC (Table 1). However, as an example, Figure ~~D~~S6~~1~~ shows ~~that~~ the theoretical d-excess values of STC vapor under ice supersaturated conditions (~~Appendix D~~Section S6). We reiterate that ice-supersaturation is an unlikely explanation for the STC z_{FT} d-excess minimum because flight altitudes were less than 2 km, and ice (cirrus) clouds are typically present at ~6 km. It is unlikely that ice hydrometeors falling from higher altitudes could be sustained at the top of the inversion and contribute to the low d-excess signal observed on VP2–VP5 through vapor deposition given the >0ºC temperatures. There was, however, a region of high-humidity upwind (northwest) of the study site at altitudes between 3-5.5 km where ice or mixed-phase condensate could have been present (Fig. S5.2). It is possible that condensation under ice-supersaturated conditions occurred prior to the STC flight, and that the resulting isotopic imprint was maintained during transport to Indianapolis and subsequently mixed downward via subsiding FT air (Fig. 9f). Both of these explanations ~~we explore~~ for the minimum in d-excess at z_{FT} on STC require an advected signal of a prior process (complete cloud droplet evaporation or vapor deposition on ice). This process must have happened relatively close in time to the STC flight, since the minimum in d-excess at z_{FT} was not observed on VP1, but the anomaly was observed two hours later when VP2-VP5 were conducted. ~~While vapor deposition in ice-supersaturated conditions might not be relevant for the STC flight, low d-excess (relative to Rayleigh at RH = 100 %) was sometimes observed in the INV layers during the Washington, D.C. Baltimore flights (Fig. 7b). Ambient temperatures observed in flight in Washington, D.C. Baltimore were sometimes less than 0ºC (Table 1), thus vapor deposition on ice crystals would be more likely for those scenarios.~~

~~3~~4.3 ~~Observations of a developing~~Developing boundary layer observations (DBL)

The ~~third~~ final airborne case study, ~~measurements was~~ere conducted on 18 March 2016 in Indianapolis (Fig. 10), ~~("DBL" for developing boundary layer, RF09)~~ . ~~This case study~~ is referred to as DBL for "developing boundary layer" because ~~M~~measurements on this day reveal considerable spatiotemporal variability in the vertical structure of the observed meteorological and isotopic variables. The boundary layer height increased over the course of the flight and may reflect a combination of a residual layer from the previous day, urban vs. rural differences in BL development, and the effects of a frontal pattern moving across the Indianapolis study area. ~~Figure 3c shows that Indianapolis was cloud free at approximately 12:30 LT and clear skies continued throughout the flight. Scattered clouds developed over Indianapolis late in the afternoon after the research flight (17:00 local time; Fig. S4). Within the BL, wind direction and wind speed were relatively constant. Wind shearing is apparent at the z_{FT} (Fig. 6). Wind speeds increase from ~5 m s^{-1} to ~18 m s^{-1} between the BL and FT, which is a larger gradient than was observed on STC. Wind speed stabilizes within the FT (Fig. 6). Wind direction varies only by ~30 ° during each of the four VPs.~~

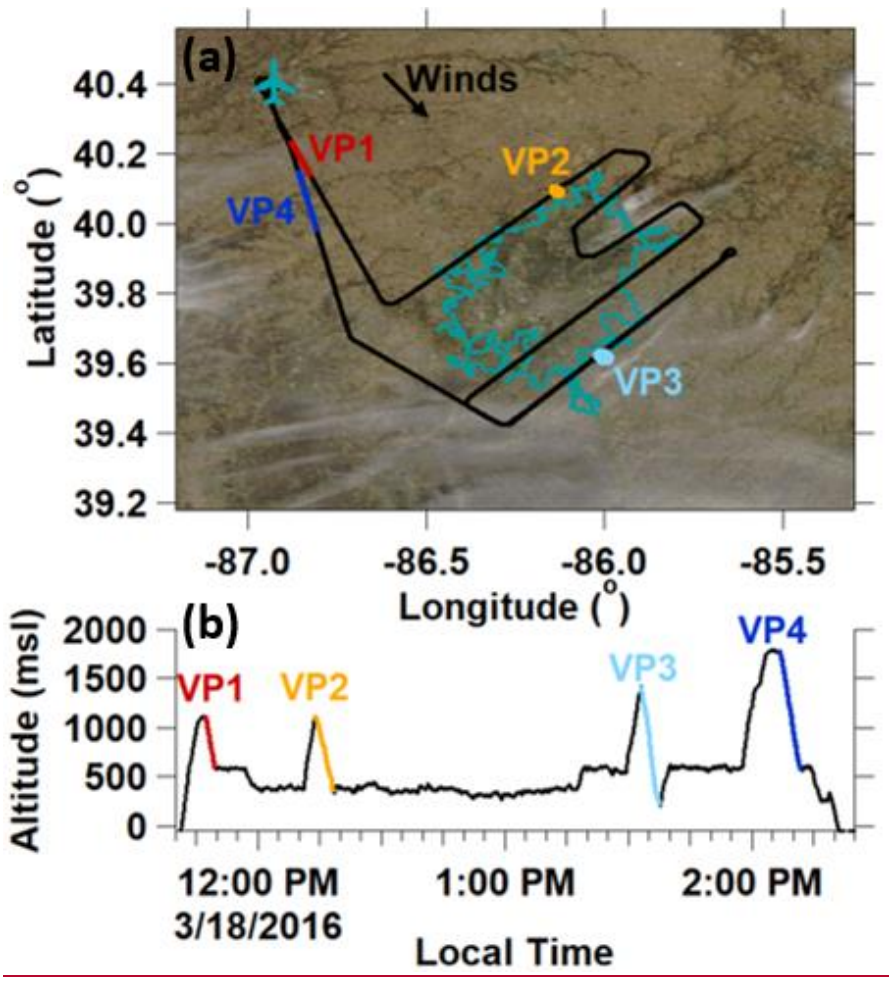

Figure 10. (a) DBL flight path overlaying the study site's cloud cover (https://worldview.earthdata.nasa.gov/) captured at approximately 12:30 local time. The teal outline indicates the Indianapolis city boundaries. The West Lafayette, IN, Purdue airport is indicated by the airplane marker. (b) DBL case study altitude time series.

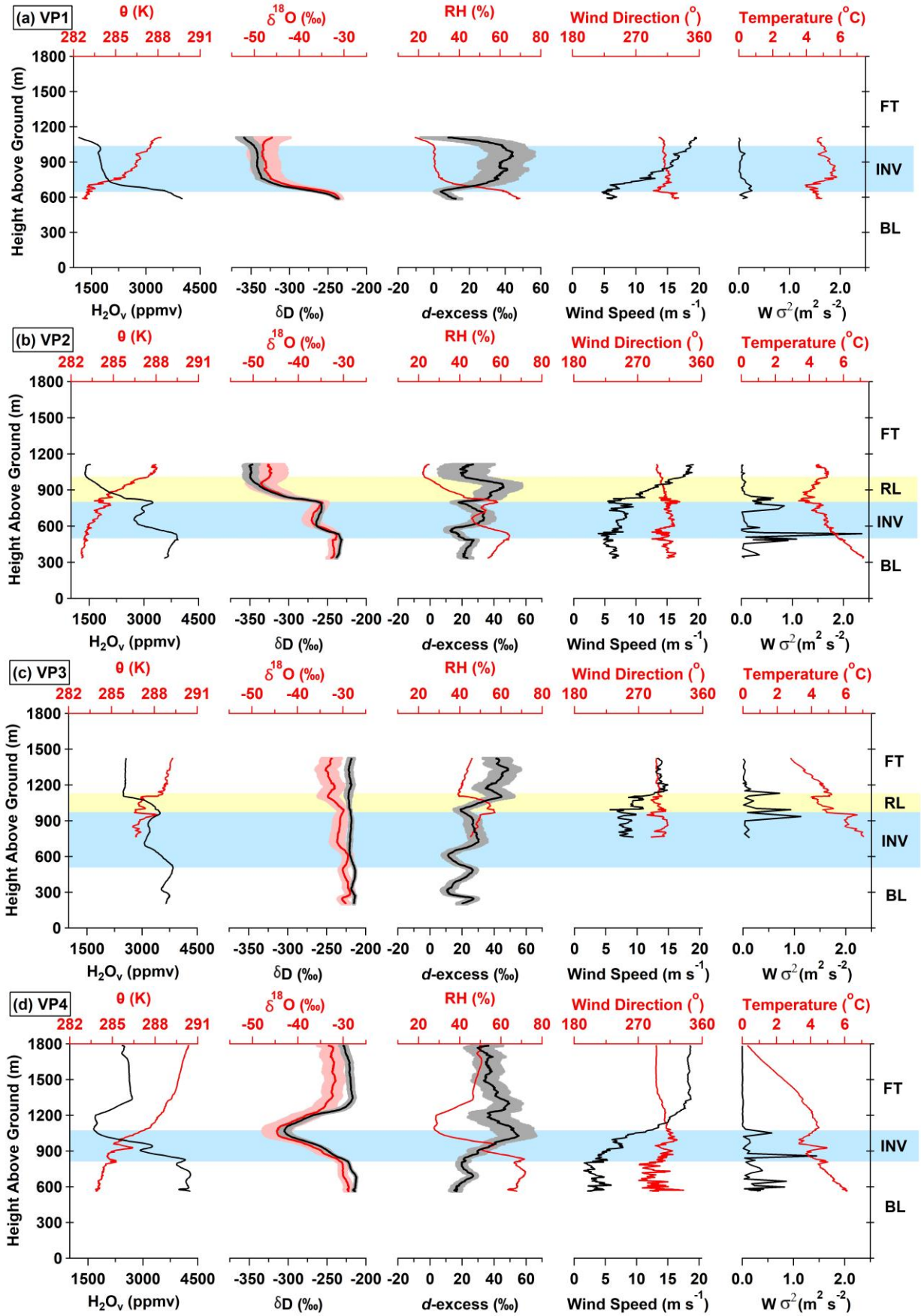
(a) VP1
(b) VP2
(c) VP3
(d) VP4
θ (K)
δ18O (‰)
RH (%)
Wind Direction (°)
Temperature (°C)
Height Above Ground (m)
FT
RL
INV
BL
H2Ov (ppmv)
δD (‰)
d-excess (‰)
Wind Speed (m s-1)
W σ2 (m2 s-2)

Figure 11~~6~~: DBL vertical profile (VP) measurements from 18 March 2016~~RF09~~ in the boundary layer (BL), inversion layer (INV; blue), previous day's residual layer (RL; yellow), and free troposphere (FT). Observations corresponding to VP1-4 are shown in (a-d), respectively.

~~Differences in the vertical structure of $\delta^{18}O$, δD, and d-excess along the four DBL VPs are shown in Figure 6.~~ A defining characteristic of the DBL case study is the variability in both the meteorological and isotopic variables between each of the four VPs (Fig. 11). Observations along VP1 show an INV layer, marked by a characteristic increase in θ and a corresponding decrease in H_2O_v (Fig. 11a), separating the BL and FT. However, ~~T~~there appears to be two distinct atmospheric layers between~~separating~~ the BL and FT in VP2 (Fig. ~~6b~~11b). The layer directly below the FT in VP2 is consistent with a~~the~~ residual layer (RL) from the previous day's boundary layer (Fig. ~~6~~11b). We define the base of the RL using the same approach described in Section 2.4 ($d\theta/dz$ and $|d(H_2O_v)|/dz$ threshold values) for determining the base of the INV (z_{INV}). ~~Indications for the presence of a RL are discussed in Section 4.3.~~ Both the RL and the INV (directly below the RL) show characteristic decreases in H_2O_v, $\delta^{18}O$, and δD values. The presence of multiple layers is supported by the increase in the variance of the vertical wind speed (W σ^2), indicating wind shear, at the interface of atmospheric layers (Fig. ~~6b~~11b ~~d~~). ~~The temporal factors influencing the presence of the RL are discussed below.~~

~~The $\delta^{18}O$ and δD values were relatively constant with altitude along VP3 (Figure 6c), however the vertical structure of H_2O_v and d-excess is similar in shape to VP2 (Fig. 6b).~~ Similarities in the vertical structure of H_2O_v and d-excess ~~features~~ between VP2 and VP3 give indications that the~~a~~ RL persisted for an additional hour after VP2 was conducted (Fig. 11c)~~and INV were present during VP3 as well as VP2~~. Despite ~~The winds measurement system on the aircraft had~~ a temporary failure of the aircraft's winds measurement system -halfway through the VP3 descent, ~~but~~ available measurements show an increase in wind speed and ~~, as well as an increase in~~ vertical wind variance (W σ^2), as well as ~~and~~ sharp ~~small~~ temperature changes~~inversions~~ at the base and top of the RL~~INV~~, supporting VP3's d-excess indications of the persisting RL (Fig. 11~~6~~c). ~~The DBL case study is an example of how d-excess can support meteorological measurements in identifying distinct atmospheric layers.The VP4 vertical structure of $\delta^{18}O$ and δD near the surface and higher in the FT (>1400 m) are constant, and are of similar enrichment to VP3 δ values. However, VP4 $\delta^{18}O$ and δD values decrease to a minimum within the INV before increasing and then plateauing in the FT.~~

~~A unique feature of DBL is the presence of a residual layer (RL), which was incorporated into the BL throughout the duration of the flight.~~ This residual layer hypothesis is supported by ~~Fig. S2, which shows that on the day prior to DBL, 17 March 2016, Rapid Refresh Model~~ ambient temperature profiles for the Indianapolis International Airport (KIND) from the day prior to DBL, 17 March 2016, which follow a nearly dry adiabatic lapse rate all the way to an altitude of 3 km (Fig. S7). This was a relatively warm, turbulent day. ~~and H_2O_v isotopologue observations were consistent with Rayleigh theory (Table 1, RF08).~~ A cold front moved into the Indianapolis study area on DBL (18 March 2016). The ambient temperature profile on DBL shows the previous day's residual layer persisted into the early afternoon, between approximately 1 - 3 km (Fig. S7~~S2~~), before being incorporated into the BL. The distinction between the RL and BL blurs as surface heating progresses throughout the day and the RL is incorporated into the BL. It would also be expected that the downwind edge of the Indianapolis city boundaries (winds were from the northwest; Fig. 11a~~3c~~) would have a more well mixed BL due to stronger turbulent mixing from the urban heat island and increased surface roughness (Grimmond et al., 2010; Stull, 1988). -Support for this is given by measurements made along~~DBL~~ VP3, which was conducted on the downwind edge of the Indianapolis city boundaries ~~observations (Fig. 6c), which~~ and reveal a considerably more homogenous structure in δD and $\delta^{18}O$ relative to VP1 and VP2 (Fig. 11c). The ambient temperatures measured along VP3 in the FT and RL are warmer relative to ambient temperatures along the other three VP's (Fig. ~~6~~11),

~~indicating~~demonstrating the influence of the urban heat island. Although the VP3 H_2O_v, δD, and $\delta^{18}O$ values are relatively more homogenous in the vertical dimension, the d-excess signatures still maintain indications of the RL, as the vertical structure of d-excess is similar to VP2 d-excess observations. ~~This is an example of how d-excess can provide more clues about atmospheric circulation than can δD or $\delta^{18}O$ alone.~~

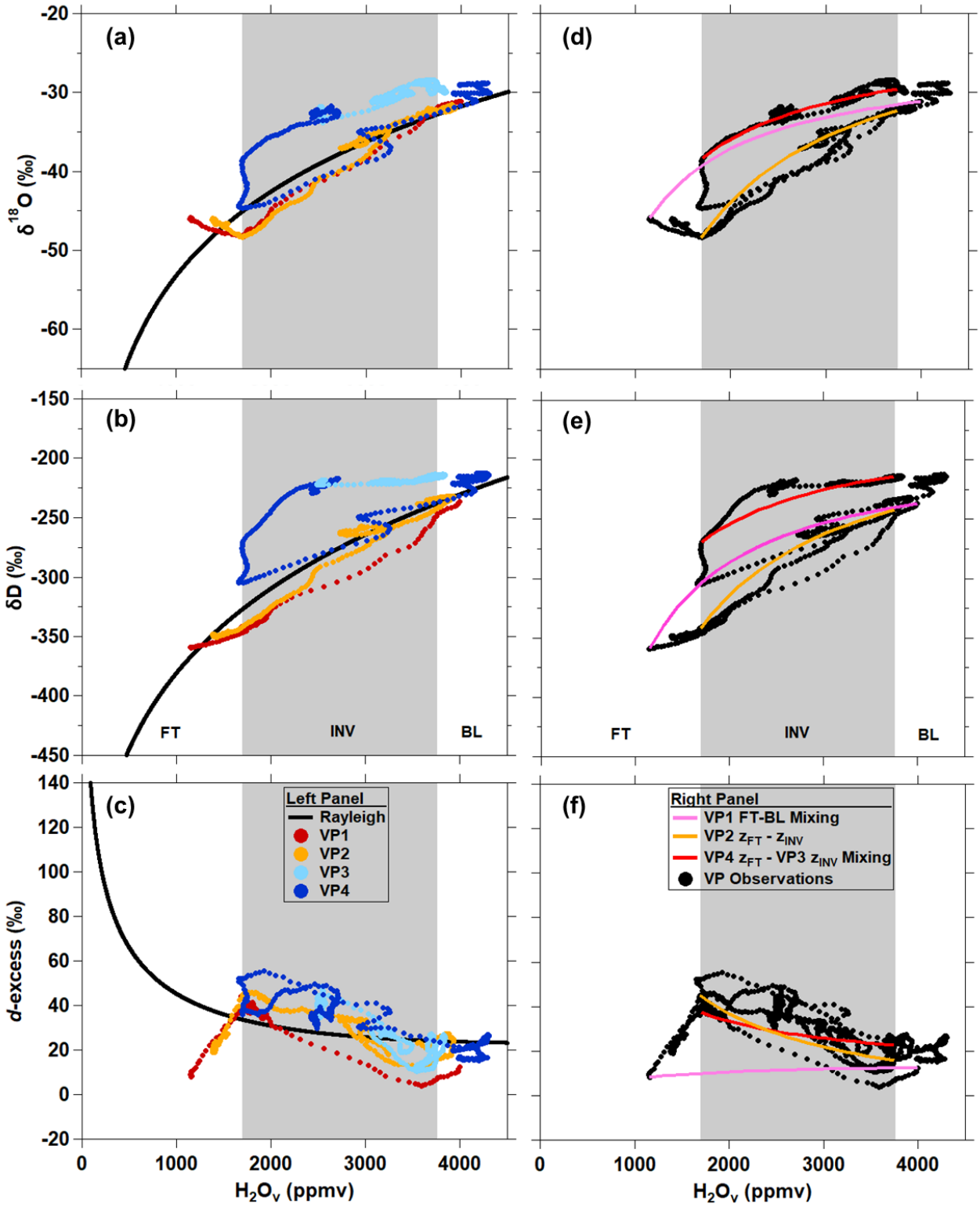

Figure 12: Comparison of vertical profile $\delta^{18}O$ (top panel), δD (middle panel), and d-excess (bottom panel) measurements to Rayleigh theory (left panel) and mixing (right panel) curves for DBL (MAR18). Individual VP descents are indicated by

the different-colored points. The bounds of the inversion layer (INV), indicated by grey shading, are defined by the average H_2O_v mole fractions observed at z_{INV} and z_{FT}.

~~Despite differences in δ value features along the four DBL VPs, the relationship between d-excess and H_2O_v mole fraction appears relatively consistent throughout the day (Fig. 4i). A positive d-excess anomaly relative to Rayleigh is present at the INV-FT interface, in contrast to the negative d-excess anomaly in STC (Fig. 4i). Inspection of the $\delta^{18}O$ (Fig. 4g) and δD values (Fig. 4h) show that δ values along VP1 and VP2 are consistent with Rayleigh predictions in the BL and in the more humid portion of the INV. As H_2O_v mole fractions decrease in the INV, the $\delta^{18}O$ and δD signatures observed on VP1 and VP2 transition to more negative values than the Rayleigh prediction, but approximately retain their original slope, suggesting agreement with the Rayleigh model if more isotopically-depleted initial conditions were considered. DBL VP3~~Measurements of ~~-~~$\delta^{18}O$ and δD values along DBL VP3 are the only observations during our airborne campaign measurements of ~~are~~ enriched, and relatively constant, δ values ~~relative to VP1 and VP2, and are~~ that extend from ~~relatively constant between~~ the BL through to the ~~and~~ FT (Fig. 11c)~~recall the grey shading in Fig. 4 represents the average range of INV H_2O_v mole fraction)~~. ~~Despite VP3 extending into the~~ FT~~,~~ H_2O_v mole fractions along VP3 only decreased to ~2500 ppmv, whereas H_2O_v mole fractions of 1700 ppmv and less were observed in the FT of VP1 and~~,~~ VP2~~, and VP4~~ (Fig. ~~4g-i~~11a-c and Fig. 12). Relatively humid conditions were also observed at the highest altitudes flown in the FT along VP4 (Fig. 11d). Enriched, vertically unvarying ~~VP4~~ $\delta^{18}O$ and δD values are unique to DBL VP3. VP4 $\delta^{18}O$ and δD values decrease across the INV (Fig. 11d),~~are~~ and track a δ-H_2O_v path similar ~~-~~to VP1 and VP2 ~~in~~ from the BL up~~through~~ to the ~~lower~~ INV-FT interface, which are similar in shape to both Rayleigh predictions or BL-FT mixing scenarios (Fig. 12). ~~However, the trend in the VP4 H_2O_v mole fraction reverses in the FT, at approximately 1370 m, and begins increasing.~~ Interestingly, VP4 FT $\delta^{18}O$ and δD values become enriched at higher altitudes, correspond~~s~~ing to an increase in H_2O_v mole fractions (Fig. 11d), and ~~instead~~ appear to track a mixing line with the VP3 δ values (red trace in Fig. 12d-e). Despite differences in δ value features along the four DBL VPs, the relationship between d-excess and H_2O_v mole fraction appears remarkably~~latively~~ consistent throughout the day (Fig. ~~4~~12c~~i~~). ~~A positive d-excess anomaly relative to Rayleigh is present at the INV-FT interface, in contrast to the negative d-excess anomaly in STC (Fig. 4i).~~

The relatively humid, isotopically-enriched FT air observed along VP3 and VP4 could have been caused by ~~A~~the shortwave trough in the mid-troposphere (3-5 km) which carried moist air into the Indianapolis study air in the late afternoon on this day~~ and likely influenced FT measurements~~ (Fig.~~ure~~ S5.3~~S6~~).~~-~~ The dewpoint profile in Fig. S7~~S2~~ shows this relatively moist mid-tropospheric air ~~descending~~subsiding over the course of the afternoon, reaching flight altitudes by the time VP3 and VP4 were~~as~~ flown~~conducted~~. The vertically unvarying, isotopically enriched VP3 observations likely reflect a combination of enhanced turbulence from the urban area and humid air from the shortwave trough mixing downward into the lower FT. In contrast, VP4 was conducted over a rural area north of Indianapolis~~ at the end of the flight~~, and likely did not experience the same degree of vertical mixing as the atmosphere downwind of Indianapolis (where VP3 was flown; Fig. 10a)~~ and a RL is not obvious (Fig. 6d). However, unlike VP1-3~~Potentially due to weaker turbulence in the rural area, a sharp decrease in δD and $\delta^{18}O$ was observed at z_{FT} on VP4 before increasing with altitude, ~~until~~ reaching enriched δ values observed in the VP4 BL and throughout VP3.

The DBL case study shows ~~the $\delta^{18}O$, δD and d-excess~~how isotopic water vapor measurements can be used as tracers to track the development of different atmospheric structures and circulations, including residual layers, urban heat island impacts, and passing fronts. δD,~~–~~ $\delta^{18}O$, and particularly d-excess can support meteorological measurements in identifying distinct atmospheric layers difficult to identify solely based on meteorological data.

~~3.4 General observations of H_2O_v isotopologues in the lower troposphere~~

~~The case study days presented above were chosen for their distinct isotopic features and because several VPs were conducted each day. However, they only represent 30% of the research flight days (Table 1). Figure 7a–c shows the Washington, D.C. Baltimore and Indianapolis VP absolute d-excess observations in the FT, INV, and BL, respectively. Figures 7d–f show the measured d-excess relative to Rayleigh distillation theory, i.e. Rayleigh-predicted d-excess has been subtracted from the observations. Overall, BL d-excess observations at the Indianapolis and Washington, D.C. Baltimore study sites are relatively consistent with Rayleigh theory when using observations on each day as the initial conditions (Fig. 7c). The greatest departures from Rayleigh theory were most commonly observed in the INV (Fig. 7b). Observations of d-excess in the INV at the Washington, D.C. Baltimore study site in particular were significantly more negative than Rayleigh predictions, by up to -80 ‰ (Fig. 7b). Very low H_2O_v mole fractions were commonly observed in the FT, as were large, positive d-excess values. Large positive d-excess values are predicted by Rayleigh distillation theory at low H_2O_v mole fractions. However, observed FT d-excess values are even more positive than the Rayleigh predictions in Fig. 7a at the lowest H_2O_v mole fractions.~~

~~The 7 March 2016 flight day in Indianapolis (RF07) stands out as an unusual set of conditions because the lower troposphere increased in H_2O_v mole fraction with altitude (Fig. 7a–c; gold trace). A warm, southerly front moved into the Indianapolis study area on this day, and rain preceded the flight observations. The relatively high H_2O_v mole fractions in the INV and FT likely reflect residual humidity from the storm. Overall, the RF07 VP observations do not exhibit distinctive isotopic features, and d-excess generally varies around Rayleigh predictions for the BL, INV, and FT (Fig. 7).~~

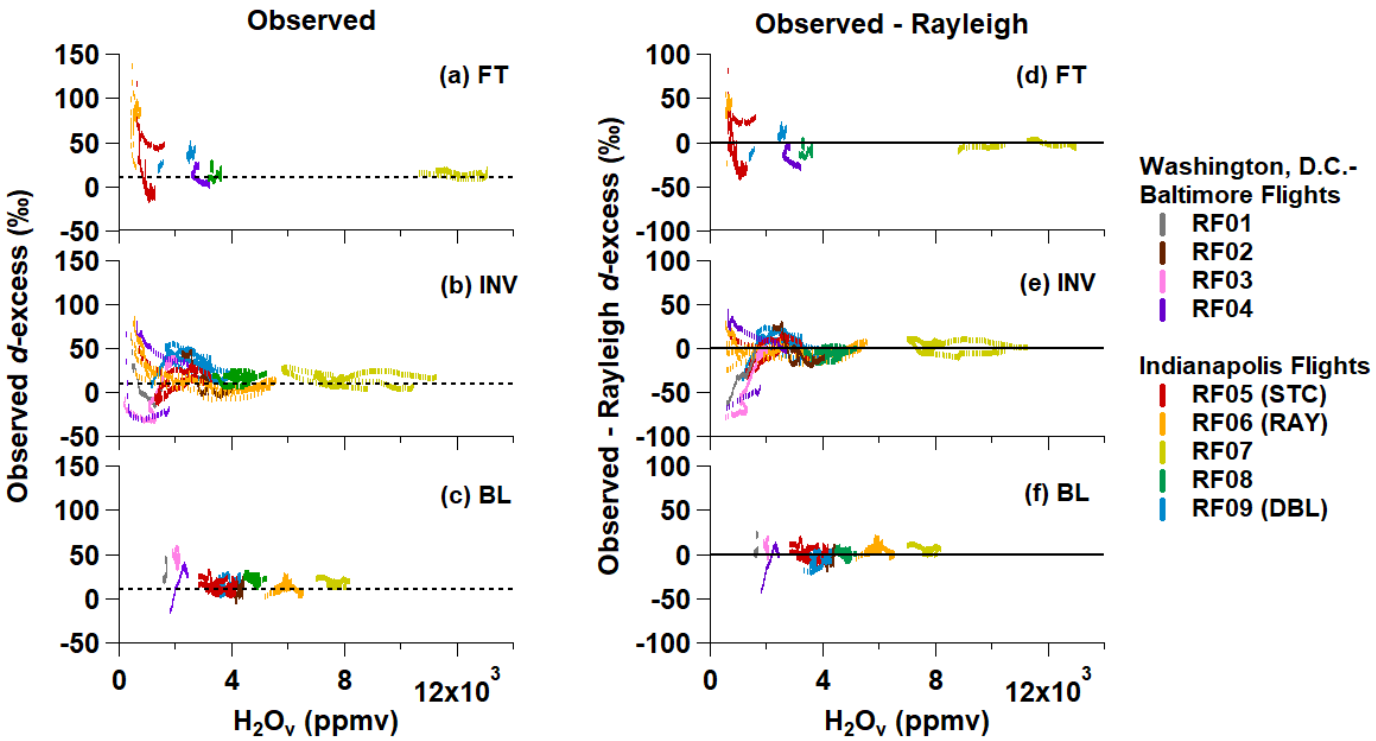

~~Figure 7: Rayleigh-subtracted d-excess observations in the (a) free troposphere (FT), (b) inversion (INV), and (c) boundary layer (BL) during all the VP descents. Colors indicate each research flight. BL, INV, and FT observations are defined by the rate of change of atmospheric variables, and not defined by H_2O_v mole fraction.~~

~~Most measurements of H_2O_v mole fraction in the FT were below 4000 ppmv; the corresponding FT measurements of $\delta^{18}O$, δD, and d-excess are plotted as a function of H_2O_v in Fig. S5. While each Washington, D.C.-Baltimore VP (Table 1) extended into the FT, H_2O_v mole fractions were often lower than the humidity range over which the TWVIA was calibrated (lower limit: 550 ppmv; Appendix B). Contributing to the scarcity of Washington, D.C.-Baltimore VP measurements is the fact that only one VP was conducted per flight, mainly as a result of congested and restricted air spaces near the capitol. Values of δD range from -30 to -60‰, $\delta^{18}O$ ranges from -200 to -400‰, and d-excess can be close to 10‰, but also increase up to 100‰ below 1000 ppmv.~~

~~4 Discussion~~

~~4.1 Rayleigh-Consistent Conditions~~

~~Previous observations have shown that Rayleigh distillation theory successfully explains most of the variability in H_2O_v isotopic composition observed in the BL (Lee et al., 2006). RAY is the simplest case study day where δ values and d-excess observations generally track the Rayleigh predictions in Fig. 4a-c. However, positive deviations from Rayleigh d-excess exist in the FT, and we hypothesize that dry FT air parcels carrying large, positive d-excess values can mix downward into more humid air parcels of smaller d-excess values near the top of the INV (Sodemann et al., 2017). As the H_2O_v mole fraction approaches zero, Rayleigh-predicted d-excess approaches 7000‰ (Bony et al., 2008). Thus, lower-altitude FT air masses can carry a more positive d-excess signature for a given H_2O_v mole fraction due to vertical mixing, than is predicted by Rayleigh theory (Fig. S5c). The d-excess signature in the FT more closely follows the FT-BL mixing line (Fig. 4c), which supports this hypothesis. Our results are consistent with Dyroff et al. (2015) who report lower troposphere δD observations over the Atlantic Ocean, and explain the vertical structure of δD at lower altitudes using Rayleigh theory, while higher altitude observations indicate mixing scenarios dictate the δD profile.~~

~~From our measurements, we can comment on what types of atmospheric conditions are likely to produce profiles consistent with Rayleigh theory, i.e. equilibrium fractionation and no vapor-condensate (cloud droplet) equilibration. The RAY meteorological and isotopic observations are very similar to those made on 17 March 2018 (RF08; Table 1). These two flight days' observations provide possible criteria for when it is appropriate to use Rayleigh theory to predict isotopic signature throughout the BL and INV. These criteria include that the study area is free of clouds/precipitation (supported by the presence of a dry adiabatic lapse rate throughout the BL) and wind speed and direction is relatively constant throughout the BL, INV, and FT. The STC and DBL case studies, which do not follow Rayleigh theory, violate one or more these criteria.~~

~~4.2 Stratocumulus Cloud Evaporation~~

~~Cloud processes may cause the d-excess anomalies from Rayleigh theory in the STC case study day. When evaluating the effect that cloud evaporation could have on vertical profiles of water vapour isotopic variability, we must consider the altitudes at which clouds form and evaporate. In the case of evaporation, this may not occur in a single layer, but throughout a range of altitudes or atmospheric layers. Stratocumulus cloud tops are typically present directly below z_{INV} (Wood, 2012). The top of the INV (z_{FT}) is approximately the upper limit of BL mixing (Wood, 2012). Lofting of cloud droplets into the INV would cause droplet evaporation, as the INV was under-saturated (Fig 5b). In the cloud evaporation scenarios discussed below, it is assumed that the cloud droplets form at the top of the BL, and the droplets undergo evaporation within the INV.~~

~~Figure 8a-b shows H_2O_v δD and d-excess predicted for several cloud evaporation scenarios. We choose to not show $\delta^{18}O$ under these cloud droplet evaporation scenarios because the results are similar to those for δD. Scenario 1 in Figure 8a shows that~~

~~the δD isotopic signature of atmospheric vapor that is influenced by 35% cloud droplet evaporation air (eq. 3 in Section 2.5) tracks the STC observations for VP3 and VP4 within the INV. While cloud evaporation scenario 1 tracks with observed d-excess in more humid portions of the INV (Figure 8b), it predicts larger positive d-excess in dryer portions of the INV (i.e. <2500 ppmv). This is the opposite of what is observed in d-excess at the upper (drier) part of the INV for VP2 through VP5. Scenario 1 does describe the steep slope in δD (and $\delta^{18}O$) values in the INV but does not explain the minimum in d-excess (Figure 8a).~~

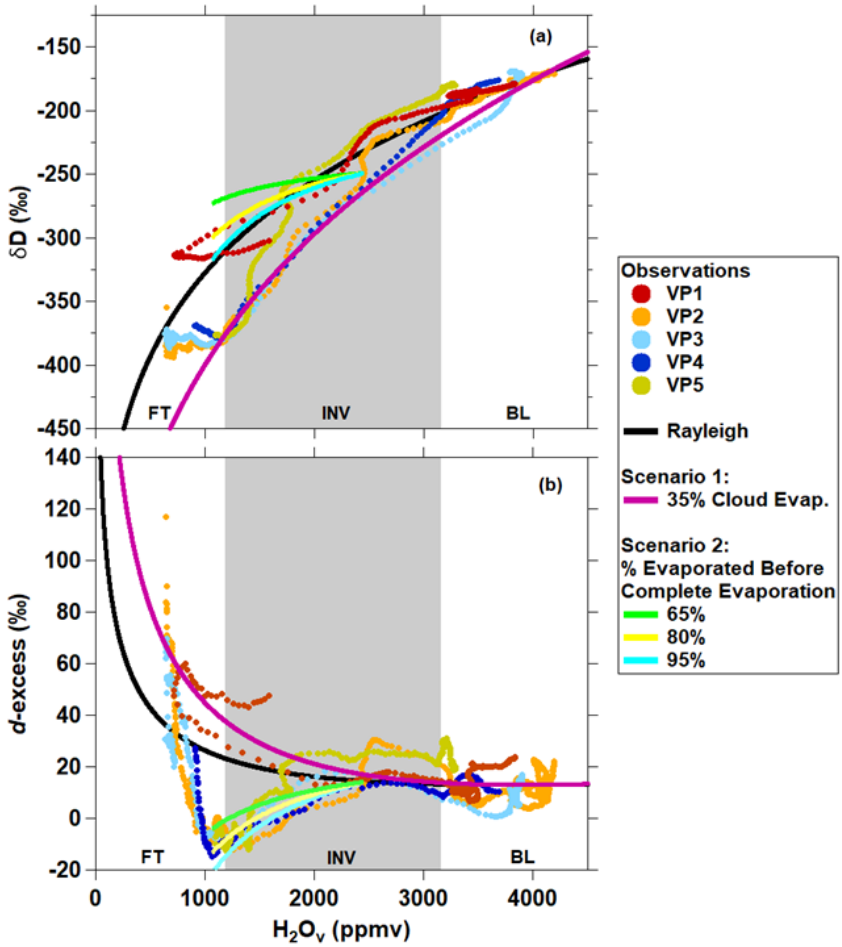

~~Figure 8: STC vertical profile (VP) (a) δD and (b) d-excesss observations plotted with different cloud droplet evaporation scenarios. The two scenarios consider partial cloud droplet evaporation (Scenario 1) or the complete evaporation of previously dehydrated cloud droplets followed by mixing (Scenario 2).~~

~~Cloud evaporation scenario 2 considers the effect of complete evaporation of a previously dehydrated cloud droplet (from eqs. 4-6 in Section 2.5). Figure 9 shows the d-excess signature of an evaporating cloud droplet that was formed at the top of the BL (consistent with stratocumulus cloud formation) evaporating into air that has an isotopic composition consistent with that observed at the top of the INV on STC. Figure 9 shows the d-excess signature of cloud droplets as they near complete evaporation, highlighting 65%, 80%, and 95% evaporation values. Figure 8 shows the effect of complete evaporation of these semi-dehydrated (65%, 80%, and 95%) cloud droplets at the top of the INV, followed by subsequent mixing with INV air (eq. 2 in Section 2.5). As can be seen from Figure 8b, scenario 2 describes the minimum d-excess signature at the top of INV. However, Figure 8a shows that scenario 2 does not agree with VP2-4 δD observations within the INV. It is possible that partial evaporation (scenario 1) occurs in the lower half of the INV, followed by complete evaporation of previously dehydrated cloud droplets at the top of the INV (scenario 2). We believe the minimum d-excess anomaly at z_{FT} for VP2-5 may result from complete evaporation of a partially dehydrated cloud droplet (Fig. 8b). We find discussion of these potential d-excess anomalies in the literature in reference to~~

~~raindrops evaporating below the cloud layer, but we believe the same isotopic fractionation would occur as liquid cloud droplets evaporate in unsaturated environments, such as at the top of the INV (Aemisegger et al., 2015; Gat, 1996; Sodemann et al., 2017).~~

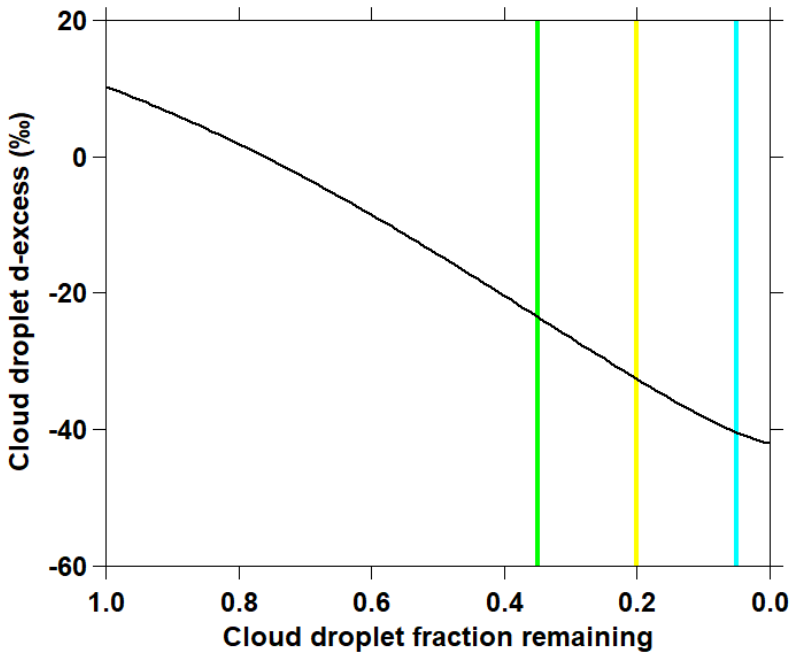

~~Figure 9. Cloud droplet (condensate) d-excess as a function of the fractional amount of the droplet lost to evaporation (calculated using eqs. 4-6). As cloud droplets dehydrate, d-excess values can become extremely negative. The d-excess signature of cloud droplets that have evaporated by 65%, 80%, and 95% are highlighted. The impact on d-excess of complete evaporation of these previously dehydrated cloud droplets, followed by mixing, is shown in Figure 8.~~

~~The slight easterly movement of the cloud layer as shown in Fig. S3 could be interpreted as the stratocumulus cloud layer being advected out of the Indianapolis study area by westerly winds rather than evaporating away. However, Fig. 5b shows that wind speeds at the cloud layer were relatively low (<6 m s^{-1}), and the clouds in Figure S3 transition from opaque to semi-transparent over the flight period. This information taken together suggests there was evaporation of the stratocumulus cloud layer during the flight.~~

~~We believe our observations provide evidence that the process of cloud evaporation may be spread throughout the INV layer with the beginning and end of evaporation separated in space. Within the INV, turbulent updrafts and downdrafts are warmer and cooler than the surrounding air, respectively (Betts, 1985). Updrafts potentially carrying partially evaporated cloud droplets to the top of the INV may facilitate complete evaporation of the droplets due to the low RH and possibly wind shear-promoted mechanical turbulence at z_{FT} (Fig. 5b). Due to higher RH values within the middle of the INV relative to z_{FT}, it is possible cloud droplet evaporation did not proceed to completion at these INV altitudes. Partial evaporation would impart a positive d-excess signal on atmospheric vapor and act to increase RH (Aemsigger et al., 2015; Sodemann et al., 2017), both of which exhibit a local maximum at ~985 m agl (Fig. 5b).~~

~~Other studies have reported negative water vapor d-excess and hypothesize that these are from kinetic fractionation of vapor during deposition on ice crystals or snow (i.e. in ice-supersaturated conditions) (Casado et al., 2016; Galewsky, 2015; Lowenthal et al., 2016; Moore et al., 2016; Samuels-Crow et al., 2014; Schmidt et al., 2005). It is unlikely that ice supersaturation is responsible for the minimum in vapor d-excess observed at z_{FT} on STC because temperatures were greater than 0°C (Table 1). However, as an example, Figure D1 shows the theoretical d-excess values of STC vapor under ice-supersaturated conditions (Appendix D). We reiterate that ice-supersaturation is an unlikely explanation for the STC z_{FT} d-excess minimum because flight~~

~~altitudes were less than 2 km, and ice (cirrus) clouds are typically present at ~6 km. It is unlikely that ice hydrometeors falling from higher altitudes could be sustained at the top of the inversion and contribute to the low d-excess signal observed on VP2-VP5 through vapor deposition given the >0ºC temperatures. While vapor deposition in ice supersaturated conditions might not be relevant for the STC flight, low d-excess (relative to Rayleigh at RH = 100 %) was sometimes observed in the INV layers during the Washington, D.C.-Baltimore flights (Fig. 7b). Ambient temperatures observed in flight in Washington, D.C.-Baltimore were sometimes less than 0ºC (Table 1), thus vapor deposition on ice crystals would be more likely for those scenarios.~~

~~4.3 Developing Boundary Layer~~

~~Unlike RAY and STC, the vertical structures of H_2O_v, δD, $\delta^{18}O$, and d-excess observed in DBL are highly variable in both space and time (Fig. 6). Despite variability in the vertical structure, a fairly consistent d-excess – H_2O_v relationship is maintained throughout the flight (Fig. 4i). Here we attempt to interpret and explain the heterogeneity in the DBL VPs.~~

~~A unique feature of DBL is the presence of a residual layer (RL), which was incorporated into the BL throughout the duration of the flight. This residual layer hypothesis is supported by Fig. S2, which shows that on the day prior to DBL, 17 March 2016, Rapid Refresh Model ambient temperature profiles follow a nearly dry adiabatic lapse rate all the way to an altitude of 3 km. This was a relatively warm, turbulent day and H_2O_v isotopologue observations were consistent with Rayleigh theory (Table 1, RF08). A cold front moved into the Indianapolis study area on DBL (18 March 2016). The ambient temperature profile on DBL shows the previous day's residual layer persisted into the early afternoon, between approximately 1 – 3 km (Fig. S2), before being incorporated into the BL. The distinction between the RL and BL blurs as surface heating progresses throughout the day and the RL is incorporated into the BL. It would also be expected that the downwind edge of the Indianapolis city boundaries (winds were from the northwest; Fig. 3c) would have more well mixed BL due to stronger turbulent mixing from the urban heat island and increased surface roughness (Grimmond et al., 2010; Stull, 1988). Support for this is given by DBL VP3 observations (Fig. 6c), which reveal a considerably more homogenous structure in δD and $\delta^{18}O$ relative to VP1 and VP2. The ambient temperatures measured along VP3 in the FT and RL are warmer relative to ambient temperatures along the other three VP's (Fig. 6), indicating the influence of the urban heat island. Although the VP3 H_2O_v, δD, and $\delta^{18}O$ values are relatively more homogenous in the vertical dimension, the d-excess signatures still maintain indications of the RL, as the vertical structure of d-excess is similar to VP2 d-excess observations. This is an example of how d-excess can provide more clues about atmospheric circulation than can δD or $\delta^{18}O$ alone.~~

~~A shortwave trough in the mid-troposphere (3-5 km) carried moist air into the Indianapolis study air in the late afternoon on this day and likely influenced FT measurements (Figure S6). The dewpoint profile in Fig. S2 shows this relatively moist mid-tropospheric air descending over the course of the afternoon, reaching flight altitudes by the time VP4 was conducted. VP4 was conducted over a rural area north of Indianapolis at the end of the flight and a RL is not obvious (Fig. 6d). However, unlike VP1-3, a sharp decrease in δD and $\delta^{18}O$ was observed at z_{FT} on VP4 before increasing with altitude until reaching δ values observed in the VP4 BL and throughout VP3. The DBL case study shows the $\delta^{18}O$, δD and d-excess measurements can be used as tracers to track the development of different atmospheric structures and circulations, including residual layers, urban heat island impacts, and passing fronts.~~

~~**4.4 Features of the lower troposphere d-excess vertical profile**~~

~~The data presented here are some of the few lower troposphere water vapour isotope observations published, so we look for common patterns that can be used to predict values in other areas. Nearly all BL observations of d-excess at the Indianapolis and Washington, D.C. Baltimore study sites agree well with Rayleigh theory (Fig. 7c). This is consistent with previous observations showing that Rayleigh distillation theory successfully explains most of the variability in H_2O_v isotopic composition observed in the BL (Lee et al., 2006).~~

~~The FT is generally drier than the BL (Fig. 7a), and FT d-excess values observed at very low H_2O_v mole fractions are often more positive than predicted by Rayleigh theory (Fig. 7a). This has been explained by very dry, depleted FT air masses, which carry large positive d-excess signatures, mixing downward towards flight-level altitudes (Bony et al., 2008; Sodemann et al., 2017). These FT air masses likely would have originated from another source region and possibly underwent multiple condensation cycles to achieve such isotopic depletion prior to mixing with more humid air across the INV. Thus, we do not necessarily expect FT air to have a d-excess signature consistent with Rayleigh theory of an ascending BL air parcel (Dyroff et al., 2015).~~

~~We observed large departures from Rayleigh theory in the INV. Figures 7b and 7e show that d-excess observations in the Washington, D.C. Baltimore INV can deviate negatively by ~80‰ relative to Rayleigh predictions. We believe the minimum in STC d-excess at z_{FT} is a result of stratocumulus cloud evaporation. Partly cloudy or overcast conditions were also present over the Washington, D.C. Baltimore study site on all four Washington, D.C. Baltimore flights (https://worldview.earthdata.nasa.gov/; https://www.ncdc.noaa.gov). It is possible that the very negative Washington, D.C. Baltimore INV d-excess measurements were a result of complete evaporation of semi-evaporated cloud droplets within the inversion. We note that the most negative Washington, D.C. Baltimore d-excess values correspond to the driest INV observations (Fig. 7b), where we would expect cloud top evaporation resulting from free troposphere entrainment to be the most prevalent.~~

5 Conclusions

The aim of this study is to observe and interpret the vertical structure of H_2O_v stable isotopic composition, specifically d-excess, in the continental lower troposphere. ~~Current literature regarding~~Previous studies presenting d-excess observations are~~is~~ heavily focused on ocean evaporation at coastal or island surface sites (Benetti et al., 2014; 2015; 2018; Delattre et al., 2015; Steen-Larsen et al., 2014; Uemura et al., 2008). Few reported observations of d-excess in the INV and FT exist (Galewsky et al., 2015; Lowenthal et al., 2016; Kelsey et al., 2018; Samuels-Crow et al., 2014; Schmidt et al., 2005; Sodemann et al., 2017), and, to our knowledge, only one study has used airborne measurements to provide high vertical resolution snapshots of the lower troposphere d-excess profile at discrete time points (Sodemann et al., 2017). Our stable H_2O_v isotope measurements over two continental sites is a starting point in filling the field's gap in understanding variability in the lower troposphere d-excess profile, and what it reveals about lower troposphere moisture processing on relatively small regional scales.

Our observations reaffirm the dominant role that Rayleigh distillation processes have on H_2O_v~~water vapour~~ isotopic ~~variability~~signature, and that isotopic signatures can be retained by air masses as they are advected from previous points of condensation. Our measurements indicate that H_2O_v isotopologues, and d-excess in particular, can act as fingerprints of earlier processes.~~ especially in the boundary layer.~~ This ~~process~~ is true for the CLR case study, in which Rayleigh distillation curves well-represent~~can predict~~ vertical profile observations from near the surface up through the atmospheric inversion layer, despite ~~that~~ the

temperature profile within the BL follow~~ed~~ing the dry, rather than the (Rayleigh-assumed) moist~~,~~ adiabat. ~~in clear-sky conditions with reasonably constant wind conditions with height.~~ Similarly, the evidence of upwind processes was also retained in the H_2O_v isotopic signature on STC. The STC measurements give clues that the observed air mass experienced prior evaporation of cloud or rain droplets. Measurements made during the rapidly changing atmospheric conditions on the DBL case study also show that H_2O_v isotopic signature can reflect near-instantaneous changes in the atmosphere. These new results highlight the potential for H_2O_v~~water vapour i~~ isotope ratios, especially d-excess, to ~~diagnose~~ identify complex processes across the atmospheric inversion layer including cloud condensation, evaporation, and mixing or entrainment of free tropospheric air into the boundary layer. These types of measurements may become increasingly valuable as we seek to understand the physical processes that sustain cloud layers and spati~~al-~~otemporally variable boundary layer mixing depths.

Our interpretation of the d-excess VPs could be further evaluated by isotope-enabled circulation and weather models (Aemisegger et al., 2015; Pfahl et al., 2012; Schmidt et al., 2005). However, the simulation of convective boundary layer ~~BL~~ processes with isotope-enabled models is complex (Bolot et al., 2013; Benetti et al., 2018). The measurements reported here could help further develop current and forthcoming isotope enabled models, particularly for simulating wintertime, continental lower troposphere processes or stratocumulus evaporation. Our observations of the d-excess profile in a stratocumulus cloud-topped ~~BL~~ boundary layer and the d-excess observations reported by Sodemann et al. (2017) near marine cumulus clouds ~~seem to indicate~~represent an opportunity to investigate cloud-class specific ~~RH and~~ d-excess relationships. Future studies could ~~interrogate~~ investigate the sensitivity of the d-excess signature to different classes of clouds and their associated unique cloud processes.

Data availability.

~~Geospositional~~Geopositional, meteorological, greenhouse gas, and water vapor isotope measurements are available for the Washington, D.C.-Baltimore and Indianapolis flight days (Table 1) are available by request and will be archived upon publication in the stable water vapour isotope database: https://vapor-isotope.yale.edu/. The authors request that they be notified if the data is to be used in publication.

~~**Appendices**~~

~~**Appendix A. Comparison of LGR and Picarro H_2O_v mole fraction**~~

~~Figure A1 compares calibrated H_2O_v mole fractions from the Los Gatos Research (LGR) Triple Water Vapor Isotope Analyzer (TWVIA) and the Picarro cavity ringdown spectrometer during the entire flight conducted on 6 March 2016 (RAY).~~

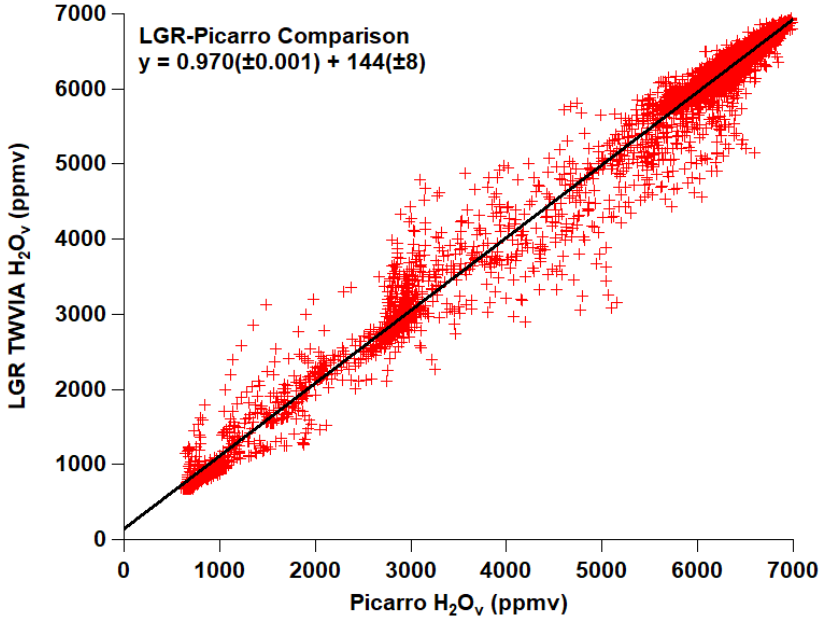

Figure A1: Comparison of calibrated LGR and Picarro H_2O_v mole fraction measurements from the entire research flight conducted on 6 March 2016 (RAY).

Appendix B. Water vapor concentration-dependence calibration

A Los Gatos Research (LGR) Water Vapor Isotope Standard Source (WVISS; model: 908-0004-9003) equipped with a secondary dry air mixing chamber for extended range operation was used to characterize the LGR Triple Water Vapor Isotope Analyzer's (TWVIA; model: 911-0034) non-linear response to water vapor (H_2O_v) concentration (Rambo et al., 2011). The WVISS samples liquid water with a known isotopic composition from a reservoir. The standard sample is then nebulized using zero (dry) air into a heated chamber (75°C), where it evaporates completely and is further diluted with zero (dry) air with programmable flow rates to output a range of H_2O_v fractions with the same isotopic signature as the liquid standard. Different combinations of nebulizer sizes (flow rates) and standard versus extended range operation were required to span a large range of H_2O_v values. The TWVIA's H_2O_v dependence (while operating in extended range mode, ~80 Torr) was evaluated over the range from 550 ppmv – 14,000 ppmv, consistent with range of H_2O_v mole fractions observed during the research flights (Table 1). Free troposphere H_2O_v mole fractions were sometimes less than 550 ppmv, but the lowest H_2O_v mole fraction the WVISS can emit is 500 ppmv and we found stable flows of H_2O_v mole fractions lower than 550 ppmv were difficult to achieve with the WVISS. We opt not to report δD and $\delta^{18}O$ values for instances when H_2O_v mole fraction is less than 550 ppmv. The δD and $\delta^{18}O$ values of the H_2O_v isotope standards, which bracket the ranges observed during the research flights (Table 1), are listed in Table B1. The WVISS was programmed to sample each H_2O_v mole fraction for ≥20 min. The δD and $\delta^{18}O$ H_2O_v dependence calibration curves were constructed from the average δD and $\delta^{18}O$ values reported during the last 200 s of each calibration period in order to remove any influence of transition instability caused by water moving onto and off of the walls of the system during the calibration H_2O_v step changes. The $\delta^{18}O$ and δD H_2O_v dependence curves shown in Fig. B1 and B2, respectively, were fit using the locally weighted polynomial regression "locpoly" function from R's "locfit" package (Bailey et al., 2015). A 100 ppmv sliding window was used for the local polynomial regression fitting over the range from 550 ppmv – 14,000 ppmv H_2O_v.

Table B1: Calibration standards

Standard*	δD (‰)	$\delta^{18}O$ (‰)	d-excess (‰)
Purdue tap water	-39.9	-8.7	29.7

~~Boulder tap water~~	~~-117.3~~	~~-15.4~~	~~5.9~~
~~USGS-46~~	~~-235.8~~	~~-29.8~~	~~2.6~~
~~South Pole Glacier Water~~	~~-434.5~~	~~-54.3~~	~~-0.1~~
~~Custom Light Blend‡~~	~~-573.7~~	~~-76.2~~	~~36.1~~

~~*Standard values are reported relative to the VSMOW-SLAP scale~~

~~‡The Custom Light Blend is a mixture of Purdue tap water, Sigma-Aldrich deuterium depleted water (≤1 ppm HDO), and Isotec 95% $H_2{}^{18}O$ (^{18}O-enriched) to achieve a depleted isotopic signature that brackets the most depleted research flight observations of δD and $\delta^{18}O$ that also has a realistic d-excess signature. Because the Custom Light Blend is isotopically more depleted than our standards, known amounts of the Custom Light Blend and Purdue tap water were combined to make three mixtures, which were analysed using an LGR liquid-water isotope analyser (T-LWIA-45-EP; model: 912-0050-0001) to determine the Custom Light Blend's isotopic signature.~~

~~The TWVIA's H_2O_v dependence curve was reproducible over all $\delta^{18}O$ isotope standard signatures considered (Table B1). The δD-H_2O_v dependence curve was reproducible for the three relatively enriched isotope standards, more enriched than -235.8‰, in Table B1 but was not always reproducible using the most depleted standards (South Pole Glacier and Custom Light Blend) over the H_2O_v range of ~3000 ppmv to ~ 8000 ppmv as is shown in the Figure B1a and B2a. At H_2O_v mole fractions above and below that range, the calibration curve remained reproducible. The cause of the 3000 ppmv – 8000 ppmv irreproducibility of the δD-H_2O_v dependence curve associated with very depleted δD values remains unknown, perhaps small leaks in the experimental setup or uncertainty associated with curve fitting. To our knowledge this behaviour has not been described in the literature. However, δD values consistent with the two most depleted standards (Table B1) were only observed in the free troposphere and correspond to low H_2O_v mole fractions (<1000 ppmv) and were outside of the irreproducible window of H_2O_v values. Therefore, it was not consequential to actual flight observations in this experiment. We note that there also appears to be large variability in the TWVIA-reported δD values <1000 ppmv H_2O_v for the two depleted standards, but there is also relatively larger variability in this H_2O_v range for the enriched standards as well. To avoid biases resulting from the depleted δD irreproducibility, the δD water vapor dependence curve is defined using calibration data from the three relatively enriched standards. However, δD calibration data from each of the five standards is used to define uncertainties (see below in Appendix C).~~

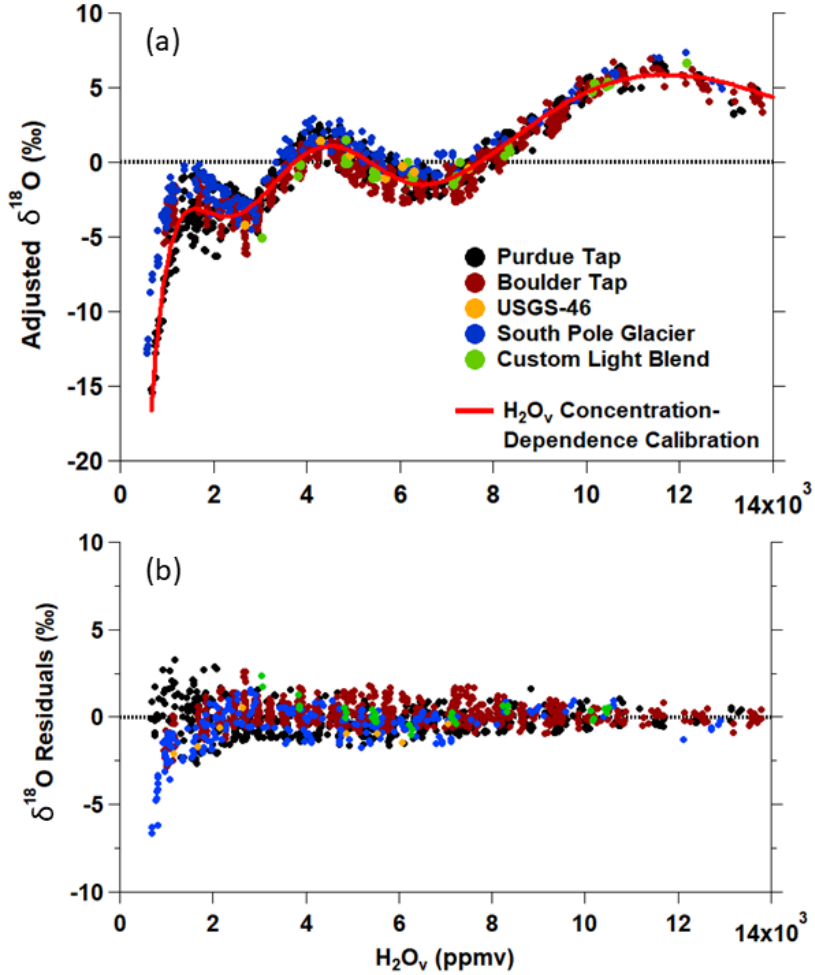

~~**Figure B1: $\delta^{18}O$-H_2O_v dependence (a) calibration curve and (b) residuals. The true $\delta^{18}O$ signature of each standard (Table B1) has been subtracted from the TWVIA measurements to give the "adjusted" $\delta^{18}O$ signature in (a).**~~

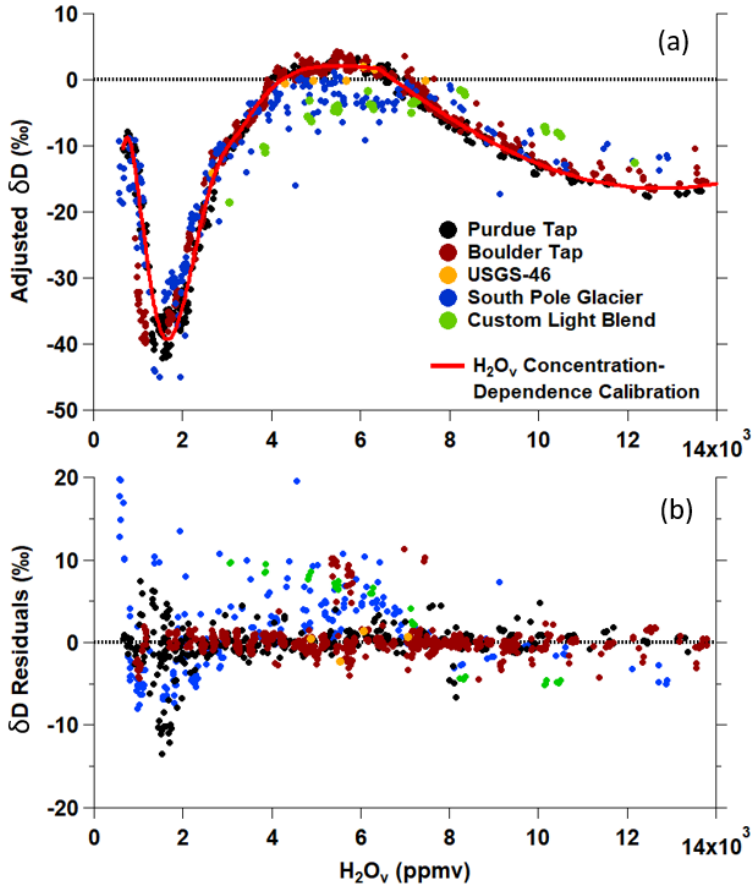

~~**Figure B2: δD-H_2O_v dependence (a) calibration curve and (b) residuals. The true δD signature of each standard (Table B1) has been subtracted from the measurements to give the "adjusted" δD signature in (a).**~~

~~To check calibration the VSMOW-SLAP scale, Figure B3 shows that the linear regressions of the isotope standards' H_2O_v concentration-dependence-corrected δ values versus true gas phase isotopic signature for (a) $\delta^{18}O$ and (b) δD have slopes near unity and intercepts near zero. $\delta^{18}O$ had a slope of 1.009(±0.001), a y-intercept of 0.08(±0.03), and an R^2 of 0.997254. The δD ordinary least-squares regression line had a slope of 0.9954(±0.0005), a y-intercept of −0.5(±0.09), and an R^2 of 0.99958. A VSMOW-SLAP correction was not applied because it would be negligible compared to the uncertainty associated with the concentration-dependence correction and the instrument precision (Appendix C).~~

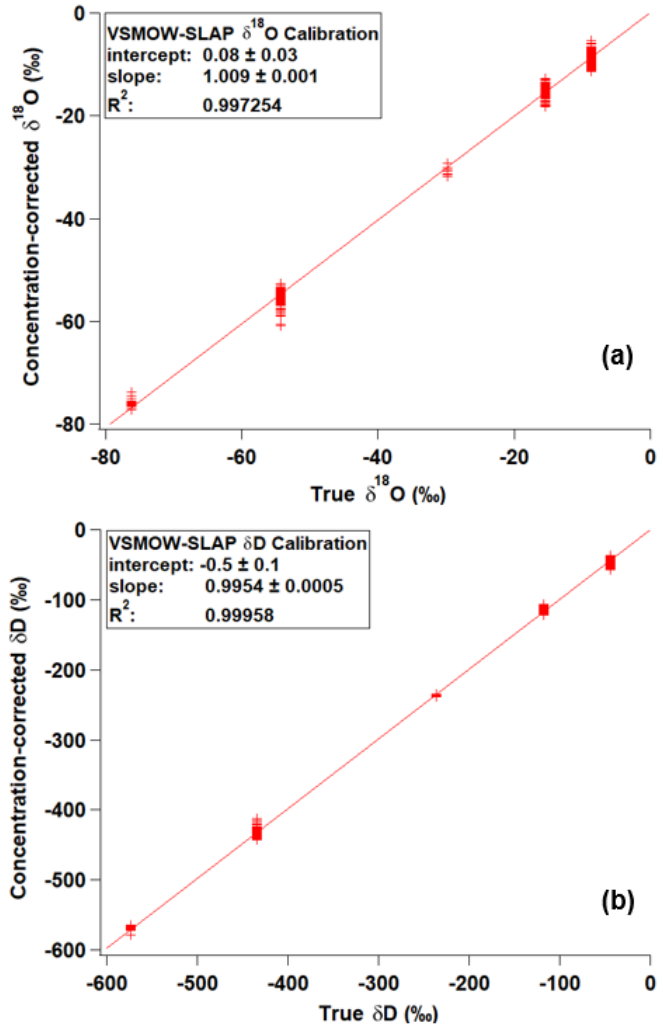

~~**Figure B3. VSMOW-SLAP calibration curves for (a) $\delta^{18}O$ and (b) δD. H_2O_v-concentration-corrected isotopic signatures are plotted against the standard's true isotopic signature. Linear regression fit slopes and intercepts are included in the figure insets.**~~

~~**Appendix C. Water vapor δD, $\delta^{18}O$, and d-excess error propagation**~~

~~**Instrument precision:**~~

~~The TWVIA instrument precision was calculated as the 1σ standard deviation for the last 20 seconds of every calibration period (Appendix B). The interval used to smooth the δD, $\delta^{18}O$, and d-excess values reported in this paper is 20 s, which corresponds to the time required for the TWVIA signal to stabilize after a change in the sample's H_2O_v mole fraction or isotopic signature. The δD and $\delta^{18}O$ precision values are calculated as a function of H_2O_v mole fraction using power functions (Fig. C1).~~

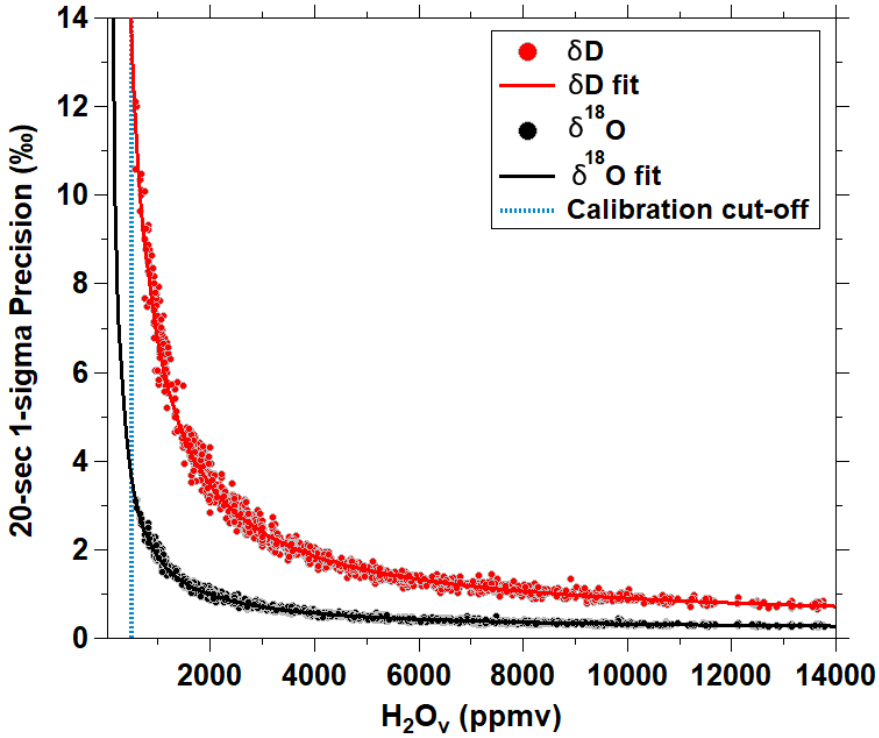

~~**Figure C1: TWVIA $\delta^{18}O$ and δD 20-s instrument precision (1σ) as a function of water vapor (H_2O_v) mole fraction.**~~

~~**H_2O_v dependence calibration uncertainty:**~~

~~The uncertainty associated with the TWVIA δD and $\delta^{18}O$ H_2O_v dependence corrections is determined from the calibration residuals shown in Fig. B1b and Fig. B2b. We note that the calibration residuals do include a small instrument precision component, as the calibration values are the average of 200 s sampling periods. The absolute value of the δD and $\delta^{18}O$ residuals from all five reference waters tested were filtered into bins defined by 100 ppmv H_2O_v mole fraction increments. Averages of the absolute δD and $\delta^{18}O$ residuals were calculated for each bin. For relatively dry conditions (i.e. below 3500 ppmv H_2O_v), the bin-averaged calibration residuals increase as H_2O_v mole fractions decrease. A best-fit linear regression was determined for the bin-averaged residuals as a function of H_2O_v mole fraction (from 550 – 3500 ppmv for δD and 550 – 3700 ppmv for $\delta^{18}O$). Bin-averaged residuals were relatively constant for H_2O_v mole fractions greater than 3500 ppmv for δD and 3700 ppmv for $\delta^{18}O$. Average H_2O_v dependence calibration uncertainties of 1.8‰ for δD and 0.9‰ for $\delta^{18}O$ were calculated from the bin-averaged residuals from 3500 – 14000 ppmv for δD and 3700 – 14000 ppmv for $\delta^{18}O$. Higher uncertainties in the δ values at low H_2O_v mole fractions is not surprising, as the manufacturer suggests the TWVIA be used for sampling air ranging from 4,000 – 60,000 ppmv H_2O_v.~~

~~**Total uncertainty:**~~

~~Total δD and $\delta^{18}O$ uncertainty is calculated by propagating the error resulting from instrument precision, $S_{precision}$, and from the calibration, $S_{calibration}$, as in eq. (C1):~~

$$\cancel{S_{total} = \sqrt{S_{precision}^{2} + S_{calibration}^{2}}.} \qquad \cancel{(C1)}$$

~~The total d-excess uncertainty is determined according to eq. (C2):~~

$$S_{total,d-excess} = \sqrt{S_{total,\delta D}{}^{2} + 8 \times (S_{total,\delta^{18}O}{}^{2})}, \quad \text{(C2)}$$

where $S_{total,\delta D}$ and $S_{total,\delta^{18}O}$ are the total δD and $\delta^{18}O$ uncertainties (given be eq. (C1)). The total uncertainty for δD, $\delta^{18}O$, and d-excess as function of H_2O_v mole fraction is presented in Fig. 1.

Appendix D. Fractionation of water vapor in ice supersaturated conditions

H_2O_v undergoing deposition in ice-supersaturated conditions is impacted by equilibrium and kinetic fractionation. The kinetic fractionation factor is calculated via Galewsky (2015) eq. (D1):

=, (D1)

where is saturation with respect to ice, expressed as a fraction. The equilibrium fractionation factor calculated for the temperature at the lifting condensation level (LCL) and is discussed in Methods 2.5. The ratio of the molecular diffusivity of the light to heavy isotopologue, , is 1.02849 for ^{18}O and 1.02512 for D (Merlivat, 1978).

The isotopic signature of an air parcel in ice supersaturated conditions () can be calculated according to eq. (D2):

= (D2)

 is the heavy to light isotopologue ratio (or) of the parcel prior to the ascent. The remaining fraction of H_2O_v left in the ascending parcel relative to initial conditions is given by .

Figure D1 shows the STC VP d-excess observations along with Raleigh vapor calculated from RH = 100 % (Methods 2.5) and vapor in ice supersaturated conditions (eq. (D2)). To match the most negative d-excess value observed at the top of the INV on STC, a supersaturation () of 1.17 (RH_i = 117% in Fig. D1) was used but does not necessarily reflect reality for the temperature or altitude of the observations. The Rayleigh curve is presented for reference.

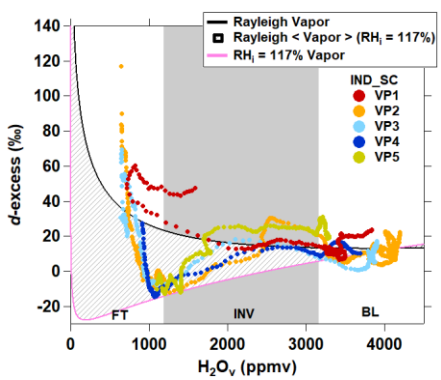

Figure D1: STC VP d-excess observations, Rayleigh vapor d-excess, and calculated d-excess of vapor in ice supersaturated (RHi) conditions up to RHi = 117 %. Ice supersaturated conditions were chosen merely to match the INV-FT interface d-excess observations, and do not necessarily reflect a realistic RH_i for the STC flight day.

Supplement link. ~~Figures~~ Sections S1-~~6~~ S7 are provided in the accompanying Supporting Information. ~~Figure S3 and Figure S4 are GIFs available in separate files.~~

Competing interests.

The authors declare no competing interests.

Author contribution.

OS, LW, and PS designed the experiments. OS collected the airborne data, with the help of KH. OS analysed the data. OS, LW, MB, and PS interpreted the results. OS prepared the manuscript with contributions from all co-authors. BS maintained the experimental aircraft.

Acknowledgments.

We thank Bruce Vaughn of the Institute of Arctic and Alpine Research (INSTAAR) for generously sharing a sample of South Pole Glacier isotope standard. We are grateful to Tomas Ratkus of Purdue University Science IT for his technological expertise while we prepared for the research flights. We thank LGR tech support for corresponding with us while we characterized the TWVIA's water vapor concentration dependence. We thank Purdue University's Jonathon Amy Facility for Chemical Instrumentation (JAFCI) for their expertise in designing and maintaining ALAR's instrument suite. We acknowledge funding support from James Whetstone and the National Institute of Standards and Technology. We also thank two anonymous reviewers for their insight and invaluable suggestions.

References

Aemisegger, F., Spiegel, J. K., Pfahl, S., Sodemann, H., Eugster, W., and Wernli, H.: Isotope meteorology of cold front passages: A case study combining observations and modeling, Geophys. Res. Lett., 42, 5652-5660, 10.1002/2015gl063988, 2015.

Bailey, A., Noone, D., Berkelhammer, M., Steen-Larsen, H. C., and Sato, P.: The stability and calibration of water vapor isotope ratio measurements during long-term deployments, Atmos. Meas. Tech., 8, 4521-4538, 10.5194/amt-8-4521-2015, 2015.

Benetti, M., Reverdin, G., Pierre, C., Merlivat, L., Risi, C., Steen-Larsen, H. C., and Vimeux, F.: Deuterium excess in marine water vapor: Dependency on relative humidity and surface wind speed during evaporation, J. Geophys. Res.: Atmos., 119, 584-593, doi:10.1002/2013JD020535, 2014.

Benetti, M., Aloisi, G., Reverdin, G., Risi, C., and Sèze, G.: Importance of boundary layer mixing for the isotopic composition of surface vapor over the subtropical North Atlantic Ocean, J. Geophys. Res.: Atmos., 120, 2190-2209, 10.1002/2014jd021947, 2015.

Benetti, M., Lacour, J. L., Sveinbjörnsdóttir, A. E., Aloisi, G., Reverdin, G., Risi, C., Peters, A. J., and Steen-Larsen, H. C.: A framework to study mixing processes in the marine boundary layer using water vapor isotope measurements, Geophys. Res. Lett., 0, doi:10.1002/2018GL077167, 2018.

Bolot, M., Legras, B., and Moyer, E. J.: Modelling and interpreting the isotopic composition of water vapour in convective updrafts, Atmos. Chem. Phys., 13, 7903-7935, 10.5194/acp-13-7903-2013, 2013.

Bony, S., Risi, C., and Vimeux, F.: Influence of convective processes on the isotopic composition ($\delta^{18}O$ and δD) of precipitation and water vapor in the tropics: 1. Radiative-convective equilibrium and Tropical Ocean–Global Atmosphere–Coupled Ocean-Atmosphere Response Experiment (TOGA-COARE) simulations, J. Geophys. Res.: Atmos., 113, doi:10.1029/2008JD009942, 2008.

Brown, D., Worden, J., and Noone, D.: Comparison of atmospheric hydrology over convective continental regions using water vapor isotope measurements from space, J. Geophys. Res.: Atmos., 113, 10.1029/2007jd009676, 2008.

Casado, M., Landais, A., Masson-Delmotte, V., Genthon, C., Kerstel, E., Kassi, S., Arnaud, L., Picard, G., Prie, F., Cattani, O., Steen-Larsen, H. C., Vignon, E., and Cermak, P.: Continuous measurements of isotopic composition of water vapour on the East Antarctic Plateau, Atmos. Chem. Phys., 16, 8521-8538, 10.5194/acp-16-8521-2016, 2016.

~~Craig, H., and Gordon, L. I.: Deuterium and oxygen 18 variations in the ocean and marine atmosphere, in proc. Stable Isotopes in Oceanographic Studies and Paleotemperatures, edited by: Tongiogi, E., Spoleto, Italy, 9-130 pp., 1965.~~

Crawford, T. L., and Dobosy, R. J.: A sensitive fast-response probe to measure turbulence and heat flux from any airplane, Bound.-Layer Meteo., 59, 257-278, 10.1007/BF00119816, 1992.

Dai, C., Wang, Q., Kalogiros, J. A., Lenschow, D. H., Gao, Z., and Zhou, M.: Determining boundary-layer height from aircraft measurements, Bound.-Layer Meteo., 152, 277-302, 10.1007/s10546-014-9929-z, 2014.

Dansgaard, W.: Stable isotopes in precipitation, Tellus, 16, 436-468, doi:10.1111/j.2153-3490.1964.tb00181.x, 1964.

Delattre, H., Vallet-Coulomb, C., and Sonzogni, C.: Deuterium excess in the atmospheric water vapour of a Mediterranean coastal wetland: regional vs. local signatures, Atmos. Chem. Phys., 15, 10167-10181, 10.5194/acp-15-10167-2015, 2015.

Dyroff, C., Sanati, S., Christner, E., Zahn, A., Balzer, M., Bouquet, H., McManus, J. B., González-Ramos, Y., and Schneider, M.: Airborne in situ vertical profiling of HDO / $H_2{}^{16}O$ in the subtropical troposphere during the MUSICA remote sensing validation campaign, Atmos. Meas. Tech., 8, 2037-2049, 10.5194/amt-8-2037-2015, 2015.

Ellehøj, M. D., Steen-Larsen, H. C., Johnsen, S. J., and Madsen, M. B.: Ice-vapor equilibrium fractionation factor of hydrogen and oxygen isotopes: Experimental investigations and implications for stable water isotope studies, Rapid Commun. Mass Spectrom., 27, 2149-2158, doi:10.1002/rcm.6668, 2013.

Field, R. D., Jones, D. B. A., and Brown, D. P.: Effects of postcondensation exchange on the isotopic composition of water in the atmosphere, J. Geophys. Res.: Atmos., 115, 10.1029/2010jd014334, 2010.

~~Fiorella, R. P., Bares, R., Lin, J. C., Ehleringer, J. R., and Bowen, G. J.: Detection and variability of combustion-derived vapor in an urban basin, Atmos. Chem. Phys. Discuss., https://doi.org/10.5194/acp-2017-1106, in review, 2018.~~

Froehlich, K., Kralik, M., Papesch, W., Rank, D., Scheifinger, H., and Stichler, W.: Deuterium excess in precipitation of Alpine regions – moisture recycling, Isotopes Environ. Health Stud., 44, 61-70, 10.1080/10256010801887208, 2008.

Galewsky, J., Strong, M., and Sharp, Z. D.: Measurements of water vapor D/H ratios from Mauna Kea, Hawaii, and implications for subtropical humidity dynamics, Geophys. Res. Lett., 34, 10.1029/2007gl031330, 2007.

Galewsky, J.: Constraining supersaturation and transport processes in a south american cold-air outbreak using stable isotopologues of water vapor, Journal of the Atmospheric Sciences, 72, 2055-2069, 10.1175/jas-d-14-0352.1, 2015.

Galewsky, J., Steen-Larsen, H. C., Field, R. D., Worden, J., Risi, C., and Schneider, M.: Stable isotopes in atmospheric water vapor and applications to the hydrologic cycle, Rev. Geophys., 54, 809-865, doi:10.1002/2015RG000512, 2016.

Garman, K. E., Hill, K., Wyss, P., Carlsen, M., Zimmerman, J., Stirm, B., Carney, T., Santini, R., and Shepson, P.: An airborne and wind tunnel evaluation of a wind turbulence measurement system for aircraft-based flux measurements*, J. Atmos. Oceanic Technol., 23, 1696-1708, http://dx.doi.org/10.1175/JTECH1940.1, 2006.

Garman, K. E., Wyss, P., Carlsen, M., Zimmerman, J., Stirm, B., Carney, T., Santini, R., and Shepson, P.: The contribution of variability of lift-induced upwash to the uncertainty in vertical winds determined from an aircraft platform, Bound.-Layer Meteo., 126, 461-476, doi.org/10.1007/s10546-007-9237-y, 2008.

Garman, K. E.: Precision of airborne wind measurement for atmospheric flight research, Purdue University, 2009.

Gat, J. R.: Oxygen and hydrogen isotopes in the hydrologic cycle, Annual Review of Earth and Planetary Sciences, 24, 225-262, 10.1146/annurev.earth.24.1.225, 1996.

Gedzelman, S. D.: Deuterium in water vapor above the atmospheric boundary layer, Tellus B, 40B, 134-147, 10.1111/j.1600-0889.1988.tb00217.x, 1988.

Gerber, H., Frick, G., Malinowski, S. P., Jonsson, H., Khelif, D., and Krueger, S. K.: Entrainment rates and microphysics in POST stratocumulus, J. Geophys. Res.: Atmos., 118, 12,094-012,109, 10.1002/jgrd.50878, 2013.

~~Gorski, G., Strong, C., Good, S. P., Bares, R., Ehleringer, J. R., and Bowen, G. J.: Vapor hydrogen and oxygen isotopes reflect water of combustion in the urban atmosphere, Proc. Natl. Acad. Sci., 112, 3247-3252, 10.1073/pnas.1424728112, 2015.~~

~~Griffis, T. J., Wood, J. D., Baker, J. M., Lee, X., Xiao, K., Chen, Z., Welp, L. R., Schultz, N. M., Gorski, G., Chen, M., and Nieber, J.: Investigating the source, transport, and isotope composition of water vapor in the planetary boundary layer, Atmos. Chem. Phys., 16, 5139-5157, 10.5194/acp-16-5139-2016, 2016.~~

Grimmond, C. S. B., Blackett, M., Best, M. J., Barlow, J., Baik, J.-J., Belcher, S. E., Bohnenstengel, S. I., Calmet, I., Chen, F., Dandou, A., Fortuniak, K., Gouvea, M. L., Hamdi, R., Hendry, M., Kawai, T., Kawamoto, Y., Kondo, H., Krayenhoff, E. S., Lee, S.-H., Loridan, T., Martilli, A., Masson, V., Miao, S., Oleson, K., Pigeon, G., Porson, A., Ryu, Y.-H., Salamanca, F., Shashua-Bar, L., Steeneveld, G.-J., Tombrou, M., Voogt, J., Young, D., and Zhang, N.: The international urban energy balance models comparison project: first results from phase 1, J. Appl. Meteorol. Climatol., 49, 1268-1292, doi:10.1175/2010JAMC2354.1, 2010.

He, H., and Smith, R. B.: Stable isotope composition of water vapor in the atmospheric boundary layer above the forests of New England, J. Geophys. Res.: Atmos., 104, 11657-11673, doi:10.1029/1999JD900080, 1999.

Held, I. M., and Soden, B. J.: Water vapor feedback and global warming, Annu. Rev. Energy Env., 25, 441-475, 10.1146/annurev.energy.25.1.441, 2000.

Held, I. M., and Soden, B. J.: Robust Responses of the Hydrological Cycle to Global Warming, J. Clim., 19, 5686-5699, 10.1175/jcli3990.1, 2006.

Herman, R. L., Cherry, J. E., Young, J., Welker, J. M., Noone, D., Kulawik, S. S., and Worden, J.: Aircraft validation of Aura Tropospheric Emission Spectrometer retrievals of HDO / H_2O, Atmos. Meas. Tech., 7, 3127-3138, 10.5194/amt-7-3127-2014, 2014.

Horita, J., and Wesolowski, D. J.: Liquid-vapor fractionation of oxygen and hydrogen isotopes of water from the freezing to the critical temperature, Geochim. Cosmochim. Acta, 58, 3425-3437, http://dx.doi.org/10.1016/0016-7037(94)90096-5, 1994.

Hurley, J. V., and Galewsky, J.: A last-saturation diagnosis of subtropical water vapor response to global warming, Geophys. Res. Lett., 37, 10.1029/2009gl042316, 2010.

Jouzel, J.: Chapter 2 - ISOTOPES IN CLOUD PHYSICS: MULTIPHASE AND MULTISTAGE CONDENSATION PROCESSES, in: The Terrestrial Environment, B, edited by: Fritz, P., and Fontes, J. C., Elsevier, Amsterdam, 61-112, 1986.

Kelsey, E., Bailey, A., and Murray, G.: The impact of mount washington on the height of the boundary layer and the vertical structure of temperature and moisture, Atmosphere, 9, 293, 2018.

Kollias, P., and Albrecht, B.: The Turbulence Structure in a Continental Stratocumulus Cloud from Millimeter-Wavelength Radar Observations, Journal of the Atmospheric Sciences, 57, 2417-2434, 10.1175/1520-0469(2000)057<2417:ttsiac>2.0.co;2, 2000.

Kunkel, K. E., Karl, T. R., Brooks, H., Kossin, J., Lawrimore, J. H., Arndt, D., Bosart, L., Changnon, D., Cutter, S. L., Doesken, N., Emanuel, K., Groisman, P. Y., Katz, R. W., Knutson, T., O'Brien, J., Paciorek, C. J., Peterson, T. C., Redmond, K., Robinson, D., Trapp, J., Vose, R., Weaver, S., Wehner, M., Wolter, K., and Wuebbles, D.: Monitoring and understanding trends in extreme storms: state of knowledge, Bull. Amer. Meteor. Soc., 94, 499-514, 10.1175/bams-d-11-00262.1, 2012.

Lai, C.-T., and Ehleringer, J. R.: Deuterium excess reveals diurnal sources of water vapor in forest air, Oecologia, 165, 213-223, 10.1007/s00442-010-1721-2, 2011.

Lawrence, J. R., Gedzelman, S. D., Dexheimer, D., Cho, H.-K., Carrie, G. D., Gasparini, R., Anderson, C. R., Bowman, K. P., and Biggerstaff, M. I.: Stable isotopic composition of water vapor in the tropics, J. Geophys. Res.: Atmos., 109, 10.1029/2003jd004046, 2004.

~~Lee, X., Smith, R. and Williams, J.: Water vapour 18O/16O isotope ratio in surface air in New England, USA, Tellus B, 58(4), 293–304, doi:10.1111/j.1600-0889.2006.00191.x, 2006.~~

Lowenthal, D., Hallar, A. G., McCubbin, I., David, R., Borys, R., Blossey, P., Muhlbauer, A., Kuang, Z., and Moore, M.: Isotopic Fractionation in Wintertime Orographic Clouds, J. Atmos. Oceanic Technol., 33, 2663-2678, 10.1175/jtech-d-15-0233.1, 2016.

de Lozar, A., and Mellado, J. P.: Evaporative cooling amplification of the entrainment velocity in radiatively driven stratocumulus, Geophys. Res. Lett., 42, 7223-7229, 10.1002/2015gl065529, 2015.

Merlivat, L.: Molecular diffusivities of $H_2{}^{16}O$, $HD^{16}O$, and $H_2{}^{18}O$ in gases, The Journal of Chemical Physics, 69, 2864-2871, 10.1063/1.436884, 1978.

~~Merlivat, L., and Jouzel, J.: Global climatic interpretation of the deuterium-oxygen-18 relationship for precipitation, Journal of Geophysical Research: Oceans, 84, 5029–5033, doi:10.1029/JC084iC08p05029, 1979.~~

Moore, M., Blossey, P. N., Muhlbauer, A., and Kuang, Z.: Microphysical controls on the isotopic composition of wintertime orographic precipitation, J. Geophys. Res.: Atmos., 121, 7235-7253, doi:10.1002/2015JD023763, 2016.

Noone, D.: Pairing measurements of the water vapor isotope ratio with humidity to deduce atmospheric moistening and dehydration in the tropical midtroposphere, J. Clim., 25, 4476-4494, 10.1175/jcli-d-11-00582.1, 2012.

Noone, D., Risi, C., Bailey, A., Berkelhammer, M., Brown, D. P., Buenning, N., Gregory, S., Nusbaumer, J., Schneider, D., Sykes, J., Vanderwende, B., Wong, J., Meillier, Y., and Wolfe, D.: Determining water sources in the boundary layer from tall tower profiles of water vapor and surface water isotope ratios after a snowstorm in Colorado, Atmos. Chem. Phys., 13, 1607-1623, 10.5194/acp-13-1607-2013, 2013.

Park, S., Baek, E.-H., Kim, B.-M., and Kim, S.-J.: Impact of detrained cumulus on climate simulated by the Community Atmosphere Model Version 5 with a unified convection scheme, Journal of Advances in Modeling Earth Systems, 9, 1399-1411, 10.1002/2016ms000877, 2017.

~~Parkes, S. D., McCabe, M. F., Griffiths, A. D., Wang, L., Chambers, S., Ershadi, A., Williams, A. G., Strauss, J., and Element, A.: Response of water vapour D-excess to land–atmosphere interactions in a semi-arid environment, Hydrol. Earth Syst. Sci., 21, 533–548, 10.5194/hess-21-533-2017, 2017.~~

Pfahl, S., Wernli, H., and Yoshimura, K.: The isotopic composition of precipitation from a winter storm – a case study with the limited-area model COSMOiso, Atmos. Chem. Phys., 12, 1629-1648, https://doi.org/10.5194/acp-12-1629-2012, 2012.

Rambo, J., Lai, C.-T., Farlin, J., Schroeder, M., and Bible, K.: On-site calibration for high precision measurements of water vapor isotope ratios using off-axis cavity-enhanced absorption spectroscopy, J. Atmos. Oceanic Technol., 28, 1448-1457, 10.1175/jtech-d-11-00053.1, 2011.

Risi, C., Bony, S., and Vimeux, F.: Influence of convective processes on the isotopic composition (δ18O and δD) of precipitation and water vapor in the tropics: 2. Physical interpretation of the amount effect, J. Geophys. Res.: Atmos., 113, 10.1029/2008jd009943, 2008.

Romps, D. M.: Exact expression for the lifting condensation level, Journal of the Atmospheric Sciences, 74, 3891-3900, 10.1175/jas-d-17-0102.1, 2017.

Roque-Malo, S., and Kumar, P.: Patterns of change in high frequency precipitation variability over North America, Scientific Reports, 7, 10853, 10.1038/s41598-017-10827-8, 2017.

Samuels-Crow, K. E., Galewsky, J., Sharp, Z. D., and Dennis, K. J.: Deuterium excess in subtropical free troposphere water vapor: Continuous measurements from the Chajnantor Plateau, northern Chile, Geophys. Res. Lett., 41, 8652-8659, 10.1002/2014gl062302, 2014.

Salmon, O. E., Shepson, P. B., Ren, X., Marquardt Collow, A. B., Miller, M. A., Carlton, A. G., Cambaliza, M. O. L., Heimburger, A., Morgan, K. L., Fuentes, J. D., Stirm, B. H., Grundman, R., and Dickerson, R. R.: Urban emissions of water vapor in winter, J. Geophys. Res.: Atmos., 122, 9467-9484, 10.1002/2016jd026074, 2017.

Schmidt, G. A., Hoffmann, G., Shindell, D. T., and Hu, Y.: Modeling atmospheric stable water isotopes and the potential for constraining cloud processes and stratosphere-troposphere water exchange, J. Geophys. Res.: Atmos., 110, n/a-n/a, 10.1029/2005jd005790, 2005.

Sodemann, H., Aemisegger, F., Pfahl, S., Bitter, M., Corsmeier, U., Feuerle, T., Graf, P., Hankers, R., Hsiao, G., Schulz, H., Wieser, A., and Wernli, H.: The stable isotopic composition of water vapour above Corsica during the HyMeX SOP1 campaign: insight into vertical mixing processes from lower-tropospheric survey flights, Atmos. Chem. Phys., 17, 6125-6151, 10.5194/acp-17-6125-2017, 2017.

Steen-Larsen, H. C., Sveinbjörnsdottir, A. E., Peters, A. J., Masson-Delmotte, V., Guishard, M. P., Hsiao, G., Jouzel, J., Noone, D., Warren, J. K., and White, J. W. C.: Climatic controls on water vapor deuterium excess in the marine boundary layer of the North Atlantic based on 500 days of in situ, continuous measurements, Atmos. Chem. Phys., 14, 7741-7756, https://doi.org/10.5194/acp-14-7741-2014, 2014.

~~Strong, M., Sharp, Z. D., and Gutzler, D. S.: Diagnosing moisture transport using D/H ratios of water vapor, Geophys. Res. Lett., 34, doi:10.1029/2006GL028307, 2007.~~

Stull, R. B.: An introduction to boundary layer meteorology, Springer Science & Business Media, 1988.

Taylor, C. B.: Vertical distribution of deuterium in atmospheric water vapour: problems in application to assess atmospheric condensation models, Tellus B, 36B, 67-70, 10.1111/j.1600-0889.1984.tb00053.x, 1984.

Thompson, A. M.: The oxidizing capacity of the earth's atmosphere: probable past and future changes, Science, 256, 1157-1165, 10.1126/science.256.5060.1157, 1992.

Tompkins, A. M.: Organization of tropical convection in low vertical wind shears: the role of cold pools, Journal of the Atmospheric Sciences, 58, 1650-1672, 10.1175/1520-0469(2001)058<1650:ootcil>2.0.co;2, 2001.

Trapp, R. J., Diffenbaugh, N. S., Brooks, H. E., Baldwin, M. E., Robinson, E. D., and Pal, J. S.: Changes in severe thunderstorm environment frequency during the 21st century caused by anthropogenically enhanced global radiative forcing, Proc. Natl. Acad. Sci., 104, 19719-19723, 10.1073/pnas.0705494104, 2007.

Trenberth, K. E.: Changes in precipitation with climate change, Clim. Res., 47, 123-138, 2011.

~~Tsujimura, M., Sasaki, L., Yamanaka, T., Sugimoto, A., Li, S. G., Matsushima, D., Kotani, A., and Saandar, M.: Vertical distribution of stable isotopic composition in atmospheric water vapor and subsurface water in grassland and forest sites, eastern Mongolia, Journal of Hydrology, 333, 35-46, https://doi.org/10.1016/j.jhydrol.2006.07.025, 2007.~~

Uemura, R., Matsui, Y., Yoshimura, K., Motoyama, H., and Yoshida, N.: Evidence of deuterium excess in water vapor as an indicator of ocean surface conditions, J. Geophys. Res.: Atmos., 113, doi:10.1029/2008JD010209, 2008.

U.S. Census Bureau, Population Division: Annual estimates of the resident population: April 1, 2010 to July 1, 2017, https://www.census.gov/programs-surveys/popest/technical-documentation/methodology.html, Accessed: March 2018.

Wang, S., Zhang, M., Che, Y., Zhu, X., and Liu, X.: Influence of below-cloud evaporation on deuterium excess in precipitation of arid central asia and its meteorological controls, Journal of Hydrometeorology, 17, 1973-1984, 10.1175/jhm-d-15-0203.1, 2016.

~~Webster, C. R., and Heymsfield, A. J.: Water Isotope Ratios D/H, $^{18}O/^{16}O$, $^{17}O/^{16}O$ in and out of Clouds Map Dehydration Pathways, Science, 302, 1742-1745, 10.1126/science.1089496, 2003.~~

Welp, L. R., Lee, X., Griffis, T. J., Wen, X.-F., Xiao, W., Li, S., Sun, X., Hu, Z., Val Martin, M., and Huang, J.: A meta-analysis of water vapor deuterium-excess in the midlatitude atmospheric surface layer, Global Biogeochem. Cycles, 26, GB3021, 10.1029/2011gb004246, 2012.

Willett, K. M., Gillett, N. P., Jones, P. D., and Thorne, P. W.: Attribution of observed surface humidity changes to human influence, Nature, 449, 710-712, http://www.nature.com/nature/journal/v449/n7163/suppinfo/nature06207_S1.html, 2007.

Wood, R.: Stratocumulus Clouds, Monthly Weather Review, 140, 2373-2423, 10.1175/mwr-d-11-00121.1, 2012.

Worden, J., Noone, D., Bowman, K., The Tropospheric Emission Spectrometer science team and data contributors: Importance of rain evaporation and continental convection in the tropical water cycle, Nature, 445, 528, 10.1038/nature05508, 2007.

Worden, J., Kulawik, S., Frankenberg, C., Payne, V., Bowman, K., Cady-Peirara, K., Wecht, K., Lee, J. E., and Noone, D.: Profiles of CH_4 HDO, H_2O, and N_2O with improved lower tropospheric vertical resolution from Aura TES radiances, Atmos. Meas. Tech., 5, 397-411, 10.5194/amt-5-397-2012, 2012.

Wright, J. S., Sobel, A. H., and Schmidt, G. A.: Influence of condensate evaporation on water vapor and its stable isotopes in a GCM, Geophys. Res. Lett., 36, 10.1029/2009gl038091, 2009.

Yamaguchi, T., and Feingold, G.: On the size distribution of cloud holes in stratocumulus and their relationship to cloud-top entrainment, Geophys. Res. Lett., 40, 2450-2454, 10.1002/grl.50442, 2013.